Aus der

Klinik für Anaesthesiologie

Klinikum der Ludwig-Maximilians-Universität München

Analysis of blood transcriptomics of the Djungarian hamster in torpor – a comparative approach with other mammalian species

Dissertation zum Erwerb des Doktorgrades der Humanbiologie

an der Medizinischen Fakultät

der Ludwig-Maximilians-Universität München

vorgelegt von

Valeria Rojas Cuyutupa

aus

Lima-Peru

2025

Mit Genehmigung der Medizinischen Fakultät der

Ludwig-Maximilians-Universität zu München

Erstes Gutachten:	Prof. Dr. Alexander Choukér
Zweites Gutachten:	Prof. Dr. Annika Herwig
Drittes Gutachten:	Prof. Dr. Bertram Müller-Myhsok

Dekan:	Prof. Dr. med. Thomas Gudermann

Tag der mündlichen Prüfung:	07.04.2025

I. **Affidavit**

Eidesstattliche Versicherung

Rojas Cuyutupa, Valeria
Name, Vorname

Ich erkläre hiermit an Eides statt, dass ich die vorliegende Dissertation mit dem Titel:

Analysis of blood transcriptomics of the Djungarian hamster in torpor – a comparative approach with other mammalian species

selbständig verfasst, mich außer der angegebenen keiner weiteren Hilfsmittel bedient und alle Erkenntnisse, die aus dem Schrifttum ganz oder annähernd übernommen sind, als solche kenntlich gemacht und nach ihrer Herkunft unter Bezeichnung der Fundstelle einzeln nachgewiesen habe.

Ich erkläre des Weiteren, dass die hier vorgelegte Dissertation nicht in gleicher oder in ähnlicher Form bei einer anderen Stelle zur Erlangung eines akademischen Grades eingereicht wurde.

München, 21.07.2025	Valeria Rojas Cuyutupa
Ort, Datum	Unterschrift Doktorandin

II. Erklärung zur Übereinstimmung

LMU LUDWIG-MAXIMILIANS-UNIVERSITÄT MÜNCHEN | Promotionsbüro Medizinische Fakultät | MMRS

Erklärung zur Übereinstimmung der gebundenen Ausgabe der Dissertation mit der elektronischen Fassung

Ihr Name: Valeria Rojas Cuyutupa

Hiermit erkläre ich, dass die elektronische Version der eingereichten Dissertation mit dem Titel:

Analysis of blood transcriptomics of the Djungarian hamster in torpor – a comparative approach with other mammalian species

in Inhalt und Formatierung mit den gedruckten und gebundenen Exemplaren übereinstimmt.

München, 21.07.2025	Valeria Rojas Cuyutupa
Ort, Datum	Unterschrift Doktorandin

III. Summary

Torpor is a complex survival strategy where endogenous metabolic rate (MR), respiratory rate and body temperature (T_b) are reversibly reduced to limit energy expenditure during periods of environmental stress. For mammals capable of torpor this process entails vast metabolic changes as they need to maintain their physiological equilibrium for hours, days or even weeks, depending on the type of torpor. During this period the homeostatic machinery is significantly impaired before the euthermic state is regained by spontaneous intrinsic heat production.

In this work transcriptional changes related to daily torpor were analysed using the Djungarian hamster (*Phodopus sungorus*) model. The aim of this work was (i) to evaluate the transcriptional dynamics between the different phases of torpor entry (ZT01), nadir / mid-torpor (ZT04), arousal (ZT07) and post-torpor phase (ZT16), (ii) to identify common transcriptional patterns in the blood of torpid *P. sungorus* and other torpid / hibernating mammals independent of analysed solid organ, and (iii) to compare blood transcriptome profiles of the different phases of *P. sungorus* daily torpor with human overwintering crews in Antarctica during different times of the mission to obtain information on possible similarities in regulation of gene expression between torpor and environmental stress related changes in humans. For data analysis the bioinformatic tool Ingenuity Pathway Analysis (IPA) was used to identify the main signalling pathways involved and their respective regulatory pattern.

The results showed (i) notable changes between torpor entry (ZT01) and torpor nadir (ZT04), while ZT01 was largely indifferent to control samples. Transcriptional proliferation, translation and protein production machinery were significantly depressed during torpor nadir (ZT04) but were restored and even upregulated during arousal (ZT07), followed by a period of slight depression in the post-torpor phase before full recovery. (ii) Based on IPA key target molecule analysis (TM_{IPA}) most cellular processes are inhibited during torpor nadir (ZT04). By literature comparison of 9 other hibernators and 10 different organs, this inhibition was shown to be independent of torpor type, duration or species.

Suppression of basic energy-consuming cellular processes, downregulation of proinflammatory immune responses and organ protection predominantly by suspending pro-apoptotic processes and promoting antioxidant production allow entry into torpor / hibernation without signs of tissue damage upon arousal. Furthermore, these data corroborate that the transcriptomic alterations required for torpor / hibernation in general and at the level of specific organs can be detected in and are reflected by blood cells. (iii) Humans overwintering at the Antarctic Concordia station show a similar downregulation pattern of the immune system as observed for ZT04 animals, however most canonical pathways in human samples were more comparable to the arousal phase (ZT07) in animals, mirroring a "continuous arousal" with EIF2, TGF-β signalling, SUMOylation and telomerase signalling as the most upregulated pathways in the overwintering crews. The post phase of human overwintering crews is similar to *P. sungorus* post phase (ZT16), representing a recovery phase of minor global downregulation striving towards control levels.

IV. **Zusammenfassung**

Torpor ist eine komplexe Überlebensstrategie, bei welcher die endogene Stoffwechselrate (MR), die Atmungsrate und die Körpertemperatur (T_b) reversibel reduziert werden, um den Energieverbrauch in Zeiten von umweltbedingtem Stress zu beschränken. Für Säugetiere, welche Torpor betreiben, bringt dieser Prozess enorme metabolische Veränderungen mit sich, da sie ihr physiologisches Gleichgewicht abhängig von der Torporart über Stunden, Tage oder sogar Wochen aufrechterhalten müssen. Während dieses Zeitraums wird die homöostatische Maschinerie stark eingeschränkt, ehe der euthermische Zustand durch spontane Eigenerwärmung wiederhergestellt wird.

In dieser Arbeit wurden transkriptionelle Veränderungen im Zusammenhang mit täglichem Torpor am Beispiel des Dsungarischen Hamsters (*Phodopus sungorus*) analysiert. Ziel dieser Arbeit war es, (i) die Transkriptionsdynamik zwischen den verschiedenen Phasen des Torporeintritts (ZT01), des Nadir (ZT04), des Erwachens (ZT07) und der Post-Torpor-Phase (ZT16) auszuwerten, (ii) gemeinsame Transkriptionsmuster im Blut von torportreibenden *P. sungorus* und anderen torportreibenden/überwinternden Säugetieren unabhängig vom untersuchten Organ zu identifizieren und (iii) Bluttranskriptom-Profile der verschiedenen Phasen des täglichen Torpor von *P. sungorus* mit denen menschlicher Überwinterer in der Antarktis zu verschiedenen Zeitpunkten der Mission zu vergleichen, um – zum ersten Mal – Informationen über mögliche regulatorische Ähnlichkeiten der Genexpression zwischen Torpor und stressbedingter Reduktion der MR im Menschen zu er-halten. Zur Datenanalyse wurde das bioinformatische Tool *Ingenuity Pathway Analysis* (IPA) verwendet, um die wichtigsten beteiligten Signalwege und ihre jeweiligen Regulationsmuster zu identifizieren.

Die Ergebnisse zeigen (i) bemerkenswerte Veränderungen zwischen dem Torporeintritt (ZT01) und des Torpornadirs (ZT04), während ZT01 weitgehend identisch zu den Kontrollproben war. Transkription, Proliferation, Translation und Proteinproduktion waren während des Torpornadirs (ZT04) signifikant unterdrückt, erholten sich allerdings während des Aufwachens (ZT07) und wurden sogar teilweise hochreguliert, gefolgt von einer

Periode leichter Depression in der Post-Torpor-Phase vor der vollständigen Erholung. (ii) Auf Grundlage der IPA-Analyse der wichtigsten Zielmoleküle (TM_{IPA}) sind die meisten zellulären Prozesse während des Torpornadirs (ZT04) gehemmt. Durch Literaturvergleiche mit 9 anderen Winterschläfern und 10 verschiedenen Organen dieser Tiere konnte gezeigt werden, dass diese Hemmung unabhängig von der Torporart, -dauer oder der jeweiligen Spezies ist. Die Unterdrückung grundlegender energieintensiver zellulärer Prozesse sowie proinflammatorischer Immunreaktionen und der intensivierte Schutz der Organe markieren den Eintritt in den täglichen Torpor/Winterschlaf. Durch die Unterbrechung pro-apoptotischer Prozesse und die erhöhte Produktion von Antioxidantien werden dabei Gewebeschäden beim Erwachen vorgebeugt. Darüber hinaus bestätigen diese Daten, dass die transkriptionellen Veränderungen, die für Torpor im Allgemeinen, aber auch auf der organspezifischen Ebene erforderlich sind, in Blutzellen nachgewiesen werden können und sich in diesen widerspiegeln. (iii) Menschen, die in der Antarktis überwintern zeigen ein ähnliches Herabregulierungsmuster des Immunsystems wie Tiere zum Zeitpunkt ZT04. Jedoch waren die meisten kanonischen Signalwege in menschlichen Probanden eher mit der Aufwachphase (ZT07) bei Tieren vergleichbar, was einem "kontinuierliches Erwachen" entspricht, wobei EIF2, der TGF-β-Signalweg, SUMOylierung und der Telomerase-Signalweg die stärksten Hochregulierung in den Überwinternden zeigten. Die Postphase der untersuchten Menschen nach ihrer Überwinterung ähnelt der Postphase von *P. sungorus* (ZT16) und stellt eine Erholungsphase mit einer geringfügigen globalen Herabregulierung dar, die sich dem Grundniveau der Kontrolltieren annähert.

V. Index of Figures

VI. Index of Tables

VII. **Abbreviations**

ATP	Adenosine triphosphate
BAT	Brown adipose tissue
BCR	B cell receptor
BDC	Baseline Data Collection or control group for overwinter samples
CD8	Cluster of differentiation 8
cDNA	complementary DNA
DAMP	Damage-associated molecular pattern
DNA	Desoxyribonucleic acid
Dr	Doctor (title)
DSI	Data Sciences International
e.g	for example
EDTA	Ethylenediaminetetraacetic acid, Ethylenediaminetetraacetic acid
EIF2	Eukaryotic translation initiation factors
ERK	Extracellular-signal Regulated Kinases
FC	Fold Change
FDR	False Discovery Rate
g	Gramm
G_0	Resting state, or gap phase
HMGB1	High mobility group protein B1
HT	Hypothermic
i.p	Intraperitoneal
IFNγ	Interferon-γ
IGF-1	Insulin like growth factor 1
IPA	Ingenuity pathway analysis
IQ	Integrity Quality
IR	Ischemic reperfusion
Keap1	Kelch-like ECH-associated protein 1
LED	Light emitting diode
LMU	Ludwig-Maximilians-Universität in Munich

MAPK	Mitogen-activated protein kinase
MDB	Membrane Desalting Buffer
MEK	MAP kinase kinase
Met-tRNA	Methionyl-tRNA
ml	Mililiter
MR	Metabolic rate
mRNA	messenger Ribonucleic Acid
NGS	Next Generation Sequencing
NK	Natural killer Cell
Nrf2	Nuclear factor erythroid 2 derived factor 2
NT	Normothermic controls
OPAC	Online Public Access Catalogue
P. sungorus	Phodopus sungorus
PAMPs	Pathogen-associated molecular patterns
RAF	Proto-oncogene serine/threonine-protein kinase
rDNase	Recombinant DNase
RIN	RNA integrity number
RNA	Ribonucleic Acid
RNA-seq	RNA sequencing
ROS	Radical Oxygen Species
rRNA	ribosomal RNA
RTL	Relative telomere length
SCN	Suprachiasmatic Nucleus
SD	short day light
SDH	Succinate dehydrogenase
SIRT	Sirtuin
SP	Short photoperiod
STDEV	Standard deviation
SUMO	Small ubiquitin-like modifier
T_a	Ambient temperature

T_b	Body temperature
TGF-β	transforming growth factor beta
TLR4	Toll like receptor 4
TM_{IPA}	Ingenuity Pathway Analysis (IPA) identified key target molecules
Tris	Tris(hydroxymethyl)aminomethane
tRNA	transfer-RNA
WAT	White adipose tissue
ZT	Zeitgeber time
ZT01	Torpor entry
ZT04	Torpor nadir/mid or deep torpor
ZT07	Arousal from torpor
ZT16	Post-torpor phase
µl	Microliter

VIII. **Table of contents**

1 Introduction

1.1 Thermoregulation in vertebrates

In the development of higher vertebrates there is a progression in the direction of a stable body temperature (T_b), however hibernators seem to go against and rather in the direction of their ancestral poikilothermic state (Xia, 1995). In living vertebrates, temperature control occurs in different ways.

In the case of fish, the geographical distribution of many species is limited by the ambient temperature (T_a) of the waters they inhabit. The capillary structure of their gills enforces temperature equilibration of blood and surrounding water. However, in fast swimming fish, such as tuna, the swimming muscles are kept warm by the heat retained in these due to their counter-current exchanger capacity allowing for a maximum T_b, which is significantly warmer than the circulating water and can buffer temporal drops in T_a (Carey & Lawson, 1973). An elevated metabolic rate (MR) coincides with a higher oxygen demand and therefore increased gill blood flow compensating metabolic heat production by increased environmental temperature exchange (Stevens et al., 2000). Its high specific warmth capacity makes water a relatively stable environment for fish compared to terrestrial vertebrates, which are exposed to rapid seasonal shifts in their environments with temperature extremes that can vary by up to 50 °C (Lyman, 1982).

Amphibians, in comparison to fish, have a very limited control of their inner milieu and without means to maintain elevated T_b levels. This taxon constantly faces the risk of dermal desiccation when sojourning in dry or hot habitats because amphibian skin is highly permeable for gases and water (Lyman, 1982). Their T_b can thus be reduced to a level below that of the environment in case of evaporative water loss (Vitt & Caldwell, 2009). For this reason, if their T_b rises, they will take refuge in a cooler place or seek out water, as amphibians are able to sense their own T_b, such as the canadian toad (*Bufo hemiophrys*) (Forget-Klein & Green, 2021).

Conversely, reptiles generally remain in warm environments without the risk of rapid desiccation by allowing their T_b to increase. They maintain a stable T_b during their active

day phase, which is slightly higher than during inactive night phases. This is regulated by sunbathing or seeking out cool shelters. However, once they are exposed to very cold weather, their T_b drops and they go into hypothermia from which they do not emerge until the T_a rises (Vitt & Caldwell, 2009).

Birds have been characterised to exhibit a high and stable T_b within a range of 39 to 43 °C throughout their lives. This capability is conferred by an endocrine system, which includes mechanisms of plastic modulation. This thermoregulatory flexibility allows individuals to rapidly respond to short and long term environmental temperature shifts (Ruuskanen et al., 2021).

Mammals show similar thermoregulatory capacities and systems to their avian relatives. Earliest mammals, such as the monotremes, generally support a T_b of around 30 °C, while marsupials span a range of 35 to 38 °C being closer to that of eutherian mammals (Lyman, 1982). Preservation of a T_b lower than its living environment is achieved through transpiration, the evaporation of body water. Significantly elevated body temperatures are hazardous for mammals, as most proteins denature at temperatures above 45 °C. However, severe disturbances of physiological functions caused by fevers below this critical value can also have lethal effects as the balance of enzyme activity, neuronal function and metabolic interactions is crucial for survival (Geiser, 2021).

Species-specific metabolism includes thermoregulatory processes that are required to keep the body well-functioning. Some mammals successfully use special strategies to reduce the amount of energy per unit time that a species needs to operate the body at rest, also known as metabolic rate (MR). This MR reduction saves energy during harsh periods of environmental stress by entering a state known as torpor.

1.2 Torpor in mammals

Torpor is a potential survival strategy used by mammals to escape from harsh environments, especially in seasons of resource scarcity (Ruf & Geiser, 2015). Throughout this process, changes occur in the organism and animals capable of torpor enter a temporary state where they reversibly reduce their endogenous MR**,** breathing rate and T_b to reduce energy expenditure. This physiological mechanism, at low MR, use of fat stores to survive for a period. It also involves a precise balance between heat generated and heat lost, as in most mammals, when body or brain temperature deviates from its functional range, it triggers death (Melvin & Andrews, 2009). Therefore, torpid mammals need to maintain their physiological equilibrium for hours, days or weeks, thus partially sacrificing their homeostatic machinery and then spontaneously rewarming themselves to regain their euthermic state (Lyman, 1982).

Torpor species are classified as heterothermic endotherm, which show two considerable variations in T_b over the course of their adulthood (Ruf & Geiser, 2015) :

- Temporal heterothermic: mammals show large fluctuations in T_b (Geiser, 2021). In a torpid state T_b is regulated around a species-specific minimum (e.g. at around 2.6 °C for marmots (Arnold, 1995) and almost 32 °C for bears (Nespolo et al., 2022)). Thereby, a new temperature set point can be achieved, during torpor, by increasing metabolic heat to avoid tissue damage, and this not only compensates for heat loss, but also, in this way, maintains the rewarming capacity (Geiser, 2011).
- Euthermic or normothermic: the active state of animals capable of torpor, which is typically characterized by a quiescent T_b and MR. A well-controlled T_b of approximately 37 °C is retained over a broad spectrum of T_a (Geiser, 2021). The euthermic condition requires two important factors: body size and species-specific MR. In mammals these two are closely associated by Kleiber's rule.

In 1947 Kleiber described an allometric relationship in mammals relating the basal MR to surface area rather than weight since the ratio of a body's heat output to its environment is roughly proportional to its surface area (Niklas & Kutschera, 2015). Exemplary, it can be observed that the MR of the small rodent *Muscardinus avellanarius* is around twenty fold higher compared to the MR of an elephant (Figure 1, the curve). During torpor, however, this rule is switched off and small animals have the same specific MR as larger mammals (Figure 1, the striped part in blue).

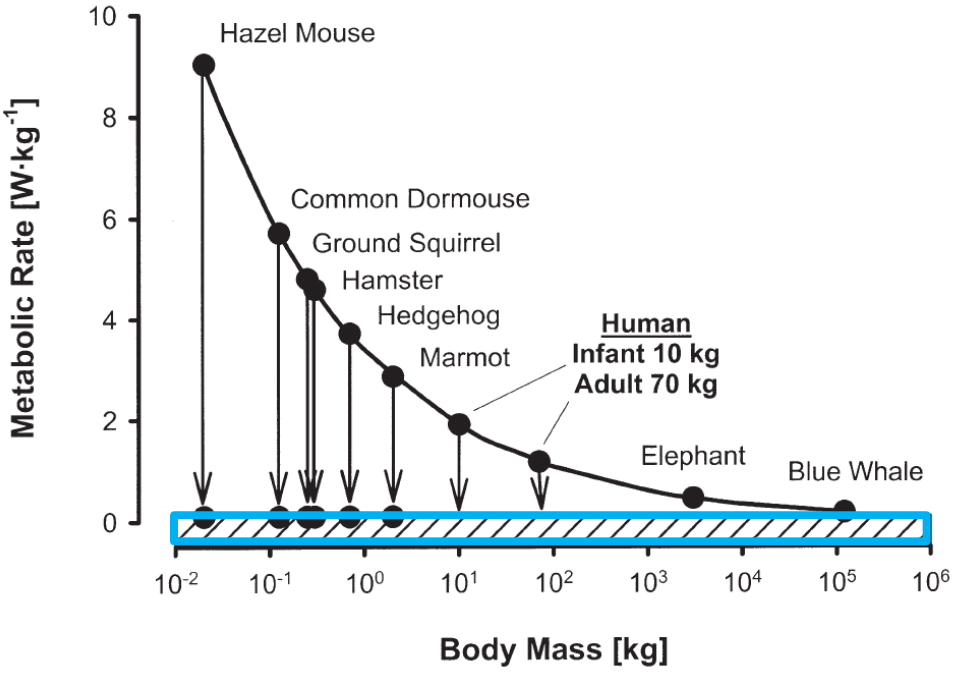

Figure 1. The Kleiber rule is "switched off" in mammals exhibiting torpor. The upper curve shows the overall increase in MR with decreasing body mass. Mammals during torpor show a uniform minimum specific MR that equals the MR of larger mammals, also human newborns, striped in the blue rectangle (Singer, 2004).

1.2.1 Mammalian torpor types and their geographical distributions

To date, 5,416 mammal species have been classified into 29 orders (Solari & Baker, 2007). Torpor-bearing mammals comprise 13 different orders (Geiser, 2021) (Table 1).

Table 1. Listed orders of mammals exhibiting torpor

Order	Family/ies	Geographical distribution
Rodentia	Bathyergidae, Cricetidae, Dipodidae, Gliridae, Heteromyidae, Muridae, Nesomyidae, Sciuridae, Zapodidae	Africa, Asia, Australia, Europe Madagascar, New Zealand, North America and South America
Chiroptera	Molossidae, Nycteridae, Phyllostomidae, Pteropodidae, Rhinolophidae, Rhinopomatidae, Vespertilionidae	Africa, Asia, Australia, Europe Madagascar, New Zealand, North America and South America
Dasyuromorphia	Dasyuridae, Myrmecobiidae	Australia and New Zealand
Erinaceomorpha	Erinaceidae, Soricidae	Africa, Asia, Europe, Madagascar and North America
Primates	Cheirogaleidae, Galagidae	Africa and Madagascar
Diprodontia	Acrobatidae, Burramyidae, Petauridae, Tarsipedidae	Australia and New Zealand
Carnivora	Hyaenidae, Mephitidae, Mustelidae, Ursidae	Africa, Asia, Europe, Madagascar and North America
Afrosoricidae	Chrysochloridae, Tenrecidae	Africa and Madagascar
Macroscelidae	Macroscelididae	Africa and Madagascar
Didelpimorphia	Didelphidae	South America
Cingulata	Chlamyphoridae	South America
Monotremata	Tachyglossidae	Australia and New Zealand
Microbiotheria	Microbiotheriidae	South America

Torpor is used by many species (Table 1, Figure 2) and their geographic distribution is diverse (Geiser, 2021). Until now, 3 types of torpor types are known in mammals:

a) Hibernation (multi-day torpor): mostly seasonal and typically between meteorological autumn and spring (Geiser, 2021). The minimum T_b ranges from -2.9 to 29.4 °C and the torpor state lasts more than one day (Geiser & Ruf, 1995). During hibernation, the MR is reduced to 4 - 25% (Christian & Geiser, 2007; Bertile et al., 2021). This type of torpor is mostly used by small mammals, with a weight varying from 10 to 1,000 g. However, it is also performed by bears that weigh around 100 - 500 kg employing a hibernation pattern that deviates from that of small hibernators (Ruf & Geiser, 2015). As a source of energy prior to the hibernation season, a fattening pattern, like hyperphagia, is often observed and dependence on stored body fat (up to 12 months), thus adopting a spherical shape (Humphries et al., 2003). Additional food storage is known for a limited subset of hibernators, for example chipmunks (*Tamias spp*.). Examples of hibernating species: Pygmy possum (*Cercartetus nanus*), little brown bat (*Myotis lucifugus*), american black bear (*Ursus americana*), european hedgehog (*Erinaceus europaeus*), arctic ground squirrel (*Spermophilus parryii*), fat-tailed lemur (*Cheirogaleus medius*).
b) Daily torpor: compared to hibernation lower seasonal specificity, but preferentially in the winter periods (Geiser, 2021). The T_b is usually reduced to 10 - 25 °C with a duration of less than or equal to one day, and the MR rate is usually reduced by 10 - 80% (Geiser, 2011). Furthermore, most species that exhibit daily torpor are small and nocturnal, with most weighing between 5 and 100 g (Geiser & Ruf, 1995). This type of torpor can be triggered by external factors such as food shortage or diurnal light cycle reduction. A common use is also adjusting energy expenses, even in times of ample food supply. Unlike hibernation preliminary generation of energy dense storage tissue is rare. Instead daily torpor is primarily entered when the body mass is already decreased (Heldmaier & Steinlechner, 1981). Examples: the mullet (*Dasycercus cristicauda*), honey possum (*Tarsipes rostratus*), white-toothed shrew

(*Crocidura suaveolens*), striped skunk (*Mephitus mephitus*), Djungarian hamster (*Phodopus sungorus*).

c) Estivation: also known as hot T_a or summer torpor, without apparent functional differences from other torpor classes (Geiser, 2010). Quantitative information on this type of torpor is limited but a new set of data is available suggesting that torpor use at moderate temperatures is not uncommon (Geiser, 2021). Some species start their estivation cycles in the ceasing summer period, often during the annual temperature peak, and can maintain their hibernating state until spring (Stawski & Geiser, 2010). The T_b is below 30 °C and lasts for days or weeks. Examples: the summer-acclimatised African dormice (*Graphiurus murinus*), marmots (*Marmota monax*), juvenile flying bats (*Eptesicusfuscus*), the South American drylands vesper mouse (*Calomys musculinus*) and juvenile insectivorous shrews (*Crocidura russula*).

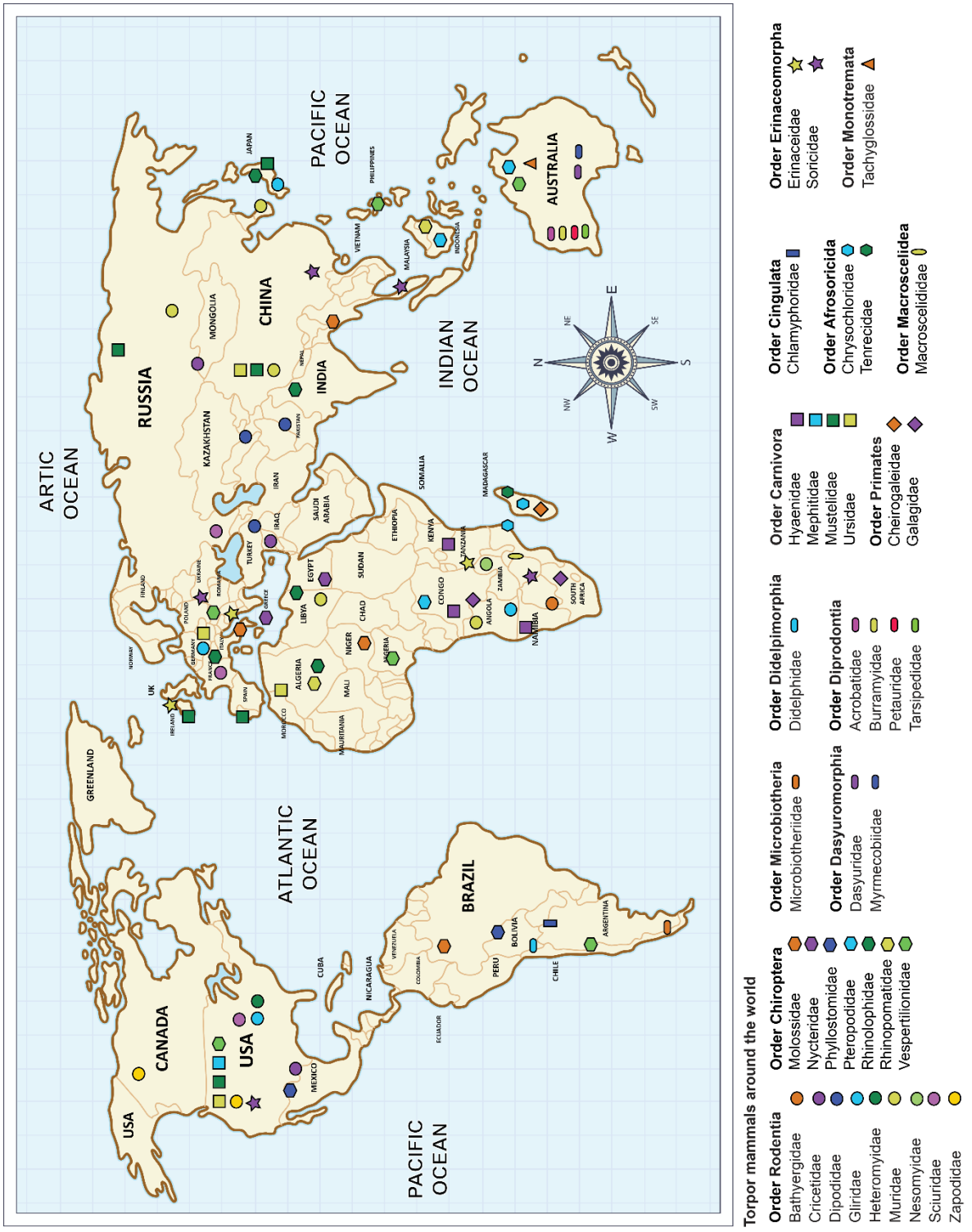

Figure 2. Torpor mammals around the world. A world map pointing out the distribution of the 13 mammalian orders to date described that are able to exhibit torpor according to Ruf & Geiser, 2015.

1.2.2 Metabolic implications of torpor

Mammalians undergo physiological changes during torpor that regulate metabolism. These are briefly described in main topics, which are energy and cell metabolism reduction, tissue and systemic responses, and cellular protection (Figure 3).

1.2.2.1 Energy and cell metabolism reduction

Torpor leads to a drop in T_b as a result of a decreased MR. Energy consumption in the organism can be reduced by up to 98% (Heldmaier et al., 2004). Due to the drastic reduction of all metabolic functions, mitochondrial respiration stops, heart-, ventilation rate and oxygen consumption are reduced. In addition, it causes a general decrease in gene expression, inhibition of protein synthesis and cell cycle arrest (Cerri et al., 2016). As crucial reorganisation of central metabolic pathways, a switch from glycolysis to lipolysis (β-oxidation), as well as the associated reduction in tissue glycolysis in torpid animals is well documented (Diedrich et al., 2023) and is triggered immediately during torpor entry (Choukèr, 2020). Glycolytic enzymes are marked for degradation via post-translational modifications and succinate dehydrogenase (SDH) is in part inhibited by high levels of oxaloacetate during torpor (Armstrong & Staples, 2010), selectively reducing the electron flux through some components of the electron transport chain, while retaining others. However, while torpor specific post-translational modifications of the electron transport chain such as phosphorylation or acetylation have been proposed as source of the observed metabolic changes, the exact mechanisms remain unclear (Staples, 2014). Moreover, the release of growth hormones, specifically insulin-like growth factor 1 (IGF-1) (Scherbarth et al., 2015; Mahlert et al., 2018; Cubuk et al., 2016), was also shown to be inhibited during torpor in some species, causing a reduction in blood glucose levels and reduced activity of different MAP-kinases (Choukèr, 2020).

1.2.2.2 Tissue and systemic responses

Species undergoing torpor spend a certain amount of time in prostration, depending on the type of torpor. It has been noted that neither muscular atrophy nor decreased bone mass occurs, although there is no mobility, digestion or absorption of nutrients during this

period. It is also known that in black bears (*Ursus americanus*), bone strength which was measured during two months of hibernation lost no more than 29% and in some muscle measures such as in soleus, the strength was not altered at all in hibernation (Harlow et al., 2001). Given that pregnant female bears give birth and suckle during hibernation, hind limb muscles have been observed only to decrease by a maximum of 4-10% (Shimozuru et al., 2013).

In both large and small torpor exhibiting mammals the absolute muscle tissue mass is largely unaffected due to active increase of striated muscle associated protein stability (Bertile et al., 2021). To compensate for the decreased rate of protein degradation, protein synthesis in those skeletal muscle cells is reduced accordingly (Jansen et al., 2019). While most innate and adaptive immune system components are suppressed in small hibernating mammals (Bouma et al., 2010, 2011) as well as the bear species *Ursus arctos* (Sahdo et al., 2013), overall immune capabilities might be retained in some other Ursidae (Chow et al., 2013). This divergent regulation even within the same genus underlines the importance of further research needed to reach a definitive conclusion, as bears enter an anuric state during hibernation, minimising urine production, where renal fluid decreases significantly during the transition from the active summer state to hibernation (Stenvinkel et al., 2013; Bertile et al., 2021).

1.2.2.3 Cell guard

In terms of cellular protection, blood flow is severely limited during torpor, but fully restored upon arousal thermogenesis, which conforms to an ischemia-reperfusion cycle (Ma et al., 2005). Rapid reperfusion causes a sudden increase in blood oxygen concentrations and subsequently mitochondrial activity. This abrupt increase in respiration is well established to induce radical oxygen species (ROS) production by insufficient oxygenic reduction in the mitochondrial electron transport chain (Choukèr, 2020). Small or moderate levels of ROS act as important second messengers during cell growth and differentiation (Sauer et al., 2001), however elevated levels are a major source of protein, lipid and DNA damage, so called oxidative stress (Schieber & Chandel, 2014). To counteract potential oxidative injury during early torpor and interbout arousal, important parts of the anti-

oxidative defence system are up-regulated, an example being superoxide dismutase 1 or glutathionine peroxidase 1 (Wei et al., 2018). Furthermore, during late torpor the Kelch-like ECH-Associated Protein 1-Nuclear Factor Erythroid 2-Related Factor 2 (Nrf2/Keap1) pathway is activated presumably in the act of protective measure against oxidative stress (Tessier et al., 2021). Additionally, dopamine and subsequently activated H_2S producing enzymes are suggested to be of relevance for preserving tissue integrity upon arousal (Dugbartey et al., 2015).

The state of torpor further increases resistance to ionising irradiation due to anti-oxidative countermeasures against radiation-induced ROS as well as potential hypothermia-induced alterations of DNA repair mechanisms (Puspitasari et al., 2021, 2022). This effect is not only observed in natural hibernators, but also in induced hibernation making it a promising tool in medical application and exploration of areas with elevated radiation levels such as space.

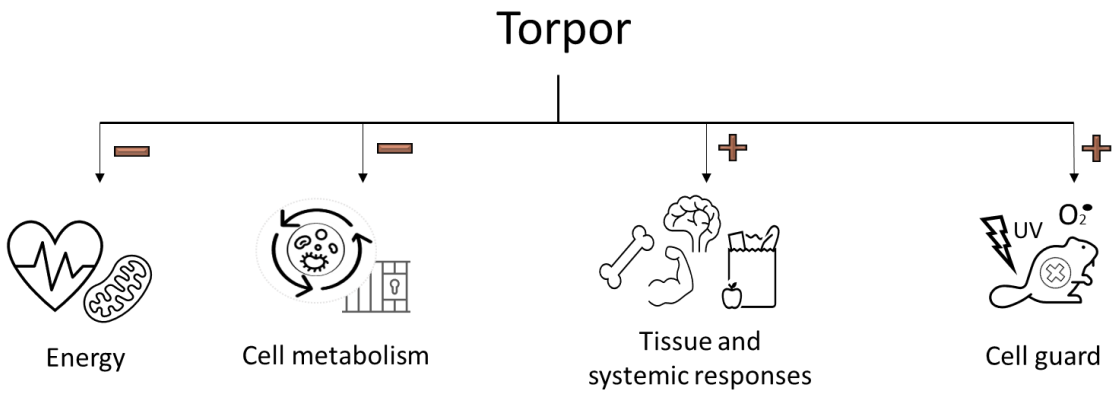

Figure 3. Illustration of the physiological regulations that take place during torpor. (1) Reduced energy, which is affected by reduced metabolic-, heart and breathing rate; (2) Reduced cellular metabolism, including inhibited/arrested gene expression, protein synthesis and cell cycle; (3) Tissue and systemic responses, preservation of muscle and bone mass, despite no digestion and absorption of nutrients. However, immune system is shut down; (4) Cell guard, during torpor there is radiation resistance and reduced oxygen radical damage. The symbols: "-" indicates reduction or inhibition; "+" indicates preservation or protection.

As described, the physiology during torpor differs strongly among different species. To investigate those mechanisms, especially those related to daily torpor, the Djungarian hamster was used as the model animal in this presented thesis.

1.3 The animal model Djungarian hamster (*Phodopus sungorus*)

Around 1968, Dr Figala, a Czech scientist, brought to Andechs two breeding pairs of *P. sungorus* for scientific work. Together with his colleagues Dr Hoffmann and Dr Goldau, observations on seasonal changes, body weight and fur were made. Already in 1980 there were many laboratories all over the world working with *P. sungorus* from Dr Hoffmann's breeding stock analysing the occurrence of torpor. Hoffmann recognised this hamster species as an animal model for pineal research. Additionally, since that time it has been used for a variety of studies concerning seasonal adaptation, reproduction, photoperiodic time measurement daily torpor and circadian characteristics (Steinlechner, 1998; Scherbarth & Steinlechner, 2010; Cubuk et al., 2017).

The Djungarian hamster originates from the Russian border region of north-eastern Kazakhstan, with different physiological and morphological parameters during summer and winter. This species is used as a model organism for mammalian torpor research because of its small size (67 - 103 mm) and thus easy housing conditions, but also because its seasonal adaptations (body mass in summer: 35 - 45 g; in winter 25 - 30 g) can be easily triggered in a laboratory context by adjusting the light-dark cycle without the need for cold exposure or food restrictions (Steinlechner & Heldmaier, 1982).

Figure 4. *P. sungorus* has different fur colours. This picture shows the usual dark brown fur, summer phenotype (right), and a white fur with the typical dark band on the back, winter phenotype (left) (Palchykova et al.2003)

This animal survives the harsh winter through a series of seasonal adaptations and daily torpor.

It can reversibly acclimatise to long and short photoperiods (Cubuk et al., 2017).

When the hamsters are adapted to winter, there is a regression of the reproductive organs, reproduction stops, food intake ceases, and the body mass is significantly reduced (Heldmaier & Steinlechner, 1981).

The morphological characteristics are very clear. The summer hamster, a robust, reproductive hamster with brown fur as opposed to the winter hamster, a slender hamster with white fur with greater thermal insulation (Figure 4) (Palchykova et al., 2003). Two phases can be denoted. The scotophase, where *P.sungorus* shows nocturnal behaviour, and the photophase, where spontaneous torpor manifests itself during the daylight hours. These torpor episodes are called spontaneous daily torpor, meaning they manifest irregularly during the daylight hours, not on a predictable daily basis (Haugg et al., 2021). During torpor, the Djungarian hamster is lying with eyes closed and a clear reduction in T_b (< 32 °C) and heart rate. Normometabolic values are reached on arousal from torpor by chemical thermogenesis without shivering. The onset of light is considered to be an important external *zeitgeber*, since torpor occurs under rigorous circadian control, with the beginning and end of torpor coincide with the onset and end of light (Haugg et al., 2021; Kirsch et al., 1991).

To properly synchronise the seasonal changes the Djungarian hamster transmits the photoperiodic signal via the pineal gland, through its hormone melatonin (Hoffmann, 1973; Larkin et al., 2003; Cubuk et al., 2016). This is controlled via the suprachiasmatic nucleus (SCN) which is consecutively regulated by the circadian clock (Bryan-Brown, 1988). This parameter is of vital importance for a reliable measurement of the photoperiod. Previous studies have further shown that torpid *P. sungorus* reduce their MR by 44% compared to normothermic resting individuals while their T_b during this on average six hours long period has a minimum around 13 °C (Heldmaier & Steinlechner, 1981; Steinlechner & Heldmaier, 1982).

1.4 Transcriptomic approaches in the field of torpor: organ sequencing

The fundamental canon of molecular biology defines the flow of information encoded as desoxyribonucleic acid (DNA) contained in the cell nucleus to the observable functions of cells and multicellular organisms, the so-called phenotype (Crick, 1970). In this process, proteins of the RNA polymerase family transcribe genes into messenger ribonucleic acid (mRNA), a short-lived information carrier (Crick, 1970). Ribosomes then transform the mRNA into proteins, functional polymers of amino acids. However, although all cells in an organism share the same genetic information, not all genes are constitutively expressed. Instead, gene expression is mediated by transcription factors and alterations in chromatin state, allowing for cell-type-specific transcriptional profiles depending on external stimuli and genetic fate (Botchkareva, 2017). Transcriptomics describe the set of molecular biology methods that allow the correlation of specific sample conditions and respective transcriptional changes at the cellular level (Shanker et al., 2015). The nowadays most commonly used method, RNA sequencing (RNA-seq), utilises recent advances in massively parallel sequencing to quantify gene expression by sequencing millions of RNA fragments. This allows to obtain frequency as well as the underlying sequences of RNA molecules captured as temporal snapshot of an isolated cell type, whole organ or specific tissue (Shanker et al., 2015).

Existing transcriptomic studies to understand gene expression differences between non-torpor and torpor states have mainly been focused on different species of squirrels and other rodents, bats, primates, and bears. Comparing these mammalian orders, the rodents are significantly over-represented because of their size and because torpor can be set off by exogenous factors such as limited food supply or reduced light. For instance, for the golden-mantled ground squirrel (*Callospermophilus lateralis*) a database of different sequenced organs and a proper annotation of the transcriptome are already publicly available. Many transcriptome studies compare different tissue types, including spleen, liver, heart, muscles, kidney, brain and brown as well as white adipose tissue, which are assumed to be highly involved in metabolic reduction (Hampton et al., 2011; Cooper et al., 2012; Grabek et al., 2015; Hampton et al., 2013; Schwartz et al., 2013; Cubuk et al., 2017). The part of the brain showing the most interesting differential expression during torpor is

the hypothalamus, which plays a role in thermoregulation, control of energy expenditure and circadian rhythm. The liver, which is the metabolic centre of the body and processes and detoxifies macromolecules to provide essential fuels for the brain, muscles and other organs throughout the body, is another promising target for torpor focused research. However, the exact transcriptional alterations, which lead to survival at a reduced MR and span the whole organism instead of singular organs, have not yet been fully uncovered.

1.5 Blood as a potential mirror of torpor related systemic changes

Blood is the largest liquid organ of the body, generally amounting for 3 - 8% of the body volume (Rasmussen & Rasmussen, 1917). It harbours a variety of different cell types, including thrombocytes (platelets), erythrocytes (red blood cells), and leukocytes (white blood cells) in a protein matrix (plasma), as well as fat, sugar, salt and water (Behrends et al., 2021a), which flows through blood vessels and comprises an extensive transport system interconnecting the entire body. This circulating system enables the exchange of energy, gas, and essential nutrients (Brandes et al., 2019) and gas, playing a unique vital role in signalling, thermoregulation and homeostasis, and has various protective functions, such as coagulation and enabling rapid immune responses (Behrends et al., 2021b).

Conventional blood analysis has long been used to perform moderately invasive disease diagnosis, yet whole blood transcriptomics were shown to enable the detection of diseases which are not normally detectable or are even fully localized in other tissues (lupus nephritis (Nagafuchi et al., 2022), rheumatic diseases (Ha et al., 2022), some rare diseases (Frésard et al., 2019), and others. Instead of measuring metabolites, immunoglobulins or surface proteins, the detection is performed indirectly by monitoring transcriptomic changes instead that relate to signal transduction or triggered immune responses according to an altered body condition (Chow et al., 2013). Blood can also reflect local and systemic metabolic changes, such as those caused by torpor. This makes the whole blood a rich source where different transcriptional states can be visible to explore the regulation of gene expression in physiological, pathological and even inaccessible tissues.

1.6 The relevance of torpor research for humans

As aforementioned, a variety of mammalian species spread all over mammalian phylogeny are capable of performing torpor, which may suggest an underlying genetic programme for MR reduction being present in the genome of most mammals. So far, neither individual molecules nor endocrine properties have been described that include or exclude humans from the torpor programme. Evidence exists that also humans are able to lower their MR on demand. During deep sleep, for instance, the MR is reduced by 15% and T_b drops – when compared to morning values - by about 1 °C (Sharma & Kavuru, 2010) and during deep meditation the MR can even be reduced around 64% (Benson et al., 1990). Another example is the adaptation to reduced MR found in Australian natives who can sleep unsheltered at low temperatures during the night (Scholander et al., 1958). Similarly, evidence has been found, dating about half a million years, that during an extreme glaciation at Atapuerca, hominids hibernated (Bartsiokas & Arsuaga, 2018).

Other developmental stages which indicate a general ability for human torpor are foetal stages and the first hours and days of life *ex utero*. Kleiber's rule is based on the increase in mass-specific basal MR with decreasing body mass where it is assumed that smaller and therefore lighter mammals have a higher specific energy expenditure than larger mammals. Human foetuses, in contrast, have *in utero* a low MR, with a specific rate of turnover that is well below the level which would be expected in adult mammals of comparable body size, thus disconnecting the metabolic allometry described by Kleiber and hence foetuses behave like “an organ of the mother” (Singer & Mühlfeld, 2007). This is considered as an adaptation to the low oxygen availability *in utero,* which also prepares to risks during birth such as temporary oxygen deprivation while transitioning to pulmonary respiration and period of circulation after birth. A similar observation can be made during torpor, where the MR drops significantly like for instance in a hibernating hazel mouse, of which the mass-specific MR during torpor is approximately equal to that of a blue whale (Singer, 2006; Singer & Mühlfeld, 2007).

Another analogy between neonates and torpid animals is the sudden activation of the oxygen supply-dependent chemical thermogenesis without shivering via brown adipose

tissue that can be observed after birth and during torpor arousal (Singer, 2004). With insufficient oxygen supply, newborns are hypothermia vulnerable, as chemical thermogenesis is suppressed. This process shows striking similarities to the tolerated drop in T_b upon entering into torpor, as well as the rewarming upon arousal from torpor due to the sudden activation of non-shivering thermogenesis in brown adipose tissue (Singer, 2004, 2006).

1.6.1 Adaptations during torpor and during human overwintering in the Antarctic Concordia station

The continent Antarctica is the harshest place on Earth, seasonally with lows of -89.2 °C, and it contains 90% of the ice on the planet (Hodgson et al., 2004). Not surprisingly, in addition to having a windy, cold, and dry climate, it is the only continent without an indigenous human population. Due to its geographical disconnection from the other continents, it has been gone unnoticed by humans for 35 million years. Its minimal flora and fauna as well as its completely undeveloped land is inadequate to provide the basic resources required for survival of larger human populations. In concession to its unique environment, Antarctica was internationally acknowledged as a nature reserve for peaceful collaborative purposes, where all human activities in the area are focused not only on year-round scientific research, but also on extremely reduced forms of tourism and sustainable fishing (De Boer et al., 2014; Khandelwal et al., 2015).

For the latter purpose there are 82 operating scientific bases that form the only permanent human habitats with a continuous flux of residents (Gröndahl et al., 2009). A typical period of residence spans between 3 to 15 months depending on the specific study conducted. Human research in the last decades was mainly devoted to the analysis of the complex seasonal variations observed in the Antarctic environment and how human physiology responds to these adverse conditions. The Antarctic summer and winter are characterized by many months of full light and darkness respectively. This significantly absent night/daylight variations disrupt the circadian rhythm and thus general mood, sleep, and executive functions (Sandal et al., 2018; Buchheim et al., 2020).

Especially during the winter period, individuals face challenging situations of stress, extreme weather and isolation. This not only leads to different psychological irregularities such as feelings of anguish, anxiety and sleep problems but also results in metabolic changes, which in turn manifest via cortisol or adrenaline mediated heartbeat acceleration and hypertension (Sandal et al., 2018).

These changes also cause everyone to go through a multifactorial stress process; selection of proper coping strategies and possible stressor evaluation encourage favourable activation levels by either focusing on the problem, by decreasing emotional reactivity, or by negating stress sources (Fletcher & Sarkar, 2013).

Expeditioners may respond differently, thus showing parallels with animals that are capable of exhibiting torpor. As mentioned before, in torpor the MR is reduced to basal levels and there are numerous adaptations to low temperatures, energy demand, lack of nutrients and general stress. To date, metabolic changes in humans overwintering in Antarctica have not been compared to metabolic adaptations in hibernating animals or animals capable of daily torpor despite environmental and physiological similarities.

2 Aim of the work

This work aims to investigate whether different mammalian species exhibit similar or comparable changes in gene expression regulation, which would support the idea of a common genetic "torpor-programme" anchored in the mammalian genome. For this endeavour the transcriptomic profile was measured in blood of *P. sungorus* in different phases of daily torpor.

In the first part, transcriptional dynamics between the different phases of torpor entry (ZT01), torpor nadir (ZT04), arousal (ZT07) and the post-torpor phase (ZT16) were assessed.

Afterwards, in the second part, relevantly regulated genes from mid torpor were subjected to an extensive comparative literature research to verify comparable transcription patterns in blood of torpid *P. sungorus* and other mammals in deep torpor/hibernation. These analyses were performed independently of the investigated organ or tissue.

Lastly, in the third part, transcription patterns in the different phases of daily torpor in *P. sungorus* were compared to transcriptomic profiles from blood of human overwintering in the Antarctic Concordia station (during different timepoints of mission) to get for the first-time insights into putative similarities in gene expression regulation which might be associated with reduction in MR.

Since there was no annotated genome for *P. sungorus*, a *de novo* assembly was performed. After differential gene expression analysis, data was imported in the bioinformatic analysis tool *Ingenuity pathway analysis* (IPA) (QIAGEN Inc., https://digitalinsights.qiagen.com/IPA) to distinguish and determine signalling pathway candidates involved in torpor and to detect protective as well as detrimental consequences of the respective regulation pattern (QIAGEN, Inc., https://targetexplorer.ingenuity.com/).

3 Material and Methods

3.1 Equipment and reagents

3.1.1 RNA Isolation Kits

Table 2. List of kits used and their manufacturers

Kit	**Manufacturer**
NucleoSpin® RNA Blood Midi	**MACHEREY-NAGEL**
Lysis Buffer DL	
Wash Buffer RB2	
Wash Buffer RB3 (Concentrate)	
Membrane Desalting Buffer MDB	
Reaction Buffer for rDNase	
rDNase, RNase-free (lyophilized)	
Liquid Proteinase K	
RNse-free H2O	
NucleoSpin® RNA Blood Midi Columns (plus Collection Tubes)	
20 Collection Tubes for lysis, elution, and washing steps	
NucleoSpin® RNA Clean-up	**MACHEREY-NAGEL**
Lysis Buffer RA1	
Wash Buffer RA2	
Wash Buffer RA3 (Concentrate)	
RNase-free H2O	
NucleoSpin® RNA Clean-up Columns (light blue rings – plus Collection Tubes)	
Collection Tubes (2 mL)	
Collection Tubes (1.5 mL)	

Qubit™ RNA IQ Assay Kit	**Thermo Fisher Scientific**
Qubit™ RNA IQ Reagent (Component A)	
Qubit™ RNA IQ Buffer (Component B)	
Qubit™ RNA IQ Standard #1 (Component C)	
Qubit™ RNA IQ Standard #2 (Component D)	
Qubit™ RNA IQ Standard #3 (Component E)	

3.1.2 Reagents

Table 3. List of reagents used that are not included in the reaction kit

Reagents	**Manufacturers**
96–100 % ethanol (to prepare Wash Buffer RA3 and to adjust RNA binding conditions)	Merck

3.1.3 Equipment

Table 4. List of equipment used for the RNA Isolation

Equipment	**Manufacturer**
Eppendorf 5430/ 5430 R centrifuge	Eppendorf
ThermoMixer® C Cooling/Heating block	Eppendorf
Rotary mixer RS-TR 5/10	Phoenix
Nanodrop One, NanoDrop™ One/OneC Microvolumen-UV/VIS-Spectralphotometer with WLAN	Thermo Fisher Scientific
Qubit 4 Fluorometer	Thermo Fisher Scientific

3.1.4 Consumables

Table 5. List of consumables

Consumable	Manufacturer
1.5 mL microcentrifuge tubes	Sarstedt
1.5 mL sterile RNase-free tips	Sarstedt
Qubit sterile RNase-free tips	Thermo Fischer Scientific

3.2 Experimental animals

3.2.1 Breeding and housing

In accordance with the local ethics committee (z.231-1, RP Tübingen), *P. sungorus* (n=36, 18 males, 18 females) were bred and raised by Professor Dr Herwig's Research Lab in December 2018 and in January 2019 in the indoor breeding colony of the Institute of Neurobiology (Ulm University, Germany) using an outbred crossing scheme. A constant environment with an ambient temperature of 20 ± 1 °C and artificial light at 200-250 lux was provided. Summer-like long photoperiods were simulated by illumination of 16 hours per day and winter-like short photoperiods (SP) by illumination of 8 hours per day.

Animals were acclimatised to SPs at an age of 16 ± 3 weeks. To allow sampling during dark phases a permanent red-light LED (<5 lux) was used. Food and tap water (Altromin hamster breeding diet 7014, Lage, Germany) were provided *ad libitum*. Once a week the diet was enriched with sunflower seeds, oat flakes, and cucumber. Makrolon Type III cages (820 cm^2) including nesting material and wooden bedding were used for single housing adult hamsters (Cuyutupa et al., 2023).

3.2.2 Radiotelemetry

Body temperature, date and time were used to determine the correct sampling time point. T_b and locomotor activity were measured using a radiofrequency transmitter (Data Sciences International (DSI), Harvard Bioscience Inc., St. Paul, MN, United States) that was

implanted at an age of 30 ± 3 weeks intraperitoneally under isoflurane anaesthesia (2.5% and 1 ml/min for induction, 0.75–2.0% and 0.4 ml/min for maintenance) and carprofen analgesia (5 mg/kg, i.p.; Rimadyl, Zoetis Deutschland GmbH, Berlin, Germany). To promote fast recovery from surgery animals were nourished with additional cucumber, sunflower seeds and oat flakes. Additional nesting material was also provided. Behaviour, posture, coat care and body mass were used as scoring parameters over a period of around a week. The Regional Council of Tuebingen, Germany (1411) approved the surgical and experimental procedures (Cuyutupa et al., 2023).

3.2.3 Sampling scheme

A spontaneous daily torpor episode has four phases with the following characteristics (Figure 5):

① torpor entry, also *zeitgeber time* 1 (ZT01), T_b: around 30 °C,
② mid-torpor or torpor nadir, also *zeitgeber time* 4 (ZT04), T_b: around 22 °C,
③ arousal, also *zeitgeber time* 7 (ZT07), T_b: around 30 °C, and
④ post-torpor state, also *zeitgeber time* 16 (ZT16), T_b: around 35 °C.

Spontaneous daily torpor, which was detected in the form of a drop of T_b < 32 °C for >= 30 minutes, was observed in all 36 SP acclimatised animals. Over different sampling times, 18 hamsters were hypothermic (HT) and expressed torpor, while 18 other non-torpor expressing animals served as normothermic controls (NT). During torpor entry (ZT01) samples were obtained from 6 NT and 5 HT animals; during torpor nadir/mid torpor (ZT04) samples from 4 NT and 5 HT animals; during torpor arousal (ZT07) samples from 4 NT and 4 HT animals, and post-torpor (ZT16) from 4 NT and 4 HT animals. Animals were sacrificed for analysis at an age of 32 ± 4 weeks inside their home cages by carbon dioxide inhalation (Cuyutupa et al., 2023).

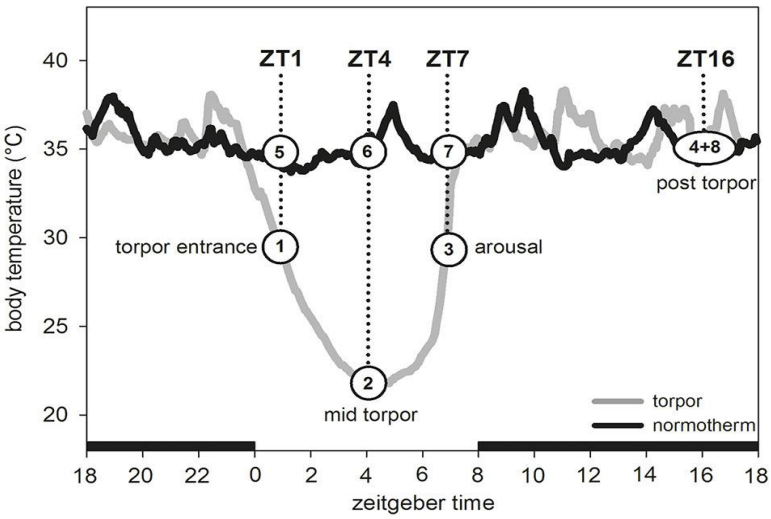

Figure 5. Illustration of the different sampling points of hamsters subjected to short day light (SD). Blood samples were taken at different zeitgeber times: torpor entry (ZT01), during torpor nadir/mid torpor (ZT04), arousal (ZT07), and post-torpor (ZT16). The grey line indicates torpor individuals, the black line indicates normothermic individuals (Cubuk et al., 2017).

3.2.4 Blood samples and processing

After the hamsters were sacrificed, a puncture was made in the right ventricle of the heart and 500 µl of whole blood were sampled. For the blood analysis, samples were taken during the previously defined torpor periods and the respective controls. Samples were deposited in microvettes containing EDTA and immediately placed on ice. These were then centrifuged for a period of 10 minutes at 2,000 rpm at a temperature of 4 °C to separate plasma from blood pellet. The two different specimen were then stored separately and kept at -80 °C until the RNA extraction (Cuyutupa et al., 2023).

3.3 RNA isolation, quality control and Next Generation Sequencing

3.3.1 Column chromatography

This method is based on the different adsorption rates of substances in a solution (mobile phase) on a solid substrate (stationary phase). It is used to perform the purification of mixed substances of different polarity at different scales. In the context of this work, only columns that bind the target RNA together with a silicon matrix were used. The principle of this method lies in the high affinity of negatively charged nucleic acids for positively charged silicon particles.

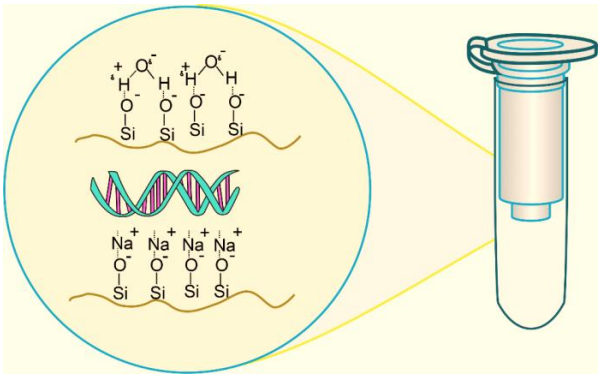

Figure 6. Column chromatography. Image based on Squidonius, 2008

Sodium ions serve here as a cation bond by attracting the negatively charged structures of the nucleic acids and, under high salt concentrations, by breaking the hydrogen bonds between the hydrogen contained in the water and the negatively charged oxygen ions contained in the silicon matrix (Squidonius, 2008), Figure 6. Once tightly bound nucleic acids can be purified by intense washing steps and then eluted with distilled water or Tris-EDTA.

3.3.2 RNA isolation from hamster blood

Frozen blood pellets (400 µl) were first resuspended in 400 µl of DL solution to enhance cell disruption and to achieve additional inhibition of RNAases. These were placed in the roller mixer for approximately 8 minutes until they were thawed. After this, the samples were split into two different tubes in equal amounts of 200 µl, as the blood was very heavy and occasionally clots were formed in the columns, thus avoiding clogging and making the assay run smoothly. Then, 5 µl of proteinase K were added to each tube and set at 20 °C for 15 minutes in a Thermoshaker. After this step, 200 µl of ethanol were augmented and after a brief vortexing, the entire sample mix was transferred to a NucleoSpin® RNA Blood Column and the samples were centrifuged for 30 seconds at 11,000 x g, the supernatant was

discarded, and the column was placed in a new collection tube. After adding 350 µl MDB (Membrane Desalting Buffer) onto the column, the samples were centrifuged for 30 seconds at 11,000 x g and the flow-through was eliminated. Following, a digest was performed with 95 µl rDNase. Subsequently an additional incubation step of 15 minutes at room temperature, two washes were performed with different solutions discarding the supernatant and the column was placed in a new collection tube, first with 200 µl Buffer RB2, then with 600 µl Buffer RB3 and centrifuged as before. The last and third wash was performed with 250 µl Buffer RB3 where the samples were centrifuged for 2 minutes at 11,000 x g. The ethanol was removed from the column. Thereafter, the columns were placed in a nuclease-free collection tubes. The supernatant from the previous step were discarded. The respective column was then relocated into a new reaction tube with 60 µl of RNase-free water and centrifugation just as the beginning. A total of 60 µl of RNA per sample was obtained.

3.3.3 RNA Clean-up

Once the RNA (60 µl) was isolated, the collection tube was filled up to 100 µl with H_2O. The samples were resuspended in 600 µl of Buffer RA1-ethanol-premix (300 µl RA1 with 300 µl ethanol, which makes a mixture of six times the volume of the RNA sample). This mixture was mixed very well by vortexing. Then 700 µl or all of the mixture was placed in a NucleoSpin® RNA Clean-up Column, centrifuged for 30 seconds at 8,000 x g, the flow-through was discarded. Then a first wash was performed with 700 µl Buffer RA3, centrifuged as before and the flowthrough was discarded. This was followed by an additional washing step with 350 µl Buffer RA3, centrifugation for 2 minutes at 8000 x g and discarding the supernatant. The NucleoSpin® RNA Clean-up column was then relocated in a nuclease-free collection tube. The cap of the column was left open, and the membrane was dried for three minutes. Afterwards, for RNA elution, the respective column was relocated to a new collection tube and the RNA was flushed by including 60 µl of RNase-free water and centrifugation for 1 minute at 8,000g. This final step yielded 60 µl of purified RNA.

3.3.4 RNA Integrity

Once purified RNA was obtained, the RNA concentrations were quantified using a NanoDrop fluorometer (Thermofisher Scientific, Waltham, MA, USA) and RNA integrity (RIN) was assessed using a Qubit with the RNA IQ Assay (Thermofisher Scientific, Waltham, MA, USA). Measurement of the RNA integrity of blood RNA was done with the Qubit™ RNA IQ Assay kit, which detects RNA degradation using the Qubit™ 4 Fluorometer. It uses two unique stains; one that binds to highly structured RNA, and the other that selectively binds to smaller, degraded RNA fragments. In this way, the quality of an RNA sample can be assessed using its integrity as a metric. RNA IQ is a numerical value indicating the integrity and quality of the RNA sample ranging from 1 to 10, with 10 being an excellent result. Additionally, 190 µl of Qubit™ working solution and 10 µl of each standard solution, which is used for calibration for the selected assay, were prepared separately. Different measuring tubes were also prepared for the samples with Qubit™ working solution and the sample to be analysed, according to the concentration ranges recommended by the kit, which vary between 180 and 199 µl. The final volume of all three standard and sample tubes was 200 µl. Dilutions were mixed by vortexing for 2-3 minutes, avoiding the formation of bubbles. The tubes were incubated at room temperature for two minutes. Then samples and according standards were measured.

Cellular RNA was then classified into different RIN (RNA integrity number) categories, ranging from values 10 to 1 with increasing degradation. These are determined by automated assignment of signal intensities of ribosomal RNAs (28S and 18S rRNAs). Progressive degradation of the RNA is accompanied by a decrease in rRNA signals and an increase in smaller RNA fragments (Schroeder et al., 2006). In the present experiments, the cellular RNA samples showed a purity of 2.08 and 2.11 and a RIN of 8.85 ± 0.76 (Mean ± STDEV) (Table 6), which passed internal quality control (Cuyutupa et al., 2023).

Table 6. Information about the hamsters (*P. sungorus*) analysed in this work. All hamsters (n=36) were capable of torpor and SD adapted. Additionally, RNA concentrations and RINs are included. Abbreviations ID: identification number; gender: m: male, f: female; SD (short day): 8 hours with and 16 hours without light; ZT: Zeitgeber; HT: torpor at day of sampling; NT: no torpor at day of sampling; RIN: RNA integrity number.

General information				Timepoint		RNA concentration			RNA quality
ID	**Gender**	**Age in weeks**	**Body temp [°C]**	**ZT**	**HT / NT**	**ng/µl**	**A260/A280**	**A260/A230**	**RIN**
18Z3 5/8	f	28	30.87	1	HT	448	2.13	2.22	7.9
18Z3 3/5	f	30	30.09	1	HT	416.1	2.1	2.26	9.4
18N3 3/5	f	33	30.53	1	HT	453.2	2.11	2.21	9
18N1 1/1	m	39	26.41	1	HT	708.6	2.09	2.27	7.7
18N3 4/4	m	30	25.20	1	HT	528.4	2.03	1.84	9.2
18F1 4/3	m	29	35.16	1	NT	440	2.07	1.98	9.1
18N1 4/1	m	30	35.26	1	NT	326.8	2.09	2.31	7.9
18Z3 2/2	m	35	34.73	1	NT	193.1	2.08	2.23	9.8
18X1 2/4	m	40	34.66	1	NT	686.4	2.09	1.94	8.8
18N3 4/6	f	30	34.24	1	NT	321.5	2.09	1.98	8.6
18F1 4/7	f	28	35.14	1	NT	612.2	2.08	2.02	8.9
18N1 3/3	f	32	24.94	4	HT	522.2	2	2.03	9.2
18Z3 3/4	f	38	23.69	4	HT	348.1	2.09	2.05	10
18Z3 5/7	f	24	25.78	4	HT	323.3	2.1	2.15	9.2
18X3 2/2	m	28	23.34	4	HT	431.9	2.09	2.28	7.9
18N3 4/2	m	29	20.66	4	HT	331	2.11	2.29	7.8
18F1 4/4	m	30	35.58	4	NT	317.8	2.09	2.14	10
18N1 4/2	m	31	36.30	4	NT	329.2	2.09	2.19	7.7
18X1 2/5	m	39	35.69	4	NT	368.1	2.09	2.28	8.6
18F1 3/3	m	33	35.20	4	NT	417.1	2.12	2.28	8.1
18X3 2/7	f	28	31.24	7	HT	313.8	2.06	1.97	8.8
18N3 3/6	f	33	32.84	7	HT	340.5	2.11	2.23	10
18Z3 2/6	f	34	29.07	7	HT	446.6	2.11	2.28	8.7
18N1 2/1	m	36	27.79	7	HT	474	2.1	2.16	7.6
18F1 4/6	f	30	36.24	7	NT	325.5	2.04	1.85	9
18N3 4/7	f	31	34.29	7	NT	190.7	2.08	2.28	8.5
18F1 3/7	f	35	34.55	7	NT	421.8	2.13	1.99	7.7
18Z3 2/4	m	34	35.27	7	NT	439.8	2.1	2.16	10
18X3 2/6	f	29	36.14	16	HT	298.4	2	1.62	9.3
18Z3 3/6	f	31	36.91	16	HT	424.2	2.12	2.27	10
18N1 3/4	f	34	35.86	16	HT	207.7	1.87	1.23	9.3
18F1 3/6	f	34	35.01	16	HT	465.2	2.08	2.04	8.9
18F1 4/2	m	30	37.93	16	NT	518.3	2.08	2.26	8.8
18Z3 3/2	m	31	35.73	16	NT	320.8	2.09	2.29	9.1
18N3 3/2	m	34	35.31	16	NT	390.4	2.07	1.9	8.3
18X1 2/3	m	36	36.33	16	NT	601.2	2.1	2.27	10

3.3.5 Next Generation Sequencing

The transcriptome of *P. sungorus* was assessed by bulk RNA-Seq employing the high-throughput capabilities of the Illumina HiSeq platform. RNA was transformed into its more stable complementary DNA (cDNA) counterpart by using virus derived reverse transcriptase. During the subsequent amplification known sequencing adapters were ligated to the cDNA fragments. These adapters were then bound by complementary surface-coupled probes to fix each fragment. Subsequently the complementary strand was synthesised using fluorescent-dye-coupled nucleotides. After each polymerisation step the process was temporarily terminated and the fluorescent properties of the last bound nucleotide were measured to derive the sequence of the respective fragment (Wang et al., 2009).

The cDNA library preparation and RNA-Seq was performed by the commercial service Eurofins Genomics Europe Sequencing GmbH Konstanz, Germany). After quality control by fragment analyser, an accurate short insert cDNA library with an insert size of 2 x 150 bp was prepared with a minimum of 30 million reads per sample, analysed separately for sequencing on HiSeq 2500 employing the paired-end module (Cuyutupa et al., 2023).

3.4 Bioinformatics

3.4.1 Genome assembly of the Djungarian hamster

The raw sequencing reads were performed by bioinformatician Dr Yiming Cheng of the Gene Centre and Department of Biochemistry of the Ludwig-Maximilians-University Munich and assessed for quality using fastqc 0.11.9 (http://www.bioinformatics.babraham.ac.uk/projects/fastqc). Pre-processing of all reads was performed by clipping adapters at 3’ and primers at 5’ ends.

Removal of adapters and low-quality bases was performed with trimmomatic (version 0.39). Additionally, reads containing uncertain base readings were eliminated as were duplicates (those with identical sequences). The cleaned reads were further processed for sequencing error correction (Figure 7). Due to the absence of an annotated *P. sungorus*

genome, a de novo assembly of the transcriptome was created. Trinity (version 2.8.6) was used to merge individual FASTQ files into reference contigs. An annotation coverage of 99.3% was measured using BUSCO (version 5) utilizing the "-m transcriptome –auto-lineage-euk" parameters. Human ortholog discovery was performed by translating each contig into all potential reading frames and blasting the obtained hypothetical proteins against human references. A BLAST bitsorce of 50 has been used as cutoff for potential hits. The best hits were then used to map the human genes to the predicted transcripts. The analysed samples were aligned with custom-made PERL scripts to the created reference genome using histat2 and gene expression data was quantified (Cuyutupa et al., 2023).

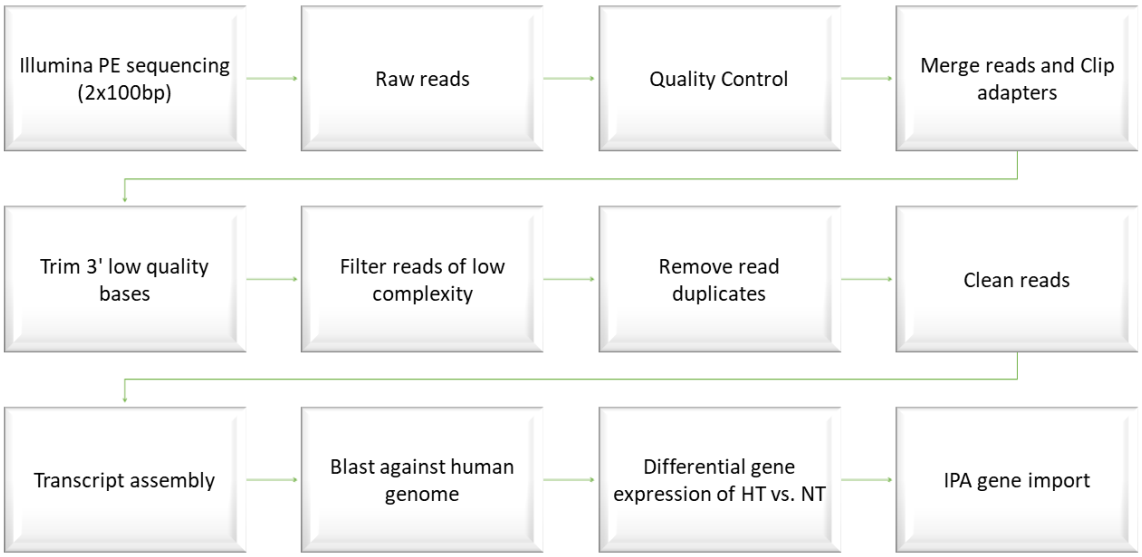

Figure 7. Flowchart depicting the bioinformatic pipeline for this work. Steps used to generate quality control and Djungarian hamster transcriptome assemblies.

3.4.2 Differential gene expression (DGE) analysis

Deseq 2 was used for the assessment of DGE of HT against NT for each ZT. To perform biological differential analysis, genes were imported into IPA (https://digitalinsights.qiagen.com/products-overview/discovery-insights-portfolio/analysis-and-visualization/qiagen-ipa/) using a fold change (FC) $\geq|1.25|$ and p-value ≤ 0.05 as cut-off. Furthermore, the IPA regulator effects tool was used to select target molecules that

represent relevant regulated genes from the *P. sungorus* transcriptome dataset. As well, this tool algorithm of IPA is widely used to formulate an initial hypothesis to explain the influence of specific transcriptional regulators and their respective inhibition or activation on the expression of the target molecule and further on down-stream metabolic processes and associated diseases. At least 1 iteration was used for this process. Merging of networks was performed if a statistically significant overlap (Fisher's exact test p-value of <0.05) was present. Additionally, potential phenotype defining mechanisms can be determined by estimating the biological impact of significantly regulated target molecules. Moreover, to analyse the longitudinal comparison of the four timepoints (ZT1-16), the tool "comparison analysis" was used, maintaining the established cut-off values and adding the significance value |z-score = 1.5|, this highlight that an equal value represents a real change and any value lower than this only a trend. Also, the networks and molecules involved in these pathways were available, which were chosen by a criterion of torpor-related themes (Cuyutupa et al., 2023).

3.5 Humans overwintering at the Antarctic Concordia station

These data were collected in an expeditionary study in 2017 and have been already published with data related to endocannabinoids, epinephrine values and some immune system changes (Strewe et al., 2018; Buchheim et al., 2020).

3.5.1 Sampling scheme

Samples were collected during the 2017 winter campaign at the Antarctic Concordia station from 8 male participants. The average age range of the study participants was 36 years, they were 1.75 m tall and 77 kg in weight and non-smokers. Blood sampling was done in 3 phases: before the deployment at the Concordia station; during the stay at the station in January, April, July; October and the post phase 5 to 6 months after the period of loneliness (Buchheim et al., 2020).

3.5.2 Blood sample processing and RNA isolation

Venous blood (2.5 ml) was collected under sterile criteria in PAXgene® RNA tubes (BD Biosciences, Germany) and reserved at -80 °C. The study was conducted in accordance

with the code of the World Medical Association (Declaration of Helsinki). The institutional review board of the Ludwig-Maximilians-Universität in Munich (LMU), Germany, and from the medical board of the European Space Agency (ESA) issued their ethical approval. RNA isolation was performed in the *Laboratory of Translational Research – Stress and Immunity* of the Hospital of the LMU employing the Paxgene Blood RNA Kit (PreAnalytiX GmBH, Germany). Sample purification was realized with RNeasy columns (Qiagen, Germany). Quality and RNA amounts were quantified with the nanoDrop fluorometer (Thermofisher Scientific, Germany). Paired-end 150bp next generation sequencing (NGS) RNA-seq was performed by Eurofins Genomics Europe Sequencing GmbH (Konstanz, Germany) on an Illumina HiSeq 2500 platform with at least 30 million reads per sample (Buchheim et al., 2020).

3.5.3 Analysis with IPA

After sequencing, the data from the Concordia crew blood samples were entered into the IPA software (QIAGEN Inc., https://digitalinsights.qiagen.com/IPA). The alignment procedure with the human genome was performed with OmicSoft Aligner OSA. Using DESeq2, comparisons were made for gene expression in comparison to the control point, which were samples taken in Europe 2-4 months prior to departure to Antarctica, termed baseline data collection (BDC). For gene expression the cut-off points used were: fold change (FC) = 2, q 0.01, false discovery rate (FDR); for post-isolation point (Post), the FC was 1.5. This database with the timepoints; January, April, July; October and Post; was used for comparisons with the *P. sungorus* blood transcriptome database (Buchheim et al., 2020).

3.6 Literature research based of transcriptomic changes during torpor in mammals

Online Public Access Catalogue (OPAC), an LMU meta-database, was used for research and collection of studies and analyses concerning transcriptome studies with focus on “torpor” and/or “hibernation” and “no torpor” and/or “no hibernation”. Those keywords were searched, and in a next step the duplicates in identified publications were discarded, resulting in 621 articles. Publications carried out in other species were also excluded, so that only 314 mammalian studies remained. Finally, 13 publications were chosen that

fulfilled the search criteria (see Figure 8), as the objective was to find matches regardless of order, species and organ. A gene expression comparison was performed, and exact matches were identified, discarding also studies with no matches, with no listed genes, i.e. only reviews, or with orthologous genes without being the identical exact same TM_{IPA} genes (Cuyutupa et al., 2023).

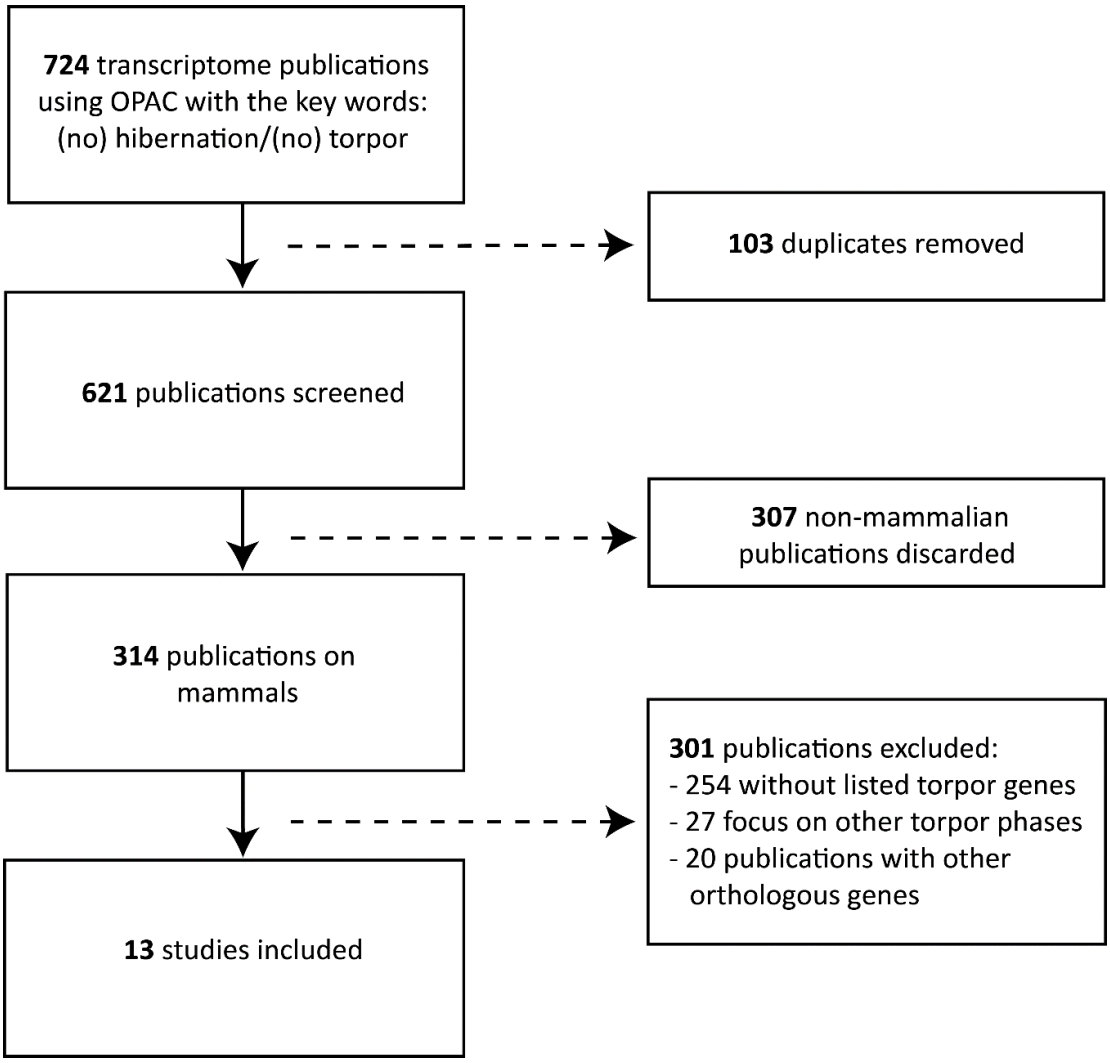

Figure 8. Descriptive flowchart of the literature analysis. From a large number of studies on transcriptomic analyses, those concerning mammals were selected. These were further filtered for reports offering a high level of detail in order to contrast the analysed genes with TM_{IPA} (Cuyutupa et al., 2023).

3.7 Data presentation

3.7.1 Gene clustering

As part of the bioinformatic analysis of the DGE associated with the four stages of torpor, the Qiagen IPA system data set (QIAGEN Inc., https://digitalinsights.qiagen.com/IPA) was used for the main analysis and then superimposed onto the Ingenuity Pathways Knowledge Base global molecular. Highly significant gene networks and canonical pathways were identified and categorised from the "IPA Pathway Knowledge Library" (https://geneglobe.qiagen.com/us/knowledge/pathways) (Krämer et al., 2014).

3.7.2 Graphic edition

Figures were created with the Adobe Illustrator (Adobe Inc., 2018) graphics editor. Heatmaps were produced with R version 4.1.0 (R Core Team, 2021) using the package pheatmap version 1.0.12 (Kolde, 2019).

4 Results

4.1 Part 1: Dynamics of the gene expression profiles and Canonical pathway analysis in the blood transcriptome of *P. sungorus* in different torpor phases

4.1.1 Overview of gene expression during the daily torpor cycle of *P. sungorus*

In order to perform a comprehensive investigation on changes of the molecular mechanisms underpinning the distinct points of daily torpor in Djungarian hamsters, gene transcription during torpor was compared within all analysed timepoints. For this purpose, blood transcriptome samples from 18 torpid animals and 18 non-torpid control animals were analysed in short photoperiods. Differential gene expression analysis between NT and HT within the four distinct *zeitgeber* time points revealed numbers of regulated genes as follows: at the entry of torpor (ZT01): 12,476 genes; at torpor nadir (ZT04): 11,422 genes, during arousal (ZT07): 11,211 genes and post-torpor (ZT16): 2,315 genes. After setting cut-offs/level of fold change (FC) $\geq|1.25|$ and significance with p-value ≤ 0.05, the number of the remaining regulated genes was as follows: ZT01 = 559; ZT04 = 1763; ZT07 = 2832; ZT16 = 306. Differentially expressed genes were classified according to the Ingenuity pathway knowledge base significance level |z-score = 1.5|. Canonical pathways indicating the value |1.5| upwards indicate a real change and any lower value only a trend.

The canonical pathway dynamics show variations between the phases entry (ZT01), torpor nadir (ZT04), arousal (ZT07) and post-torpor (ZT16). A total of 484 genes (Figure 9) were identified to be part of torpor-related changes in canonical signalling pathways which were ranked in a Top 20. These genes were regulated differently at each sampling time point and are listed in Table 7 of the Appendix.

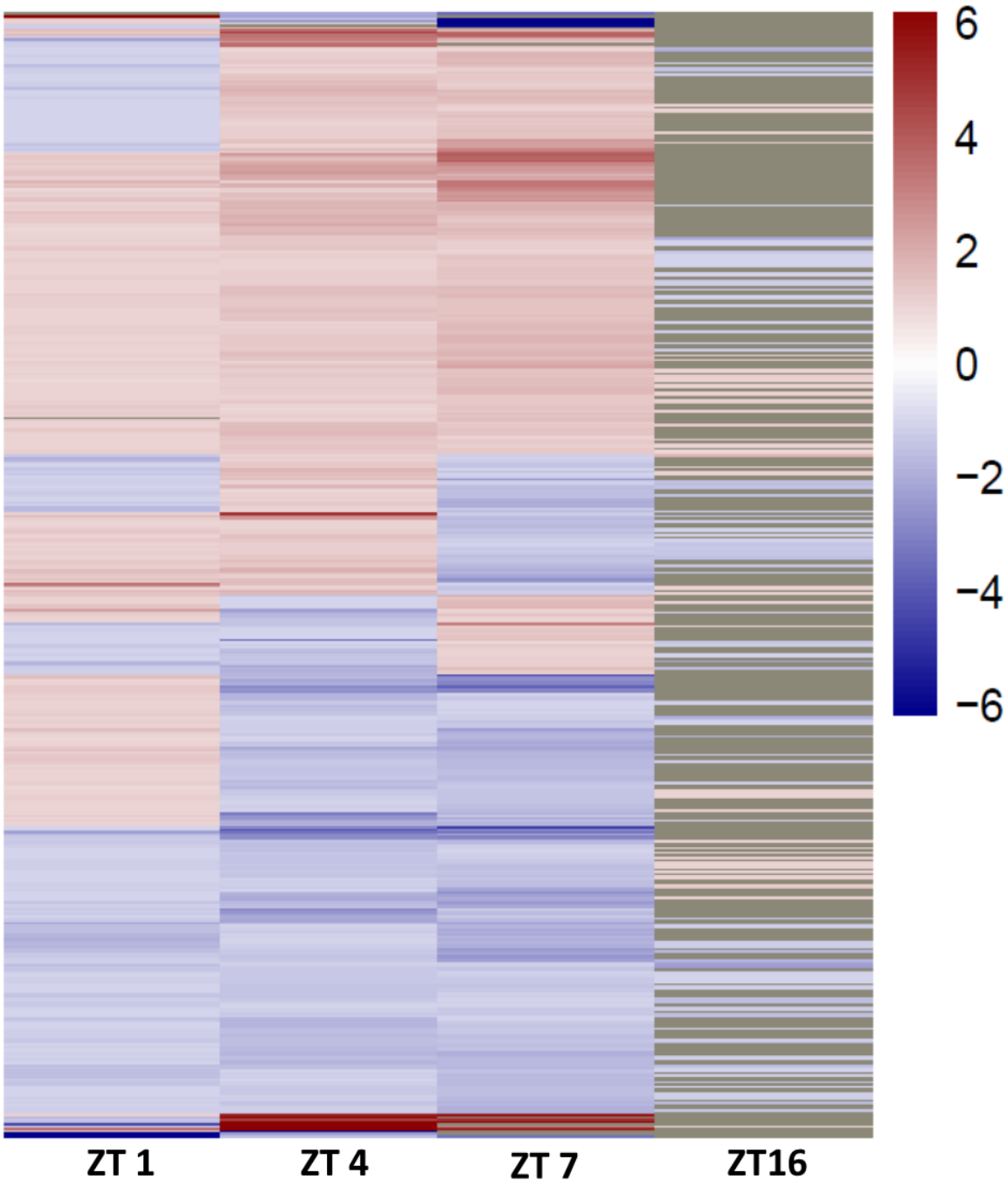

Figure 9. Gene expression levels at each timepoint of daily torpor in the *P. sungorus* blood transcriptome. Gene expression levels were indicated by colour bar. Cut-off criteria were set with fold change (FC) ≥|1.25|, p-value ≤ 0.05 and |z-score = 1.5|.Blue colour indicates downregulation, red colour indicates upregulation, while grey colour indicates no change compared to the controls.

4.1.2 Top 20 Canonical pathways

To obtain an in-depth impression of the molecular mechanisms underlying daily torpor, the data from each phase were subjected to IPA core analysis (QIAGEN Inc., https://digitalinsights.qiagen.com/IPA). DGE results were classified into torpor-associated canonical pathways (Figure 10). These 20 canonical pathways (Krämer et al., 2014) were categorized into five essential physiological systems, which ranged from Gene expression and Protein metabolism, Immune system, Cellular growth and maintenance to senescence. The significance value |z-score = 1.5| was set to indicate a real change and any value below this indicates only a trend.

Within the timepoints:

a) Entry of torpor (ZT01): significant differences were shown in 6 of the 20 canonical pathways. These were downregulated and were tRNA Charging, Leukocyte Extravasation Signalling, Insulin Secretion Signalling Pathway, Senescence Pathway, Sirtuin Signalling Pathway. The only pathway that was highly upregulated during this phase was Natural Killer Cell Signalling. All except tRNA Charging (|z-score = -2.24|) were non-significant and only showed a trend (|z-score < 1.5|).
b) Torpor nadir (ZT04): in this phase most of the pathways were downregulated and show a significant change (|z-score > 1.5|), except for Insulin Secretion Signalling Pathway (|z-score = -2.19|) which was upregulated compared to the ZT01 phase and the NRF2-mediated Oxidative Stress Response (|z-score < 1.5|). Sirtuin Signalling Pathway (|z-score = 2.61|), and SUMOylation (|z-score < 1.5|) were both upregulated at this timepoint.
c) Arousal (ZT07): in this phase most of the canonical pathways were upregulated, with the exception of the Assembly of RNA Polymerase II Complex (|z-score < 1.5|), Chemokine Signalling (|z-score < 1.5|) and Crosstalk between Dendritic Cells and Natural Killer Cells (|z-score = -1.51|).
d) Post torpor (ZT16): at this stage the canonical pathways were altogether downregulated, most of them show a significant change (|z-score > 1.5|), and some show no significant difference to control hamsters.

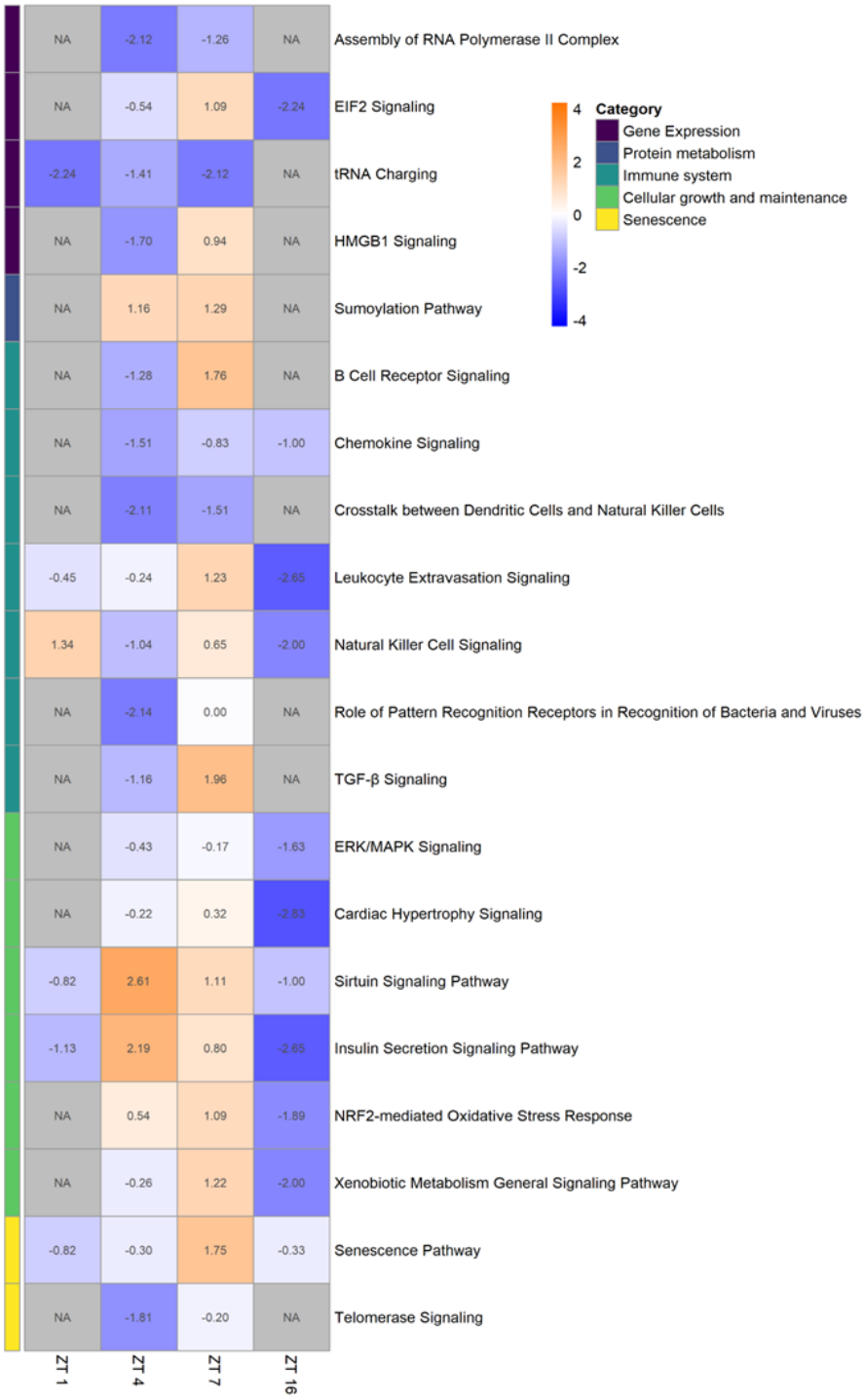

Figure 10. Heatmap showing Top 20 canonical Pathways. Comparative transcriptome analysis between HT and NT, based on IPA predictions across the four distinct zeitgeber timepoints (ZT): at the entry of torpor (ZT1), at torpor nadir (ZT4), during arousal (ZT7) and after torpor (ZT16). The blue colour indicates downregulation, the orange colour indicates upregulation and grey colour indicates no detectable change compared to the controls. Numbers inside the boxes are the significance value (|z-score = -1.5|) to indicate a real change, any value below this indicates only a trend.

Additionally, this Top 20 of most important differentially expressed pathways were grouped into 5 categories based on cellular function (Figure 10). Pathways definitions were generated from the IPA database as the number of involved molecules with the torpor dataset of this work (QIAGEN, Inc., https://targetexplorer.ingenuity.com/):

(1) Gene expression: there were four pathways related to gene expression. These were **Assembly of RNA Polymerase II Complex**, which denotes the first step of highly dynamic eukaryotic gene expression in mammals and forms part of the general transcription factors in the DNA promoter. The **tRNA Charging** pathway involves signalling after tRNA aminoacylation, which is of utmost importance for the initiation of translation, in which the aminoacyl tRNA and the mRNA transcript bind to the ribosome. These two pathways involve 16 molecules. The third pathway related to gene expression is **HMGB1 Signalling**, where the high mobility group protein B1, involves 39 molecules, the intracellular process of transcriptional regulation, DNA replication and repair as well as nucleosome assembly. **EIF2 Signalling** (eukaryotic translation initiation factors) elucidates the role of EIF2 in the regulation of transcription. For this pathway 21 involved molecules were identified.

(2) Protein metabolism: the **SUMOylation Pathway**; this pathway comprises various aspects of protein function, such as transcription, subcellular localisation, DNA repair and the cell cycle. Of the involved molecules, 32 were identified here.

(3) Immune system: the pathway with the most identified involved molecules (56) was **B Cell Receptor Signalling**, which involves B cell activation prompted by the B cell receptor (BCR) mediated antigen binding. This is important for processing and presentation of an antigen to T helper cells. The next pathway, **Chemokine Signalling**, is involved in the control of leukocyte migration during development, homeostasis and inflammation. **Crosstalk between Dendritic Cells and Natural Killer Cells** is involved in signalling the regulation of immune defence against viruses and tumours and the secretion of chemokines and cytokines. The latter two

pathways comprise 23 of the identified molecules. **Leukocyte Extravasation Signalling** is a process by which leukocytes migrate from the blood into tissues during inflammation. From this pathway, 44 relevant molecules were identified. **Natural Killer Cell Signalling** (59 molecules) is a pathway which is linked to lymphocytes and involves the cascade of cytolytic processes and the secretion of cytokines and chemokines. The **Role of Pattern Recognition Receptors in Recognition of Bacteria and Viruses** pathway contains 38 differentially expressed enzymes relevant for recognition of pathogen-associated molecular patterns and dysfunctional cells. Furthermore, for the pathway **TGF-β Signalling** 29 proteins related to leukocyte activity, competence and proliferation were identified.

(4) Cellular growth and maintenance: For the **ERK/MAPK Signalling** 59 molecules were identified. This pathway regulates the growth factor-mediated action of a wide range of cell development events including mitosis, differentiation, senescence, and apoptosis following irradiation in function of MAPK pathway. **Cardiac Hypertrophy Signalling** (59 molecules) mediates the cardiac growth response by activating receptors and downstream signalling peptide release. **Insulin Secretion Signalling** points out the increase in glucose uptake in fasting states at different levels of stress in which insulin increases, including 67 of the identified molecules. The **Sirtuin Signalling Pathway** covers signals that regulate diverse processes related to aging, cellular stress and metabolism, while comprising 94 of the identified molecules. **NRF2-mediated Oxidative Stress Response** which is an antioxidant pathway that is activated in response to ROS presence, with 68 molecules. **Xenobiotic Metabolism General Signalling Pathway** which deals with the regulation of endogenous primary and secondary toxic substances by active transport and subsequent enzymatic degradation, 41 associated molecules were identified therein.

(5) Senescence: Two signalling pathways were identified, the first **Senescence Pathway** involves cell cycle arrest and the release of inflammatory cytokines, restricting the propagation of cells under various types of stress and inducing

telomere shortening, which is detected in part through DNA damage responses, in which 106 of the identified molecules act. The second pathway, **Telomerase Signalling** (42 identified molecules) targets the mechanisms that regulate telomere length, and genome-wide studies have helped to map the genes involved in telomere length control, which are crucial for cancer initiation and tumour survival.

4.2 Part 2: Whole-body regulatory mechanisms during torpor are reflected in blood transcriptomics

In the second part of this work, as already published in (Cuyutupa et al., 2023), the focus was set on gene expression regulation in ZT4 and its comparison with findings in transcriptomic alterations in different mammalian species and organs. This comparative analysis was performed using target molecules identified in the dataset from the *P. sungorus* transcriptome in torpor nadir (ZT04 = 11.422), as the most notorious changes of torpor are demonstrated in this phase. By IPA, these genes were classified with the threshold criteria ($P \leq 0.05$, FC ± 1.25), and thereby 1,763 genes were shown to be differentially expressed between torpor vs. non torpor group. Significantly up- or downregulated genes and target molecules (TM_{IPA}) (QIAGEN, Inc., https://targetexplorer.ingenuity.com/) were obtained using |z-score = 1.5| to indicate a real change, otherwise values below this indicates only a trend. These TM_{IPA} (215 genes) were subjected to a comparative literature analysis including 13 publications related to transcriptomic changes in torpor. The literature search was focused on the keywords torpor or/and hibernation and that the studies were conducted in mammals. Only those that provided a detailed list of identical up- or downregulated genes were considered for comparative analysis (see Figure 8) with TM_{IPA}, regardless of species, duration and torpor type. By this, 13 different transcriptome studies were chosen under these criteria and were analysed in comparison with TM_{IPA}. The rate of matches between TM_{IPA} derived from *P. sungorus* and the data extracted from the literature was 68.8%. This ratio could be attributed to the fact that ZT04 comprises the nadir phase of daily torpor, which best corresponds to the deep torpor/hibernation state reported in the literature.

4.2.1 Analogies in different species and organs based on torpor nadir matches

From the 13 studies applying the criteria which were specified above, genetic matches with the *P. sungorus* were found in 9 species and ten different organs (Figure 11).

The species *Ictidomys tridecemlineatus* showed the highest overlap with more than 120 matching genes in various organs, followed by *Myotis lucifugus* with > 60 matching genes in a single organ. Other hibernating species showed only minor overlap over a range of different organs (Figure 11).

Figure 11. Circular chart illustrating the target molecule overlap according to IPA when comparing existing literature on mammalian hibernators to the Djungarian hamster. The bars are clustered by the different species with distinct torpor types. The gene count per organ is denoted next to the respective cluster (Cuyutupa et al., 2023).

4.2.2 Degrees of kinship in the overlapping torpor species

The order classification of these species showed different phylogenetic correlations as shown in Figure 12. These species belong to the taxa Theria, which includes marsupials (Metatheria) and higher mammals (Eutheria).

P. sungorus belongs to the Eutheria group, within phylogenetic proximities are the mice (*Mus musculus*), being of different families. On the one hand the *P. sungorus* of the family Cricetidae (the Voles) and the mouse of the family Muridae (rats and mice), both belonging to the superfamily Muroidea and to the order Rodentia (the rodents). The next species belonging to the same order, which showed overlap in gene regulation and torpor, are the sciurid family (the squirrels), the arctic ground squirrel (*Urocitellus parryii*) and the thirteen-lined ground squirrels (*Ictidomys tridecemlineatus*). Next closest were two species of the order Primates.

Both rodents and primates belong to the superorder of placental mammals Euarchontoglires which is composed of two clades Glires (the rodent and rabbit group) and Euarchonta (which includes the primates, colugos and tupayas). Matches in gene regulation of *P. sungorus* occurred with two species, from the Cheirogaleidae (fork-marked lemur) and the lemuriformes, the grey mouse lemur (*Microcebus murinus*) and the dwarf lemur (*Cheirogaleus medius*).

Next closest in kinship to the order Artiodactyla (even-toed ungulates) and Pholidota (scaly anteaters), were two species of the order Chiroptera (vampires) of the families Rhinolophidae (horseshoe bats) and the greater Vespertilionidae (microbats). These were the little brown bat (*Myotis lucifugus*) and the greater horseshoe bat (*Rhinolophus ferrumequinum*). Thus, there were also matches with a species of the order carnivora the black bear (*Ursus americanus*). Finally, and most distantly related is a species belonging to the rank of metatheria within the order microbiotheria. This species is the bush monkey/monito del monte (*Dromiciops gliroides*).

A brief description of the species that showed regulatory matches with the *P. sungorus* transcriptome can be found in the supplementary material and was recently published (Cuyutupa et al., 2023).

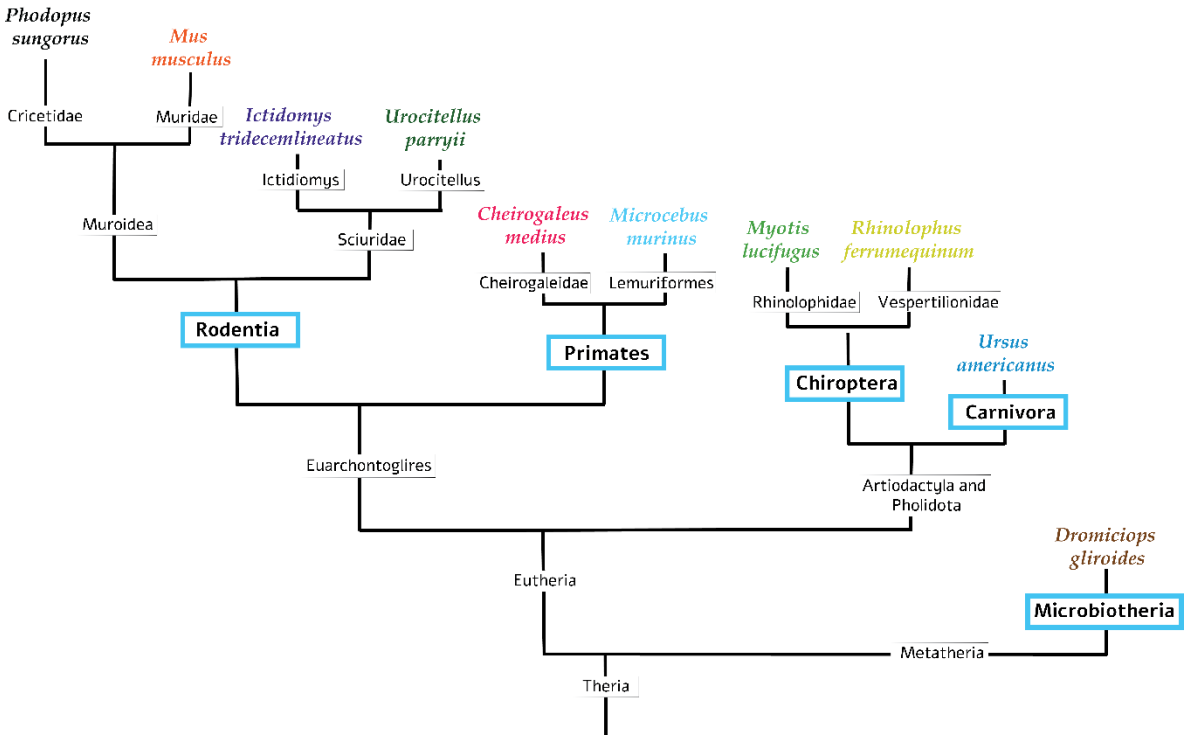

Figure 12. Species arranged in a cut-out simplified phylogenetic tree, to make visible the distances to *P. sungorus*. The blue boxes highlight the orders, and at the top are the family names of the species, with which similarities in genetic regulation were found (Cuyutupa et al., 2023).

4.2.3 Cellular maintenance and physiological changes during torpor

By the IPA network analysis tool, the assumed (predicted) consequences which are based on transcriptional regulation of TM_{IPA} were displayed. Here physiological processes were selected according to the belonging in one of the following categories “Basic cellular mechanisms”, “Immune system” and “Other organs” (Figure 13 and 14).

a) Basic cellular mechanisms, which includes physiological processes such as transcription, metabolism of protein, cellular homeostasis, autophagy, apoptosis and necrosis that are essential for cell subsistence and homeostasis.

b) Immune system, that broadly encompasses predictions about the inhibition or activation of processes associated with the focusing on lymphopoiesis, recruitment of leukocytes, migration of cells, quantity of T lymphocytes, quantity of B lymphocytes, activation of T lymphocytes and viral infection.
c) Other Organs, covering the protective effect, which was detected in blood cells, liver, kidney and heart. The processes in these organs were proliferation of heart cells, angiogenesis, proliferation of hepatocytes, proliferation of kidney cells, protective effects liver lesion, liver regeneration, damage of kidney, infarction of heart, apoptosis of cardiomyocytes and inflammation of heart and nephritis.

The prediction according to Figure 13 indicates that the diseases and functions related to the three categories of mechanisms, the basic cellular mechanisms, the immunological system and the other organs, are inhibited during the nadir torpor and this is to be expected, as it is known that the mechanisms involved in gene expression, cell cycle, immunological system and cell proliferation in orphans in these mechanisms are arrested by the low temperature regulation and energy saving that occurs during the deep torpor.

The relation of TM_{IPA} to functions or diseases in the different torpor phases were predicted to be very different. The heatmap which is displayed in Figure 14 depicts the predictions (either activation or inhibition) on the activity of the physiological processes as shown in Figure 13, but for all four torpor timepoints (ZT01-16). These changes are based on the direction and magnitude of regulation of TM_{IPA}, which were initially identified for ZT04.

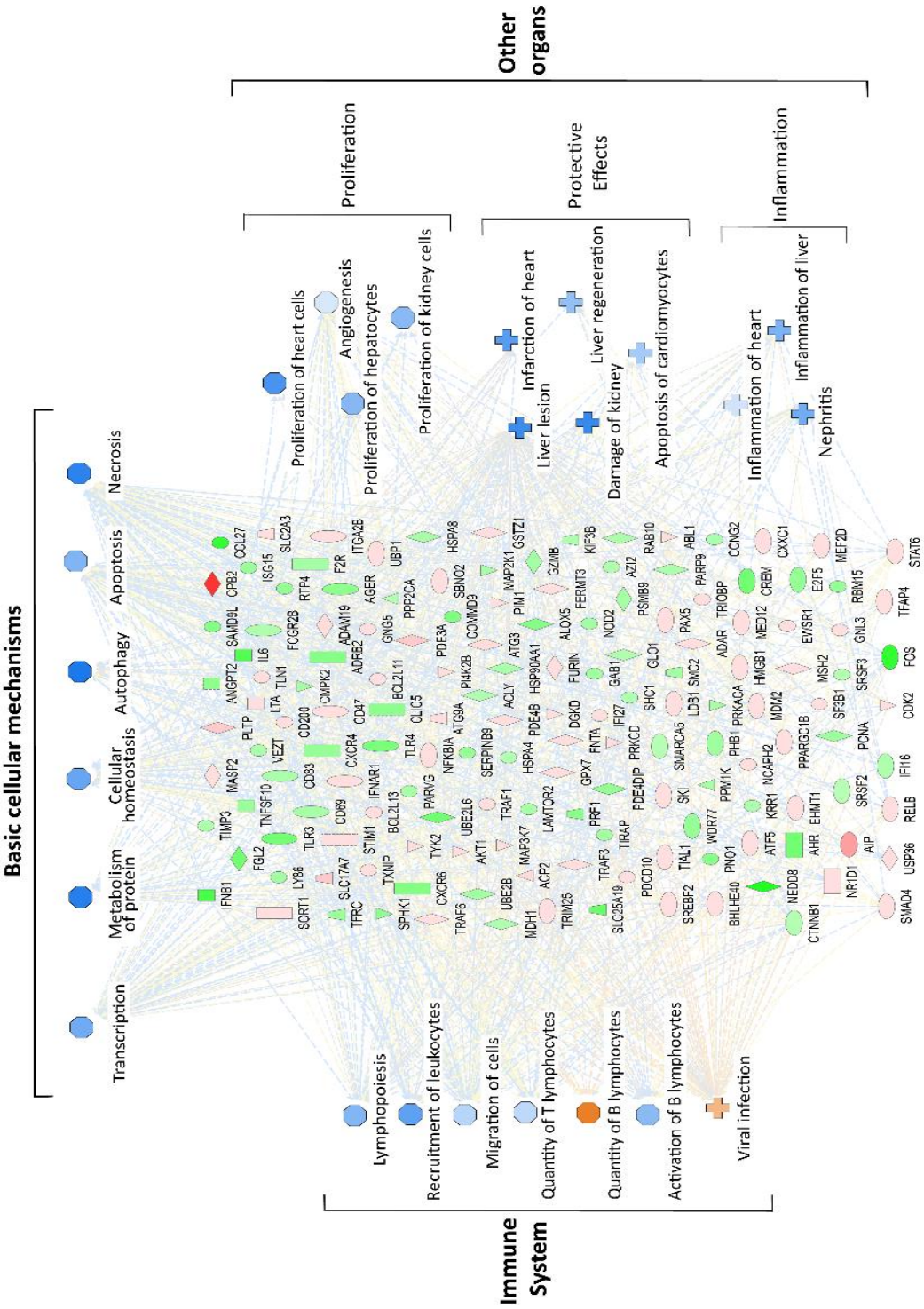

Figure 13. Physiological changes based on prediction of key target molecules (TM_{IPA}) regulation. Categories: Basic cellular mechanisms, immune system, and other organs. Diseases and functions expected are denoted in the colouring. Blue symbols: downregulation, orange symbols: upregulation, crosses: diseases, octagons: functions. Regulated genes in dataset (green: decreased measurement, red: increased measurement) (Cuyutupa et al., 2023).

Also here, significance value |z-score = 1.5| was set to indicate a real change and any value below this indicates only a trend (Figure 13). According to these results, changes in daily torpor at the four *zeitgeber* timepoints were as follows:

a) Entry of torpor (ZT01): in the category Immune system, diseases and functions are minimally upregulated, with no significant change (|z-score < 1.5|), except for migration of cells (|z-score = -4.39|). In the Basic cellular mechanisms category, there are significant changes in up- or downregulated pathways, except for metabolism of protein and apoptosis (|z-score < 1.5|). In the category other organisms there is a noticeable change in most of them both up- and downregulated (|z-score > 1.5|), however no change for Infarction of heart, Inflammation of heart, Nephritis (|z-score < 1,5|).
b) Torpor nadir (ZT04): all Basic cellular mechanisms, Immune systems and others were downregulated and showed a significant change (|z-score > 1.5|), except for Quantity of B lymphocytes (|z-score = 1.62|) and Viral Infection (|z-score = 1.16|), which were upregulated.
c) Arousal (ZT07): most pathways were upregulated and show a significant change (|z-score > 1.5|), with the exception of metabolism of protein, autophagy, quantity of T lymphocytes, inflammation of heart and nephritis which were down-regulated, as well as proliferation of kidney cell and infarction of heart which did not differ significantly from controls and also do not show a significant change (|z-score < 1.5|).
d) Post torpor (ZT16): in this phase all mechanisms are downregulated in Basic cellular mechanisms, Immune systems, others show a significant change (|z-score > 1.5|), with the exception of apoptosis (|z-score = 3.12|), necrosis (|z-score = 2.06|) and infarction of hearth (|z-score = 1.56|) which are upregulated.

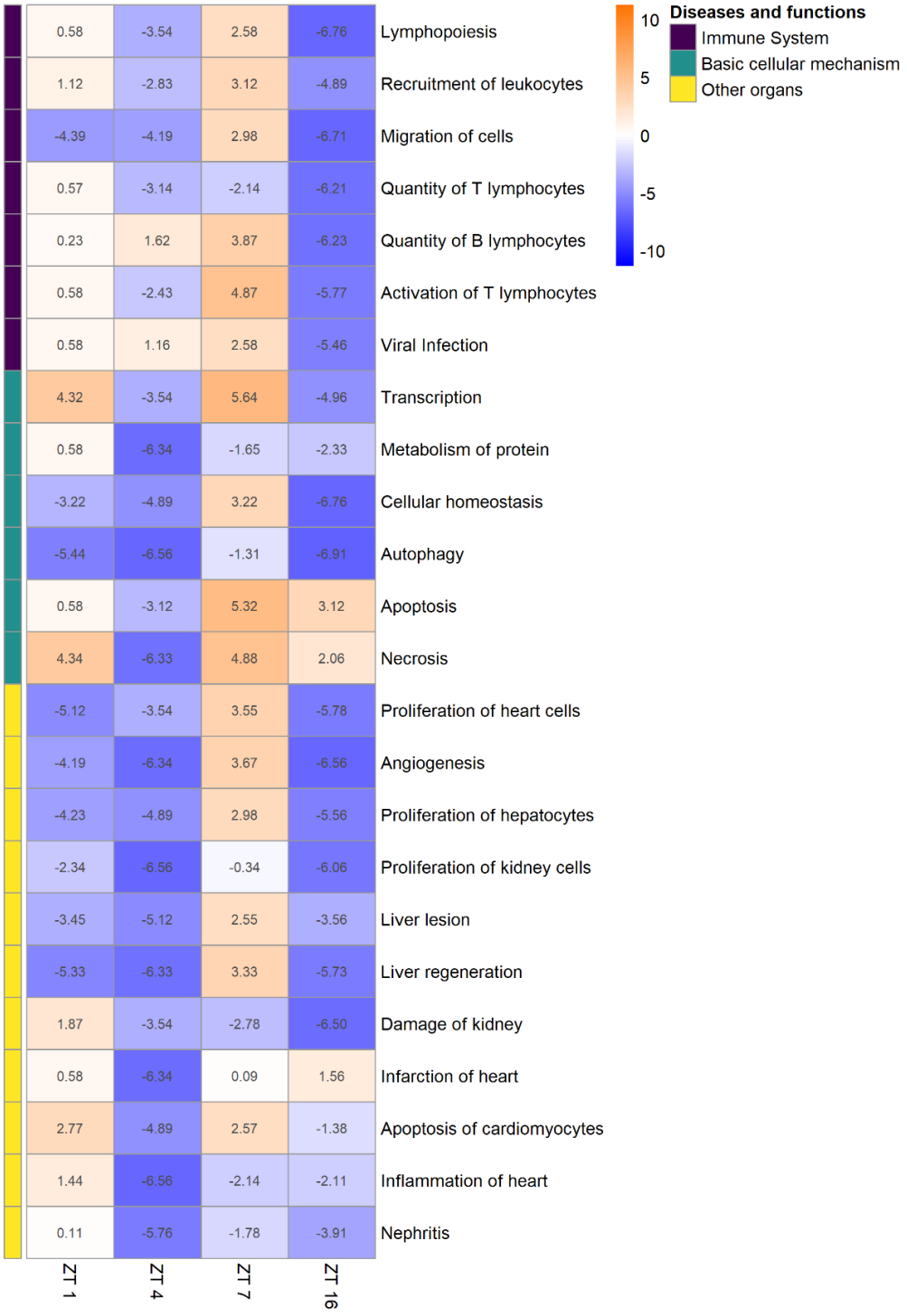

Figure 14. Enriched diseases and functions, based on IPA predictions, through all daily torpor timepoints (ZT01-ZT16). Blue coloured squares denote downregulation, orange squares indicate upregulation. Numbers inside the boxes are the significance value (|z-score = 1.5|) to indicate a real change, any value below this indicates only a trend.

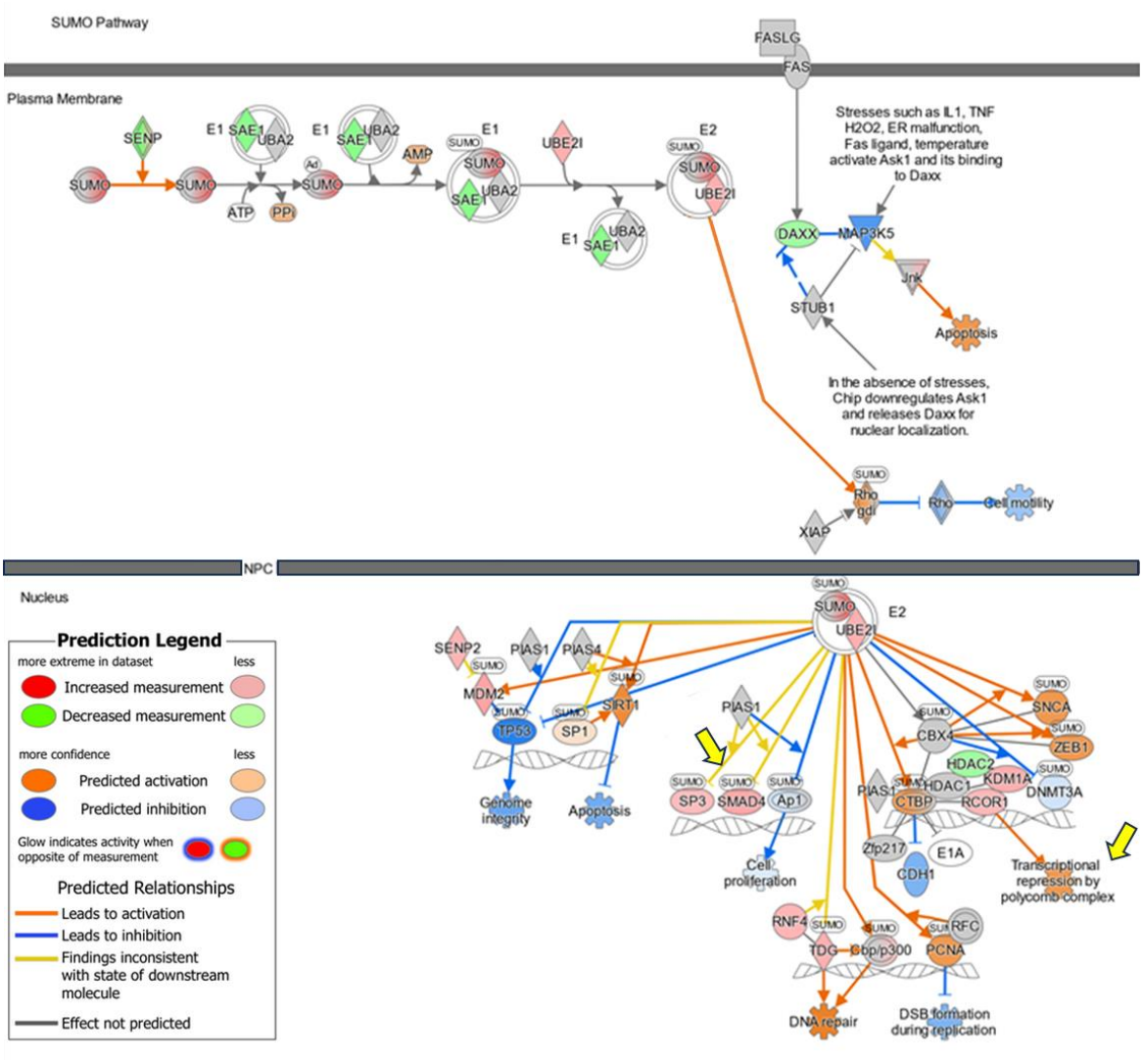

Figure 15. SUMOylation Pathway predicted to be upregulated during torpor nadir and arousal (ZT04 and ZT07). The pathway described as small ubiquitin like modifier (SUMO) conjugation contains a multitude of ubiquitination target proteins that are themselves part of a wide variety of cellular processes. SUMOylation has the ability to amplify TGF-β/SMAD, SMAD proteins transmit extracellular TGF receptor signals to the cell nucleus to subsequently regulate gene transcription.

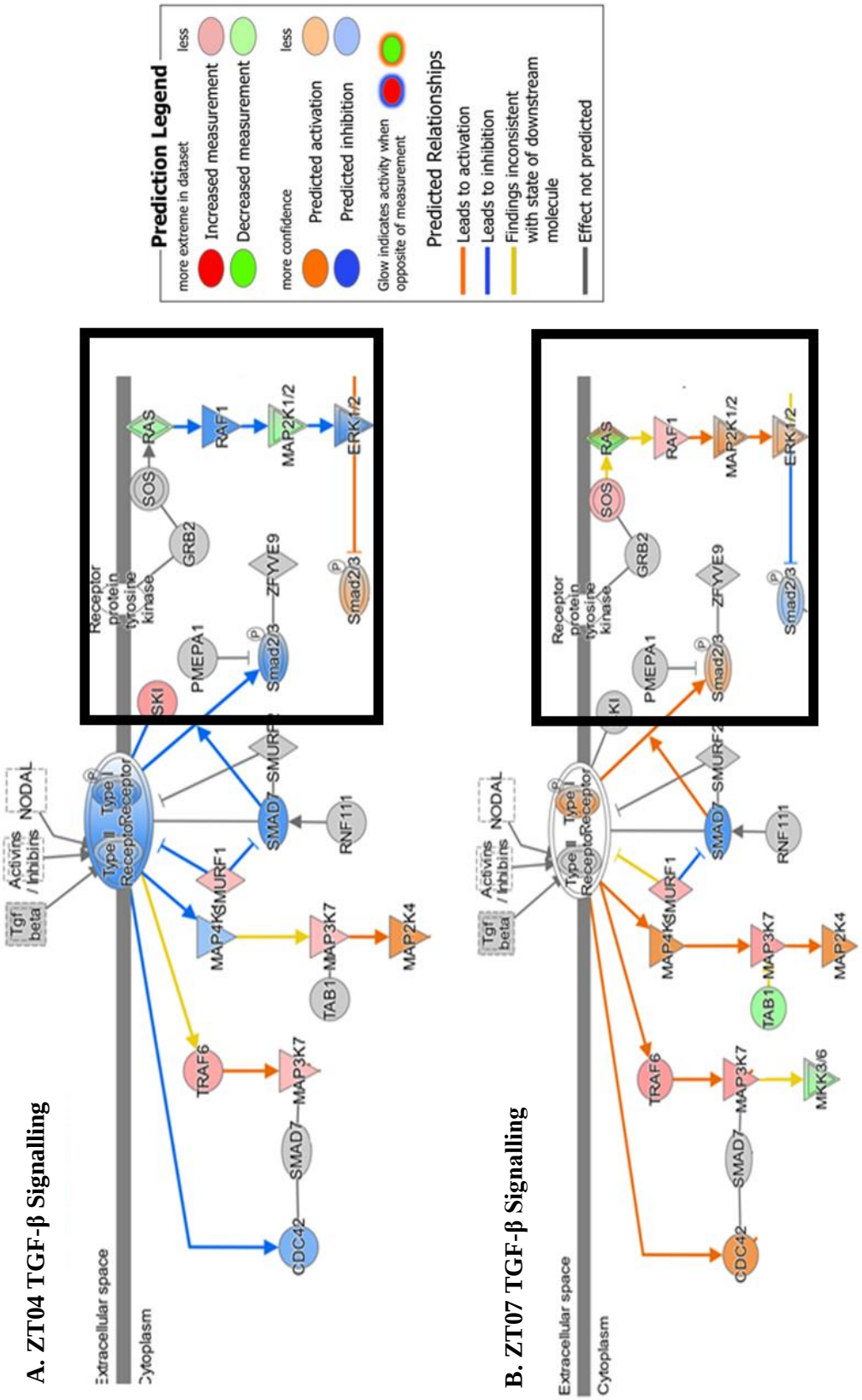
Prediction Legend
more extreme in dataset
less
Increased measurement
Decreased measurement
more confidence
less
Predicted activation
Predicted inhibition
Glow indicates activity when opposite of measurement
Predicted Relationships
Leads to activation
Leads to inhibition
Findings inconsistent with state of downstream molecule
Effect not predicted
A. ZT04 TGF-β Signalling
B. ZT07 TGF-β Signalling
Extracellular space
Cytoplasm
Tgf beta
Activins / Inhibins
NODAL
Type I Type II Receptor
Receptor protein tyrosine kinase
SKI
SOS
GRB2
RAS
RAF1
MAP2K1/2
ERK1/2
PMEPA1
Smad2/3
ZFYVE9
SMURF1
SMURF2
SMAD7
RNF111
MAP4K
MAP3K7
TAB1
MAP2K4
TRAF6
CDC42
MKK3/6

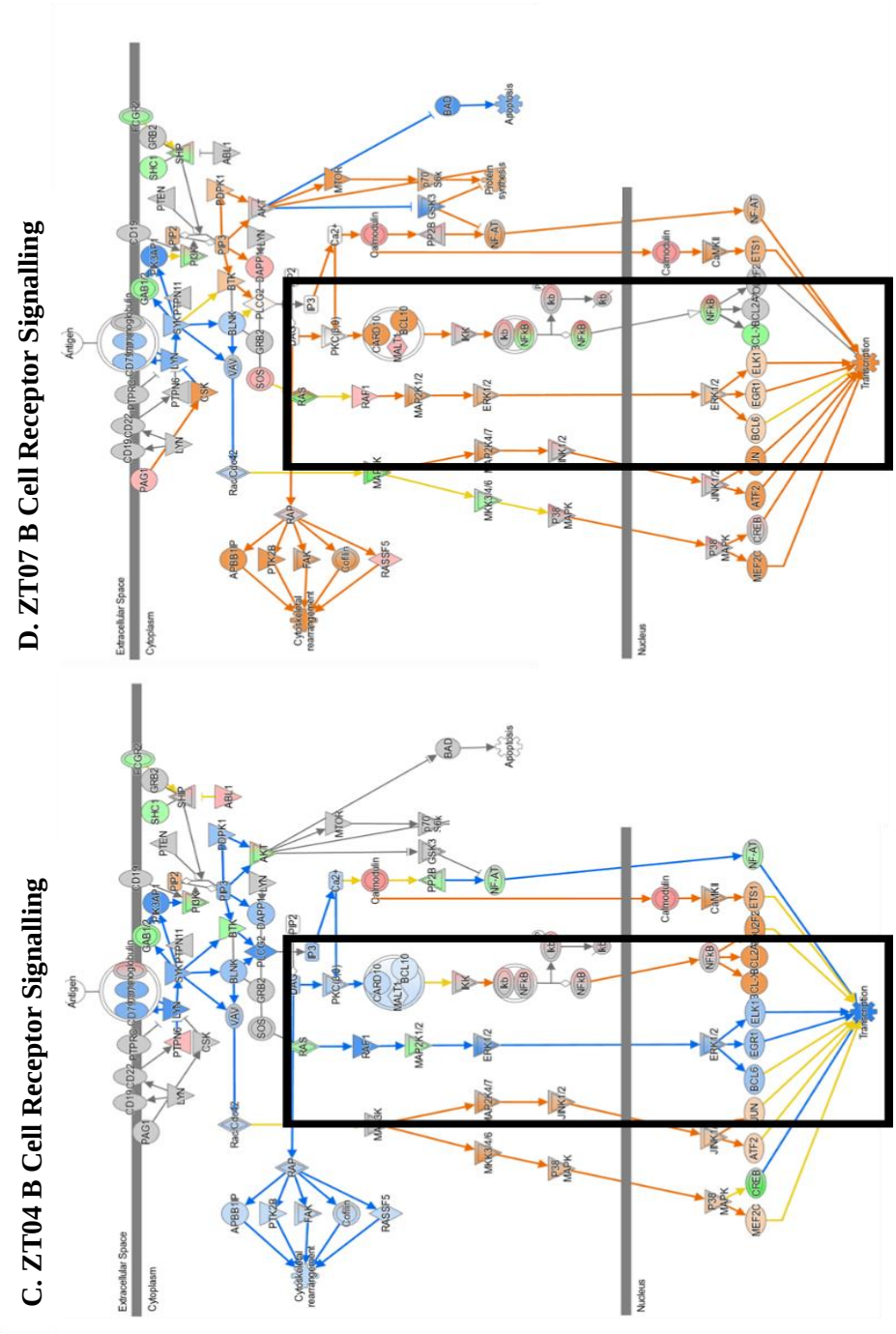

Figure 16. The ERK/MAPK signalling cascade is a crucial regulator of signalling in the immune system. In Figure A it acts by inhibiting the regulation of Smad2/3 which acts with TGF-β signalling. During nadir torpor TGF-β is predicted to be downregulated, phosphorylation of Smad2/3 inhibits transcription and translation. In contrast, during arousal, Figure B shows how this cascade is upregulated and inhibits Smad2/3 phosphorylation, thus allowing transcription and translation to proceed. Figure C and D relate this cascade to the regulation of B Cell Receptor Signalling where it is inhibited or upregulated, respectively.

4.3 Part 3: Comparison of metabolic adaptations reflected in blood transcriptomics of *P. sungorus* and humans overwintering at the Antarctic Concordia station

The results for this third part of the work, focus on *P. sungorus* blood transcriptome gene expression data from a comparison of the Top 20 canonical pathways, described in the first part, during daily torpor (NT versus HT) and the changes found in the expeditioners (January - Post versus BDC). These data were normalised before comparisons with their respective controls. To indicate a real change, significance value |z-score = 1.5| was set and any value below this indicates only a trend (Figure 17).

Overall, the January samples were taken after the crew arrived at the station, in April and July many changes were recognised, and these were downregulated in October and upon return. Within the Gene Expression category, significant upregulation of EIF2 Signalling (|z-score > 1.5|) was seen throughout the entire duration of the stay (except for Post; with shows no change) and is comparable to the arousal phase of *P. sungorus* (ZT07). In comparison, Assembly of RNA Polymerase II Complex and tRNA Charging did not show any significant changes in humans overwintering at the Antarctic Concordia station in comparison to BDC. These two canonical pathways were shown to be downregulated during torpor in *P. sungorus* (ZT04). HMGB1 Signalling shows a varied dynamic with the lowest peak before and after the stay and the highest peak during July (|z-score < 1.5|). The upregulation in this category (July) is comparable to the arousal phase of torpor (ZT07), which was also highly regulated.

In the Protein Metabolism category, activation of SUMOylation Pathway is denoted throughout the whole mission in Antarctica (|z-score > 1.5| in January) and a surprising drop in activity after the stay (|z-score = -2|), and these results are comparable with both the torpor nadir phase (ZT04) and the daily torpor arousal phase (ZT07).

In the category of the immune system (|z-score > 1.5| in the Post phase), the mechanisms that were downregulated were Crosstalk between Dendritic Cells and Natural Killer Cells, Leukocyte Extravasation Signalling, Natural Killer Cell Signalling and Role of Pattern Recognition Receptors in Recognition of Bacteria and Viruses and these results are

comparable with the nadir torpor phase (ZT04), where these canonical pathways are also downregulated. However, on the other side, there are three pathways that were upregulated in different months, and these were B Cell Receptor Signalling in April and July which is comparable with the arousal phase of torpor. An upregulation of Chemokine Signalling, which can be observed in April and July, doesn´t correspond to torpor results where this pathway is completely downregulated. Moreover, TGF-β Signalling (|z-score < 1.5|), which was active during all the months sampled, is comparable with the arousal phase of torpor (ZT07).

In the category Cellular growth and maintenance, with a significant change (|z-score > 1.5|) in the Post phase, an almost uniform upregulation of all mechanisms in the months of April and July is remarkable for most of the canonical pathways: Cardiac Hypertrophy Signalling, ERK/MAPK Signalling, Insulin Secretion Signalling Pathway, Sirtuin Signalling Pathway, Xenobiotic Metabolism General Signalling Pathway. Except for NRF2-mediated Oxidative Stress Response which was downregulated during all sampling timepoints. The activation of these canonical pathways during hibernation at Concordia station is mostly comparable with the arousal phase of torpor (ZT07), as can be seen in Figure 17.

In the Senescence category, an activation of the two signals of both the Senescence Pathway (|z-score > 1.5| in the Post phase) and Telomerase Signalling (|z-score > 1.5|, January - July) is clearly visible throughout all timepoints in mission, which is at least for the Senescence Pathway comparable to the arousal phase (ZT07). However, despite this similarity, senescence-associated pathways are predicted to be downregulated during torpor.

Previously published results by Buchheim and colleagues (Buchheim et al., 2020) were related to viral infections and the immune system and fit the general impression of a dysfunctional immune status.

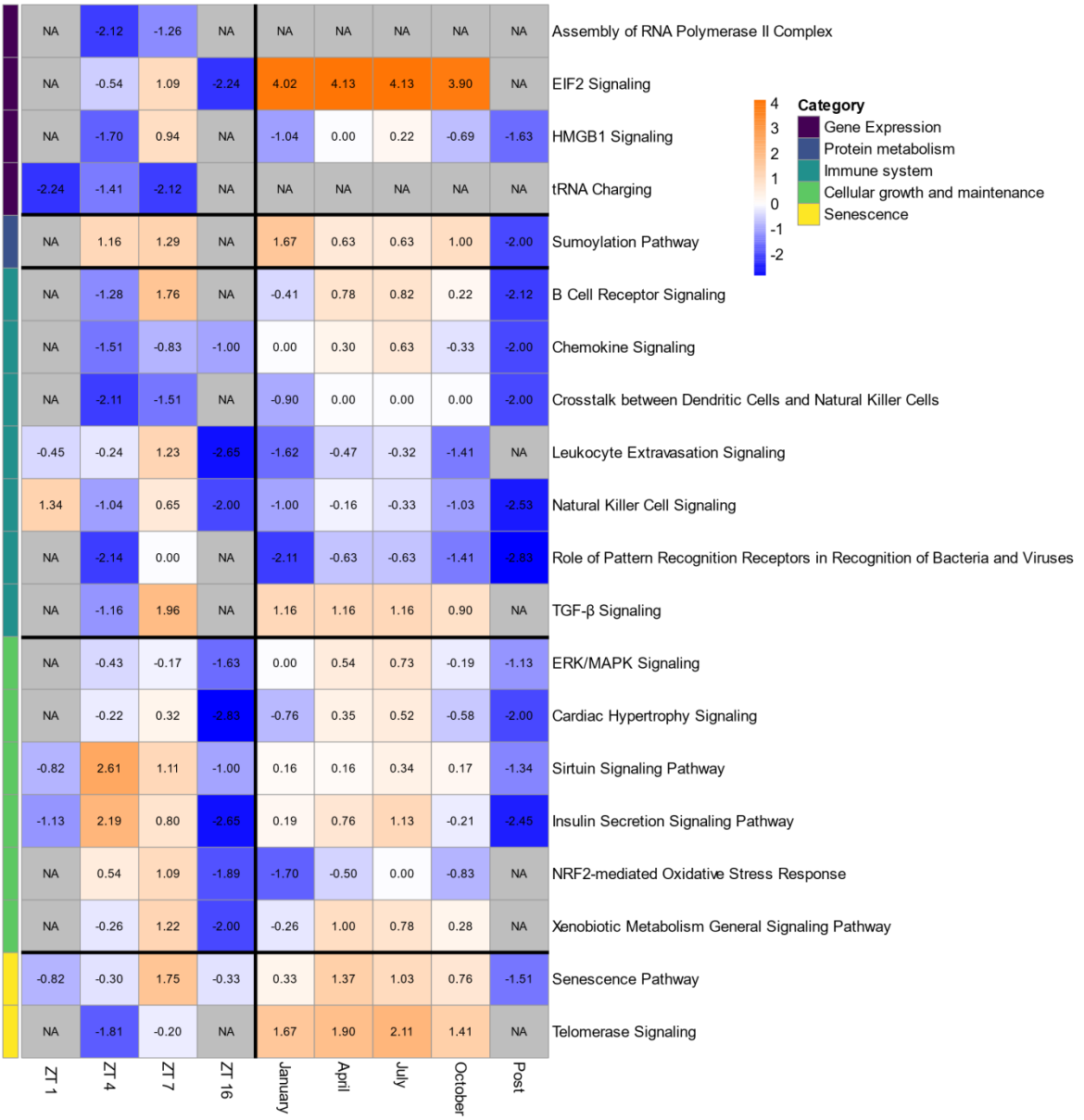

Figure 17. Comparative heatmap of *P. sungorus* and humans at the Concordia station. This based on IPA predictions across the four distinct *zeitgeber* timepoints (ZT01-ZT16) and measurements on Concordia station crewmembers (January-Post). 5 Categories: Gene expression, Protein metabolism, Immune system, Cellular growth and maintenance and Senescence. Orange indicates upregulation, while blue indicates downregulation. The dark lines served to better frame the categories, numbers inside the boxes are the significance value (|z-score = -1.5|) to indicate a real change, any value below this indicates only a trend.

5 Discussion

Drastic shutdown of cellular mechanisms to save energy and ensure survival occurs during torpor and hibernation, but up to this date it is still unclear how these mechanisms operate in detail. However, the existence of a conserved genetic programme in all mammals has previously been suggested. Although daily torpor lasts only a few hours, it is a multidynamic event with many adaptive changes. In this work the most noteworthy, regulated signals during daily torpor found in the blood transcriptome of *P. sungorus* will be discussed in the first part. In the second part the evaluated target molecules of torpor nadir will be discussed according to the comparative findings with the literature. And finally, in the third part comparative results between *P. sungorus* and human blood transcriptome analysis sampled from humans overwintering at the Antarctic Concordia station will be discussed.

5.1 Part 1: Transcriptional gene dynamics between the different torpor phases of torpor entry, nadir (deep torpor), arousal and the post-torpor phase

5.1.1 Gene expression and metabolism of proteins

Modulation of gene expression is essential for the cellular machinery, but hardly understood in the context of torpor. Many different components and steps interact to achieve a responsive expression landscape; these include transcription factors, protein synthesis and post-translational modifications, which are for example employed to target the protein end product to its appropriate subcellular destination (Thomas & Chiang, 2006; Ling & Groop, 2009). Analysis of signalling pathways using IPA revealed predictions about RNA Polymerase II Complex, EIF2 signalling, tRNA charging und HMGB1 signalling.

Although control mechanisms should be gradually activated during torpor entry (ZT01), which are then maintained during torpor nadir (ZT4) and reversed later, for the majority of pathways, no changes occurred during ZT01 compared to the respective normothermic controls (grey colour in Figure 10). This lack of regulation is consistent with the only minor temperature reduction in this phase compared to later stages of torpor. During deep torpor

in mammals, mechanisms to reduce the MR are engaged like reducing transcription and translation (Tessier & Storey, 2014) by activating different pathways in response to the stress signal due to the torpor phenotype (Yan et al., 2008).

In all four of the initially mentioned pathways significant downregulation started to be evident during the torpor nadir (ZT04), probably because during this torpor phase a quickly reversible reduction of translation must be achieved through the interaction of mRNA processing factors and other proteins, protecting and stabilising the mRNA pool to increase stress tolerance during arousal (van Breukelen & Martin, 2001). This can also be observed for the EIF2 and HMGB1 signals, which are upregulated in the arousal phase (ZT07) but downregulated in the post torpor phase (ZT16). Furthermore, RNA polymerase II assembly is downregulated during torpor nadir (ZT04), but slightly upregulated in the arousal phase (ZT07) and is then restored to control levels in the post torpor phase (ZT16). This is consistent with previous studies in which the presence of active polymerase II analysed in hepatocytes and nuclei of brown adipocytes of hazel dormice (*Muscardinus avellanarius*) drops to very low levels during torpor, but remains detectable, indicating a drastic reduction under hypometabolic conditions, but not a full block of transcriptional activity (Malatesta et al., 2008). Furthermore, nuclear accumulation of pre-mRNA during hibernation could play an important role in preserving and maintaining cellular activity as a restorative strategy of RNA metabolism upon arousal (Malatesta et al., 2008).

On the other side, downregulation of global protein synthesis via EIF2 was detected only during torpor nadir (ZT04). Potentially different types of cellular stress, including torpor, cause the aggregation of misfolded proteins in the lumen of the endoplasmic reticulum (ER), termed ER stress (Palam et al., 2011). Mammalian cells activate ER-associated protein degradation to prevent this type of abnormal accumulation. EIF2 signalling down-regulates global protein synthesis as a stress adaptation (Palam et al., 2011). The mechanism involved in EIF2 guides the tRNA charge (Met-tRNA) to the ribosomal translation initiation site, which is imperative to start translation and successive elongation (van Breukelen et al., 2004). Upon EIF2 signalling downregulation, as presented here, a direct impact on low tRNA charging at the torpor nadir (ZT04) is expected. Contrary, an

EIF2 upregulation is observed during arousal (ZT07) although the tRNA charging is still low but almost comparable with the initial phase (ZT01). In the post torpor phase (ZT16) no difference compared to control individuals was detected. Additionally, the predicted downregulation of EIF2 is consistent with comparable findings in murine microbats species and daurian squirrels (Huang et al., 2020). This response to the hibernation phenotype showed that only a small fraction of translation initiation complexes is active when general metabolism is suppressed, while a larger fraction is phosphorylated and thus inhibited (van Breukelen & Martin, 2002). Increased EIF2 activity during periods of arousal has also been linked to the restoration of protein levels essential for survival (Frerichs et al., 1998). Moreover, high mobility group protein B1 (HMGB1) is a multivariate functional protein that plays a role in gene regulation, DNA repair, autophagy induction, acting as a chemokine and damage-associated molecular pattern (DAMP) causing inflammation (Logan & Storey, 2018). HMGB1 was found to be downregulated at nadir torpor (ZT04), however its signalling was upregulated during the arousal stage (ZT07) and showed no difference within the post torpor phase (ZT16). These findings are similar to those of brown adipose tissue (BAT) analysed in the ground squirrel, where HMGB1 is increased during arousal and thermal stress, when body temperature returns to euthermic levels. Here it was linked to levels of proinflammatory markers or tissue damage (Qiu et al., 2016), suggesting that it may be upregulated during arousal in response to oxidative stress in *P. sungorus*.

Death is an imminent consequence of global translation machinery shutdown, yet torpid animals are capable of minimising the rate of protein synthesis as measure of energy conservation without existential risks (O'Hara et al., 1999). Translational regeneration during the arousal phase (ZT07) seems to be a key component in achieving this. Furthermore, a limited but crucial number of proteins continue to be synthesised during torpor in order to ensure organ subsistence (Hittel & Storey, 2002).

At the torpor entry (ZT01) and post torpor (ZT16) stages, no differences were found with the controls, but SUMOylation activity was detected just during torpor nadir (ZT04). These results are comparable to those performed in the kidney, liver and brain of 13-lined ground squirrels, where SUMOylation was shown to be massively increased (Figure 15) (Lee et al.,

2007). Since torpor is an innate model of resistance to extremely low blood flow, hypothermia is a general inducer of SUMO conjugation due to special adaptive changes and to counteract CNS damage (Lee et al., 2007; Storey, 2010; Lee & Hallenbeck, 2013), and can enhance the activity of the TGFβ/SMAD (Lin et al., 2020). Limited energy availability and post-translational modifications as a regulatory mechanism for tolerance play a very important role during this process. SUMOylation is likely active during the arousal phase (ZT07), where blood flow is restored. Conjugation of ubiquitin decreases rapidly in the post-torpor phase, indicating a close relationship of hibernation and SUMO conjugation. While unbound SUMO is ubiquitous in all cellular compartments, the majority of conjugated SUMO is found in the nucleus, consistent with transcription being the main target of SUMOylation (Girdwood et al., 2004). The cytoprotective properties provided by SUMOylation are impressive and therefore important for cell survival; however, additional research is still needed to thoroughly elucidate the SUMOylation machinery that confers this hypothermia resistance (Sajeev et al., 2021). The current results hereby suggest that the increase in SUMOylation during ZT04 may be primarily caused by decreased body temperature and act as a tolerance strategy to hypothermia-induced ischemia (Lee et al., 2007).

5.1.2 Immune System

Although the majority of pathways showed no difference in regulation when comparing the ZT01 phase to control individuals, the Natural killer (NK) Cell Signalling was found to be upregulated. NK cells are part of the innate immune system and specifically recognise and kill aberrant cells such as virus infected, tumorous or severely stressed cells (Paul & Lal, 2017). Thus, upregulation might either represent a protective measure against viral infections and stress induced damage during torpor entry or might be a co-regulated consequence of ZT01 related stress reactions and regulatory responses observed during deep torpor (ZT04).

In general, all immuno-related pathways are predicted to be downregulated during torpor nadir (ZT04), most likely because there is no stimulation by cytokines or chemokines. Their secretion typically promotes leukocyte migration during development, homeostasis

and inflammation (Tessier et al., 2015); therefore their absence impedes any activating immune responses until their re-activation during the arousal phase (ZT16). In addition, chemokines, a group of cytokines, which selectively recruit leukocytes to areas of tissue inflammation or injury (Baggiolini et al., 1993; Lukacs et al., 1995), are also shown to be downregulated during ZT04. In addition, Crosstalk between Dendritic Cells, Leukocyte extravasation signalling and Role of Pattern Recognition Receptors in Recognition of Bacteria and Virus pathways and the transforming growth factor beta (TGF-β) pathway are predicted to be downregulated during ZT04. Also, B cell receptor signalling is predicted to be downregulated during torpor (Figure 16, C and D). This may be because there is no stimulation by cytokines or chemokines, which are also downregulated and therefore there is no activation response of this mechanism. Until its activation during the arousal phase (ZT16) (Figure 16, A and B). These pathways are mostly upregulated again during arousal (ZT07). Immune latency being a result of torpor is widely recognised as an energy conservation strategy by decreasing the functions of innate and adaptive immune cells (Wu & Storey, 2016; Tessier et al., 2021). The immune processes predicted by IPA to be inhibited are consistent with studies in Syrian hamsters (*Mesocricetus auratus*) and hibernating ground squirrels in which the reduction in body temperature resulting from metabolic suppression in torpor is the main driving force constituting a versatile, yet rapidly reversible system of reduced immune function (Bouma et al., 2010; Wei et al., 2018). Furthermore, previous studies in bats and torpid 13 lined ground squirrels showed that during torpor, cytokine levels were decreased in the duodenum, jejunum, ileum and large intestine and the immune system became active immediately before the mammals returned to their active state (Kurtz et al., 2021). In addition, this decrease is also attributed to the downregulation of the leukocyte extravasation signalling pathway, since leukocytopenia is closely associated with torpor entry. This resembles analyses in squirrels, where endothelial processes such as adhesion, accumulation, activation and subsequent extravasation of circulating leukocytes decreased in localised foci of inflammation and confirmed the occurrence of leukocytopenia with the onset of torpor (Bouma et al., 2010). Extravasation is active in the arousal phase (ZT07) and is downregulated again during the post torpor phase (ZT16).

The TGF-β pathway is associated with a large variety of cytokines and plays an important role as inhibitor of cellular proliferation (Wu & Storey, 2012). In the blood of *P. sungorus*, a downregulation was observed which is consistent with results from ground squirrels, as this signalling pathway is able to induce cell cycle arrest by expression of cyclin-dependent kinase inhibitors via TGF-β/Smad signalling (Wu & Storey, 2016) (see Figure 17) and induces torpor associated cell cycle arrest in the G1 and S transition phases (Wu & Storey, 2012, 2018). The immune system returns to its baseline state in the post torpor phase (ZT16).

5.1.3 Cell growth and maintenance

In the ZT01 phase ERK/MAPK signalling such as cardiac hypertrophy signalling show no significant regulation compared to control animals. However, in the ZT04 phase a downregulation of both can be observed, probably because the ERK signalling pathway depends on G-protein activation, leading to subsequent phosphorylation-mediated activation of a three-level cascade including MAPK kinases (Biggar et al., 2015b). MEK, RAF and ERK are kinases involved in the ERK cascade, which ultimately phosphorylates various targets and are connected to mechanisms that affect all epithelia (Biggar et al., 2015b; Ihermann-Hella et al., 2014) e.g. intestine (Hommes, 2003), skin, kidney, etc. (Cuarental et al., 2019), and specifically in the pathways obtained in this work, it plays a significant part in the cardiac hypertrophy signalling activation system (Tessier et al., 2021). It is therefore not surprising that upon ERK/MAPK downregulation in the torpor nadir phase (ZT04), the Cardiac Hypertrophy Signalling is subsequently down-regulated, thereby controlling cell proliferation, growth and survival. This is consistent with studies in lemurs in both BAT and WAT, where a major decrement of relative ERK1/2 and MAPK protein phosphorylation levels was observed during torpor due to decreased levels of mitogenic stimuli, implying suppression of proliferation and cell growth during torpor in response to cellular stress and implying the enforcement of tissue-specific survival programmes (Biggar et al., 2015b). Processes responsible for the maintenance of glucose metabolism and the circadian clock, which are related to the insulin secretion signalling pathway and Sirtuins, are also part of cellular homeostasis (Zhou et al., 2018). These two appear to be closely related in their regulation. Here, both showed a similar pattern of

regulation during torpor (see Figure 10). In the ZT04 phase, upregulation of insulin secretion was predicted, as well as upregulation of the Sirtuin signalling pathway. Upregulation of SIRT1 increases insulin secretion and is involved in anti-apoptotic and protective functions as result of cellular stress through various pathways, such as distinct histone targets alterations and the transcription factor p53 (Rouble & Storey, 2015). Remarkably, hibernating organisms do not show signs of hyperglycaemia with the consequent glycosuria and gradual depletion of energy, which is known from fasting states, despite the elevated insulin resistance (Gilbert et al., 2015; Zhou et al., 2018). In torpor conditions, insulin secretion is maintained at levels that provide sufficient insulin to limit hepatic glucose release (Bertile et al., 2021).

In addition, the increased amount of circulating insulin leads to a further suppression of hepatic glucose release due to torpid individuals not feeding or reabsorbing nutrients (Palumbo et al., 1983). Consistent with this regulation, analysis of the protein level of SIRT1, SIRT2, SIRT3 and SIRT6 in 4 ground squirrel tissues showed increased relative levels of liver muscle BAT during the torpor-arousal cycle (Rouble & Storey, 2015). In other systems, increases in SIRT6 are established as consequence of oxidative stress, bolstering repair of DNA double-strand breaks to resolve genomic detriment from increased ROS prevalence, and are noted to be downregulated during the post torpor phase (ZT16), which appears to indicate a resting phase (Rouble & Storey, 2015). Nuclear factor erythroid 2-related factor 2 (Nrf2) is a basic leucine transcription factor responsible for modulating a number of detoxification and antioxidant enzymes thus the "general signalling pathway of xenobiotic metabolism" also involves the regulation of Nrf2 (Y. Li et al., 2012). Nrf2 is active during the ZT04 torpor phase, as it is indispensable for maintaining cellular homeostasis, especially in response to oxidative stress, by transcriptional regulation of a wide range of different xenobiotic transporters, detoxification proteins and antioxidant carriers (Tessier et al., 2021). This is consistent with results in the nadir torpor phase (ZT04), and further increases their activation during the arousal phase (ZT16) as reaction to oxidative stress, activating a number of antioxidative genes and linking this alarm signal to the immune system (Tessier et al., 2021). This is also consistent with pre-existing data of the late torpor phase in thirteen-lined ground squirrels, where in liver, heart and brown

adipose tissue the level of ROS was increased and an excess of pro-oxidants were detected (Wei et al., 2019; Tessier et al., 2021). This caused Nrf2/Keap1 signalling and thus phosphorylation of Nrf2. Furthermore, it was suggested that activation of Nrf2 transcription factors is maximal during the arousal of the torpor (ZT07), when tremendous increases in blood oxygen occur within minutes, making the hibernator more susceptible to harmful ROS (Wei et al., 2019). This in turn indicates a working together in the organism, if the gene expression machinery is running and activated during arousal (ZT07) and goes into a downregulated or resting state in the post torpor phase (ZT16).

5.1.4 Senescence

Two aging-related signalling pathways were identified, first the "senescence pathway" and second "telomerase signalling", which are downregulated during torpor (ZT04) and upregulated during arousal (ZT07). These findings are also in agreement with available reports on ground squirrels, where this process could not actually be observed during torpor but is rather assumed to be a transitional arrest period during torpor (ZT04), thereby suspending cell division and growth (Wu and Storey, 2012). Natural hypometabolic suppression of cell cycle pathways in the torpor state might also explain these observations. It has been observed in telomere studies in *P. sungorus* that attenuated cell turnover during torpor may minimise relative telomere length (RTL) loss (Turbill et al., 2012). In addition to reducing energy expenditure, the use of torpor may also delay somatic aging during periods of unfavourable environmental conditions. This is also denoted by changes in telomerase signalling that regulates telomere length (López-Otín et al., 2013). The IPA prediction indicates that telomerase enzyme activity, which would guard cells against premature ageing, is strongly downregulated (ZT04). If the senescence or aging pattern is inactive or down-regulated, telomerase has no role in protecting against aging, a behaviour seen in the nadir phase (ZT04), in contrast to the arousal phase (ZT07) where senescence related pathways can be observed to be activated while telomerase signalling is still down-regulated, this could be due to the fact that aging is still active if telomerase is not active or downregulated and is reversible with telomerase activation (Jaskelioff et al., 2011). The process of senescence decays in the post torpor phase (ZT16), thus telomerase signalling does not differ from that of controls.

5.2 Part 2: Whole-body regulatory mechanisms during torpor are reflected in blood transcriptomics

Gene expression results of the *P. sungorus* blood transcriptome will be discussed in the three proposed categories, Basic cellular mechanisms, Immune system and Other organs; based on the findings of TM_{IPA} during nadir torpor, as already published in (Cuyutupa et al., 2023).

5.2.1 Basic cellular mechanisms

During torpor nadir (ZT04), network analysis of 148 TM_{IPA} predicted an overall inhibition of diseases and function on this category (Figure 13 and 14). This is in consistent to previous analysis outlining that a balanced transcription is required according to cell function demands, as protein biosynthesis is an energetically costly cellular process (van Breukelen & Martin, 2002). Furthermore, transcriptional depression during torpor is argued to be a reversible process as low temperatures are associated with inhibition of transcription onset and subsequent elongation (Zhang et al., 2015). In this work, the T_a were maintained constant at 20 ± 1 °C suggesting that the main reason for the observed transcriptional downregulation is energy conservation rather than cold. TM_{IPA} regulation during nadir torpor (ZT04; Figure 13) indicates that both cellular homeostasis and autophagy signalling pathways were downregulated. Sustaining signalling pathway function, proper regulation of ion pumps and adequate protein turnover according to energy demands are extremely critical for maintaining a cellular physiological balance (Biggar et al., 2015a). Cell cycle control, growth and survival during torpor are controlled by effects of central cellular keys such as AMPK and mTOR (Storey et al., 2010). Autophagocytosis degrades damaged cell structures to build new cells or to provide ATP and metabolites. Autophagy is activated during torpor (Mizushima & Levine, 2010; Dias et al., 2021), contrary to the IPA prediction. However, torpor associated autophagy is typically assessed in the arousal phase, during which functionally impaired proteins are cleared and energy demand is high (Wiersma et al., 2018), and thus does not well reflect the metabolic state during torpor nadir. The predicted down-regulation of apoptosis and necrosis match existing literature pointing to diminished apoptotic activity and in return promotion of cellular survival,

modification of signalling pathways, establishment of reversible post-translational protein modifications, and mechanisms that prevent antioxidative damage (Logan & Storey, 2017; Jain & Jani, 2020), also contributing to the prevention of necrotic tissue damage (Bouma et al., 2011). The TM_{IPA} based prediction of inhibited basic cellular mechanisms in torpid *P. sungorus* clearly shows that the full blood transcriptome is a function representation of changes affecting the whole organism.

5.2.2 Immune System

According to TM_{IPA} predictions, the immune system associated processes also show inhibition or activation of expression profiles (Figure 13 and 14). In line with TM_{IPA} prediction results inhibition of lymphopoiesis during winter periods was previously described by Bouma et al. 2010. Further, the predicted inhibition of leukocyte recruitment and migratory potential matches retention of the majority of the immune cell pool as observed in lung intestine, and spleen (Bouma et al., 2010, 2013). Decreased T_b is considered to be the main factor in regulation of immune cell number and function during torpor (Bouma et al., 2011). Yet, the predicted low number of T-lymphocytes in the Djungarian hamster implies the underlying mechanisms to be partially independent of body temperature. IPA predictions are further confirmed by showing an increased number of B-lymphocytes despite overall lymphocyte retention, which corresponds to findings in the intestinal connective tissue of ground squirrels and bats (Bouma et al., 2011; Kurtz et al., 2021). Additionally, this demonstrates that the transcriptomic alterations found in blood resemble the protective immune state in the gut during torpor, both in microbial defence and inflammation. The limited repertoire of immune cells during dormancy may increase susceptibility to infection (Bouma et al., 2010). Moreover, the predicted decrease in T-lymphocyte activation is consistent with observations made in hibernating artic yacutian ground squirrels, where T-lymphocytes showed reduced proliferation after stimulation with the mitogen Concanavalin A (Novoselova et al., 2000). Increased rates of viral infections were predicted based on the downregulation of various genes related to antiviral immunity during torpor. Previous studies in hibernators reported a reduction in IFNγ production after stimulation and decreased numbers of activated CD8+ T cells through cytolytic mechanisms (Bouma et al., 2010). Despite these results torpid mammals do not experience

viral infection or reactivation. Most likely viral quiescence is caused by the overall reduction of metabolic and transcriptional activity of the host during torpor (Gerow et al., 2019).

5.2.3 Other organs

Organ damage is inevitable due to the cellular stress caused by torpor, however modulations of gene expression during the daily torpor cycle make the organism capable of resisting such injury. The adaptive effects that were identified in blood cells in different organs such as the heart, kidney and liver, inhibition of proliferation, different protective effects and inflammation during the torpor nadir and comparison with the different other phases can be seen in Figure 13 and 14.

The transcriptomic state further implies reduced blood vessel formation (angiogenesis), probably due to a stop of cellular proliferation during dormancy as it is an energy intensive process. Additionally, it has been observed that during hibernation a great amount of cells is reversibly arrested in the G0 step of the cell cycle until arousal (Dias et al., 2021).

In cardiac tissue of torpid animals cardiomyocytes show G0-associated hypertrophy to compensate for the elevated workload due to increased blood viscosity and reduced blood vessel elasticity (Zhao et al., 2011; Xie et al., 2021). Yet, during torpor the renal function is extremely depressed resulting in minimal glomerular filtration rate and thus urine production, mainly due to vasoconstriction of the kidney due to hypothermia and decreased blood flow caused by sparse cardiac output (Jani et al., 2012, 2013).

Despite this, no structural remodelling has been observed to date, which ensures readily available renal function directly after arousal. The reduction of hepatocyte proliferation during torpor is mainly caused by reversible cessation of cellular activity (Wu & Storey, 2012). Tissue damage is rapidly regenerated by hepatocytes of active animals during the summer season due to their formidable proliferative capabilities.

The lower functional performance of heart, kidney, and liver as well as regarding immunity indicate overall decreased inflammatory levels during torpor. The transcriptional

downregulation the transmembrane receptor TLR4 observed in the TM_{IPA} further supports this. TLR4 is a high abundance receptor during cardiac inflammation (Fairweather, 2007), suggesting a diminished organ specific inflammatory capacity during torpor. Furthermore, hepatic inflammation, immune activation and corresponding signalling pathways have previously been described to be greatly suppressed in torpid animals (Kurtz et al., 2006).

Hibernators have evolved a protective mechanism that exploit signalling pathway plasticity to precisely regulate ion exchange rates for fine-tuning basal cardiac functions such as contraction and relaxation. Additionally, the upregulation of antioxidant enzymes and anti-apoptotic genes throughout a torpor cycle serves to protect against cardiac tissue damage (Givre et al., 2021; Xie et al., 2021). In the kidney similar adaptations help to resist blood (re-)perfusion related injury and low T_b (Jani et al., 2013). Furthermore, these organ protective adjustments associated with torpor and ischemic reperfusion (IR) have also been observed in liver hepatocytes where upregulation of both antioxidant and anti-apoptotic proteins occurs (Kurtz et al., 2021). Unpublished data also indicates, protection against an impaired glucose metabolism and brain damage in hibernating animals (Betz & Enerbäck, 2015; de Veij Mestdagh et al., 2021).

Overall, protection from organ damage in torpid animals is provided by adaptations such as reduced MR, respiratory rate, T_b and pre-protection mechanisms mainly present in the heart, liver and kidney. Otherwise, in the case of species, that do not exhibit torpor, specific adaptions hibernators would suffer from heart attacks, cardiac arrhythmias, organ damage and IR lesions during arousal. Even more incredible, this genetic programme seems to be activated independently of T_b.

5.3 Part 3: Comparison of metabolic adaptations reflected in the blood transcriptome of *P. sungorus* and humans overwintering at the Antarctic Concordia station

This part focused on the adaptive metabolic processes in the blood samples of Concordia expeditioners and how they respond differently, thus showing parallels with animals that are capable of exhibiting torpor, as during torpor MR is reduced to basal levels and

numerous adaptations caused by low temperatures, energy demand, lack of nutrients and cellular stress occur. To date, metabolic changes in humans overwintering in Antarctica have not been compared with metabolic adaptations in hibernating animals or animals capable of daily torpor, despite environmental and physiological similarities. This question is addressed here in a comparative manner. For the studies that frame adaptations of the metabolism, subjects voluntarily agree to be part of the research in the Antarctic stations. This environment is extremely harsh, inhospitable and cold, which altogether leads to severe stress on the body causing changes that are detectable in the organisms through different stress response tests. Comparative results together with torpor analysis at the transcriptomic level revealed that gene expression regulations were very pronounced for the EIF2 signalling pathway at all sample times and comparable with the arousal phase of torpid animals (ZT07). In addition to strong upregulation of the EIF2 signalling pathway most immune pathways were inactivated. EIF2 modulates proteostasis, extends lifespan and is likely to be high in Concordia hibernates as low glucose, nitrogen or amino acid conditions activate EIF2α kinases (Jiménez-Saucedo et al., 2021). It may be that the high levels of stress result from the growing insufficiency of vital nutrients produced by cellular processes (Choukèr, 2020). Furthermore, EIF2 activity has been associated with senescence in animal models, where a decrease in longevity was revealed in incapable cells of phosphorylating EIF2α and thus reduce overall translation (López-Otín et al., 2013). Aging is counteracted in two ways, by reducing the generation of new proteins; and by promoting limited gene translation (Martín et al., 2013). In these results the sensing signal is upregulated (January to October) in all phases, which is comparable to the arousal phase (ZT07) thus the telomerase signal is upregulated in all months of the season (January to October). The higher the activity and upregulation of the senescence pattern, the stronger the telomerase activity to counteract aging. The upregulation of the ERK/MAPK pathway and the other cell growth and maintenance pathways (April and July comparable to the arousal phase, ZT07) is coupled to glucose deprivation (Graham et al., 2012) and modulates transcription to handle oxidative cellular stress (López-Otín et al., 2013). As a response, elevated levels of insulin are secreted, as shown for the time points January, April and July in comparison to torpor and arousal (ZT04, ZT07). While stopping protein synthesis seems to be coupled to potential severe cellular damage (Sanchez et al., 2019),

stress associated activating phosphorylation of EIF may enhance the cell viability by activation of autophagy pathways (Pakos-Zebrucka et al., 2016). Nevertheless, EIF2α dependent regulation of immune response and autophagy via post-translational modifications is still an active research topic. TGF-β, an important, pleiotropic signalling molecule, regulates amongst others lymphocyte viability, growth, and phenotypic conversion (Fortunel et al., 2000). Furthermore, it is a key component in the intricate process of leukocyte activation, chemotaxis, and immune tolerance, significantly influencing the overall immune response (Li et al., 2006). Thus this upregulated signal (January to October) inhibits the self or non-detrimental antigen immuno-recognition while retaining the ability to respond to pathogenic agents (Figure 17). What can be seen is that the B cell signalling pathways are active (B cell Receptor Signalling and Chemokine Signalling) in the months of April and July and is comparable to the ZT07 phase of torpor.

5.4 Limitations

The data was compiled from a keyword-based literature search. It is thus possible, that some literature on specific hibernating species could not be retrieved with the used keyword filter. All reviewed organs have well documented immune system specific genetic changes upon hibernation. A potential explanation for the high similarity of the compared data is the ubiquitous presence of tissue resident immune cells, that will even persist in perfused tissue. Overall, a distinct, common gene set related to a decreased immune capacity during torpor can be observed when comparing blood and other organs.

Also, it is questionable how well the washing and cleaning procedures of the organs treated in each of these studies were carried out, how free of blood they were and, therefore, whether this is the reason for the number of similarities in our analysis. In addition, for complete analysis and identification of up- and downregulated genes within a species, a more detailed transcriptome analysis of all organs from the same specimen, with and without blood, could be considered in the future to verify validations. Furthermore, database about the progression of infections in humans overwintering at the Antarctic Concordia station during and after the isolation period at Concordia were not collected at

the day of the blood sample. Thus, the use of drugs to combat discomfort or symptoms of illness was not collected, in order to check whether this had an influence on the results.

6 Conclusions

(1) The suppression of cellular processes in the five presented categories (gene expression, protein metabolism, immune system, cellular growth and maintenance, and senescence), whether due to low temperatures or to conserve energy, is a compensation of all systems to keep the animal organism in torpor state with life, and in turn, in species capable of torpor, a reversible process. In this part of the work, it was shown that during torpor entry (ZT01), there were in general no remarkable changes, and in most cases no differences with the controls. In contrast to this, the machinery of transcriptional proliferation, translation and protein production was largely arrested during nadir torpor (ZT04) and active during arousal (ZT07). The torpor nadir-arousal torpor phase (ZT04-ZT07) during the daily torpor, has an "off-on system", where it is not yet clear which mechanism shuts-down first, nor how long time exactly everything is fully active. On the other hand, the data show that the post-torpor phase is a relative resting phase after the rapid "switched-on" in the arousal phase.

(2) Processes during torpor based on TM_{IPA} findings are shut down, as comparison with the literature have shown, with other hibernators regardless of torpor type (daily torpor, hibernation or estivation), duration (days or months) or species (rodents, primates, carnivores, and others). While the nadir phase is heavily associated with global cellular stress, tissue damage during this process is actively counteracted by increased production of antioxidants and downregulation of pro-apoptotic, immune-related, and generally energy intensive pathways. Additionally, the presented data clearly shows that blood mirrors the torpor induced genetic programme of other organs.

(3) Canonical pathways presented comparatively with the torpor timepoints (ZT01-16) and the samples of the humans overwintering at the Antarctic Concordia station,

have a lot of similarity in the immune system with the ZT04 phase of the daily torpor, however they seem to be in general in a “continuous arousal” phase as there is a great analogy with the arousal phase (ZT07). With EIF2, TGF-β signalling, SUMOylation and Telomerase Signalling as the most highly upregulated pathways in the humans overwintering at the Antarctic Concordia station. In contrast, the Post phase of both (*P. sungorus* and humans overwintering at the Antarctic Concordia station), appears to be like a resting phase for the organism where either a downregulated mechanism is shown or in some cases no change was found at all compared to the controls with the controls.

7 Outlook

The presented results suggest blood transcriptomics as an accessible and representative analysis method to track and unravel torpor associated metabolic changes in mammals. To further validate this claim blood and tissue of different organs of the same individuals in the respective torpor stages need to be compared in a future work. However, evaluation software, reference genomes of different torpor type, model organisms and the levels of statistical testing for various torpor exhibiting species need to be standardised first to allow for comparable results that also enable integration from and into the work of other groups dedicated to torpor inversion.

Additionally, to provide evidence of torpor as an anchoring system in human newborns a comparative transcriptome analysis of newborn blood samples is currently in progress. Three different timepoints are evaluated, (i) intra-utero life, to show potential torpor related adaptations, (ii) the transition to extra-uterine life, and (iii) postnatal life to verify the capacity for torpor is inhibited or silenced due to metabolic increase in humans a few days after birth.

8 References

Armstrong, C., & Staples, J. F. (2010). The role of succinate dehydrogenase and oxaloacetate in metabolic suppression during hibernation and arousal. Journal of Comparative Physiology B, 180(5), 775–783. https://doi.org/10.1007/s00360-010-0444-3

Arnold, W. (1995). Social Behaviour and Telemetric Assessment of Thermoregulation in Hibernating Marmots. In E. Alleva, A. Fasolo, H.-P. Lipp, L. Nadel, & L. Ricceri (Eds.), Behavioural Brain Research in Naturalistic and Semi-Naturalistic Settings (pp. 395–411). Springer Netherlands. https://doi.org/10.1007/978-94-011-0091-5_22

Baggiolini, M., Dewald, B., & Moser, B. (1993). lnterleukin-8 and Related Chemotactic Cytokines—CXC and CC Chemokines. In Advances in Immunology (Vol. 55, pp. 97–179). Elsevier. https://doi.org/10.1016/S0065-2776(08)60509-X

Bartsiokas, A., & Arsuaga, J. L. (2018). Hibernation, puberty and chronic kidney disease in troglodytes from Spain half a million years ago [Preprint]. PeerJ Preprints. https://doi.org/10.7287/peerj.preprints.27370v1

Behrends, J. C., Bischofberger, J., Deutzmann, R., Ehmke, H., Frings, S., & Grissmer, S. (2021a). Physiologie (4., unveränderte Auflage). Thieme. doi:10.1055/b000000462

Behrends, J. C., Bischofberger, J., Deutzmann, R., Ehmke, H., Frings, S., & Grissmer, S. (2021b). Physiologie (4., unveränderte Auflage). Thieme. doi:10.1055/b000000462

Benson, H., Malhotra, M. S., Goldman, R. F., Jacobs, G. D., & Hopkins, P. J. (1990). Three Case Reports of the Metabolic and Electroencephalographic Changes during Advanced Buddhist Meditation Techniques. Behavioral Medicine, 16(2), 90–95. https://doi.org/10.1080/08964289.1990.9934596

Bertile, F., Habold, C., Le Maho, Y., & Giroud, S. (2021). Body Protein Sparing in Hibernators: A Source for Biomedical Innovation. Frontiers in Physiology, 12, 634953. https://doi.org/10.3389/fphys.2021.634953

Betz, M. J., & Enerbäck, S. (2015). Human Brown Adipose Tissue: What We Have Learned So Far. Diabetes, 64(7), 2352–2360. https://doi.org/10.2337/db15-0146

Biggar, K. K., Wu, C.-W., Tessier, S. N., Zhang, J., Pifferi, F., Perret, M., & Storey, K. B. (2015a). Modulation of Gene Expression in Key Survival Pathways During Daily Torpor in the Gray Mouse Lemur, Microcebus murinus. Genomics, Proteomics & Bioinformatics, 13(2), 111–118. https://doi.org/10.1016/j.gpb.2015.03.001

Biggar, K. K., Wu, C.-W., Tessier, S. N., Zhang, J., Pifferi, F., Perret, M., & Storey, K. B. (2015b). Primate Torpor: Regulation of Stress-activated Protein Kinases During Daily Torpor in the Gray Mouse Lemur, Microcebus murinus. Genomics, Proteomics & Bioinformatics, 13(2), 81–90. https://doi.org/10.1016/j.gpb.2015.03.002

Botchkareva, N. V. (2017). The Molecular Revolution in Cutaneous Biology: Noncoding RNAs: New Molecular Players in Dermatology and Cutaneous Biology. Journal of Investigative Dermatology, 137(5), e105–e111. https://doi.org/10.1016/j.jid.2017.02.001

Bouma, H. R., Carey, H. V., & Kroese, F. G. M. (2010). Hibernation: The immune system at rest? Journal of Leukocyte Biology, 88(4), 619–624. https://doi.org/10.1189/jlb.0310174

Bouma, H. R., Dugbartey, G. J., Boerema, A. S., Talaei, F., Herwig, A., Goris, M., van Buiten, A., Strijkstra, A. M., Carey, H. V., Henning, R. H., & Kroese, F. G. M. (2013). Reduction of body temperature governs neutrophil retention in hibernating and nonhibernating animals by margination. Journal of Leukocyte Biology, 94(3), 431–437. https://doi.org/10.1189/jlb.0611298

Bouma, H. R., Kroese, F. G. M., Kok, J. W., Talaei, F., Boerema, A. S., Herwig, A., Draghiciu, O., van Buiten, A., Epema, A. H., van Dam, A., Strijkstra, A. M., & Henning, R. H. (2011). Low body temperature governs the decline of circulating lymphocytes during hibernation through sphingosine-1-phosphate. Proceedings of the National Academy of Sciences, 108(5), 2052–2057. https://doi.org/10.1073/pnas.1008823108

Brandes, R., Lang, F., & Schmidt, R. F. (Eds.). (2019). Physiologie des Menschen: Mit Pathophysiologie. Springer Berlin Heidelberg. https://doi.org/10.1007/978-3-662-56468-4

Bryan-Brown, C. W. (1988). Blood flow to organs: Parameters for function and survival in critical illness. Critical Care Medicine, 16(2), 170-178. PMID: 3277775.

Buchheim, J.-I., Billaud, J.-N., Feuerecker, M., Strewe, C., Dangoisse, C., Osterman, A., Mehta, S., Crucian, B., Schelling, G., & Choukér, A. (2020). Exploratory RNA-seq analysis in healthy subjects reveals vulnerability to viral infections during a 12- month period of isolation and confinement. Brain, Behavior, & Immunity - Health, 9, 100145. https://doi.org/10.1016/j.bbih.2020.100145

Carey, F. G., & Lawson, K. D. (1973). Temperature regulation in free-swimming bluefin tuna. Comparative Biochemistry and Physiology Part A: Physiology, 44(2), 375–392. https://doi.org/10.1016/0300-9629(73)90490-8

Cerri, M., Tinganelli, W., Negrini, M., Helm, A., Scifoni, E., Tommasino, F., Sioli, M., Zoccoli, A., & Durante, M. (2016). Hibernation for space travel: Impact on radioprotection. Life Sciences in Space Research, 11, 1–9. https://doi.org/10.1016/j.lssr.2016.09.001

Choukèr, A. (Ed.). (2020). Stress Challenges and Immunity in Space: From Mechanisms to Monitoring and Preventive Strategies. Springer International Publishing. https://doi.org/10.1007/978-3-030-16996-1

Chow, B. A., Donahue, S. W., Vaughan, M. R., McConkey, B., & Vijayan, M. M. (2013). Serum Immune-Related Proteins are Differentially Expressed during Hibernation in the American Black Bear. PLoS ONE, 8(6), e66119. https://doi.org/10.1371/journal.pone.0066119

Christian, N., & Geiser, F. (2007). To use or not to use torpor? Activity and body temperature as predictors. Naturwissenschaften, 94(6), 483–487. https://doi.org/10.1007/s00114-007-0215-5

Cooper, S. T., Richters, K. E., Melin, T. E., Liu, Z., Hordyk, P. J., Benrud, R. R., Geiser, L. R., Cash, S. E., Simon Shelley, C., Howard, D. R., Ereth, M. H., & Sola-Visner, M. C. (2012). The hibernating 13-lined ground squirrel as a model organism for potential cold storage of platelets. American Journal of Physiology-Regulatory, Integrative and Comparative Physiology, 302(10), R1202–R1208. https://doi.org/10.1152/ajpregu.00018.2012

Crick, F. (1970). Central Dogma of Molecular Biology. Nature, 227, 561–563. https://doi.org/10.1038/227561a0.

Cuarental, L., Sucunza-Sáenz, D., Valiño-Rivas, L., Fernandez-Fernandez, B., Sanz, A. B., Ortiz, A., Vaquero, J. J., & Sanchez-Niño, M. D. (2019). MAP3K kinases and kidney injury. Nefrología (English Edition), 39(6), 568–580. https://doi.org/10.1016/j.nefroe.2019.12.004

Cubuk, C., Bank, J. H. H., & Herwig, A. (2016). The Chemistry of Cold: Mechanisms of Torpor Regulation in the Siberian Hamster. Physiology, 31(1), 51–59. https://doi.org/10.1152/physiol.00028.2015

Cubuk, C., Kemmling, J., Fabrizius, A., & Herwig, A. (2017). Transcriptome Analysis of Hypothalamic Gene Expression during Daily Torpor in Djungarian Hamsters (Phodopus sungorus). Frontiers in Neuroscience, 11. https://doi.org/10.3389/fnins.2017.00122

Cubuk, C., Markowsky, H., & Herwig, A. (2017). Hypothalamic control systems show differential gene expression during spontaneous daily torpor and fasting-induced torpor in the Djungarian hamster (Phodopus sungorus). PLOS ONE, 12(10), e0186299. https://doi.org/10.1371/journal.pone.0186299

Cuyutupa, V. R., Moser, D., Diedrich, V., Cheng, Y., Billaud, J.-N., Haugg, E., Singer, D., Bereiter-Hahn, J., Herwig, A., & Choukér, A. (2023). Blood transcriptomics mirror regulatory mechanisms during hibernation—A comparative analysis of the Djungarian

hamster with other mammalian species. Pflügers Archiv - European Journal of Physiology, 475(10), 1149–1160. https://doi.org/10.1007/s00424-023-02842-8

De Boer, B., Lourens, L. J., & Van De Wal, R. S. W. (2014). Persistent 400,000-year variability of Antarctic ice volume and the carbon cycle is revealed throughout the Plio-Pleistocene. Nature Communications, 5(1), 2999. https://doi.org/10.1038/ncomms3999

de Veij Mestdagh, C. F., Timmerman, J. A., Koopmans, F., Paliukhovich, I., Miedema, S. S. M., Goris, M., van der Loo, R. J., Krenning, G., Li, K. W., Mansvelder, H. D., Smit, A. B., Henning, R. H., & van Kesteren, R. E. (2021). Torpor enhances synaptic strength and restores memory performance in a mouse model of Alzheimer's disease. Scientific Reports, 11(1), 15486. https://doi.org/10.1038/s41598-021-94992-x

Dias, I. B., Bouma, H. R., & Henning, R. H. (2021). Unraveling the Big Sleep: Molecular Aspects of Stem Cell Dormancy and Hibernation. Frontiers in Physiology, 12, 624950. https://doi.org/10.3389/fphys.2021.624950

Diedrich, V., Haugg, E., Van Hee, J., & Herwig, A. (2023). Role of glucose in daily torpor of Djungarian hamsters (Phodopus sungorus): Challenge of continuous in vivo blood glucose measurements. American Journal of Physiology-Regulatory, Integrative and Comparative Physiology, 325(4), R359–R379. https://doi.org/10.1152/ajpregu.00040.2023

Dugbartey, G. J., Talaei, F., Houwertjes, M. C., Goris, M., Epema, A. H., Bouma, H. R., & Henning, R. H. (2015). Dopamine treatment attenuates acute kidney injury in a rat model of deep hypothermia and rewarming – The role of renal H2S-producing enzymes. European Journal of Pharmacology, 769, 225–233. https://doi.org/10.1016/j.ejphar.2015.11.022

Fairweather, D. (2007). Regulating Inflammation in the Heart. International Journal of Biomedical Science : IJBS, 3(1), 9–13. PMID: 23675015; PMCID: PMC3614623. 23675015

Fletcher, D., & Sarkar, M. (2013). Psychological Resilience: A Review and Critique of Definitions, Concepts, and Theory. European Psychologist, 18(1), 12–23. https://doi.org/10.1027/1016-9040/a000124

Forget-Klein, É., & Green, D. M. (2021). Toads use the subsurface thermal gradient for temperature regulation underground. Journal of Thermal Biology, 99, 102956. https://doi.org/10.1016/j.jtherbio.2021.102956

Fortunel, N. O., Hatzfeld, A., & Hatzfeld, J. A. (2000). Transforming growth factor-beta: Pleiotropic role in the regulation of hematopoiesis. Blood, 96(6), 2022-36. PMID: 10979943.

Frerichs, K. U., Smith, C. B., Brenner, M., DeGracia, D. J., Krause, G. S., Marrone, L., Dever, T. E., & Hallenbeck, J. M. (1998). Suppression of protein synthesis in brain during hibernation involves inhibition of protein initiation and elongation. Proceedings of the National Academy of Sciences, 95(24), 14511–14516. https://doi.org/10.1073/pnas.95.24.14511

Frésard, L., Smail, C., Ferraro, N. M., Teran, N. A., Li, X., Smith, K. S., Bonner, D., Kernohan, K. D., Marwaha, S., Zappala, Z., Balliu, B., Davis, J. R., Liu, B., Prybol, C. J., Kohler, J. N., Zastrow, D. B., Reuter, C. M., Fisk, D. G., Grove, M. E., … Care4Rare Canada Consortium. (2019). Identification of rare-disease genes using blood transcriptome sequencing and large control cohorts. Nature Medicine, 25(6), 911–919. https://doi.org/10.1038/s41591-019-0457-8

Geiser, F. (2010). Aestivation in Mammals and Birds. In C. Arturo Navas & J. E. Carvalho (Eds.), Aestivation (Vol. 49, pp. 95–111). Springer Berlin Heidelberg. https://doi.org/10.1007/978-3-642-02421-4_5

Geiser, F. (2011). Hibernation: Endotherms. In John Wiley & Sons, Ltd (Ed.), eLS (1st ed.). Wiley. https://doi.org/10.1002/9780470015902.a0003215.pub2

Geiser, F. (2021). Ecological Physiology of Daily Torpor and Hibernation. Springer International Publishing. https://doi.org/10.1007/978-3-030-75525-6

Geiser, F., & Ruf, T. (1995). Hibernation versus Daily Torpor in Mammals and Birds: Physiological Variables and Classification of Torpor Patterns. Physiological Zoology, 68(6), 935–966. https://doi.org/10.1086/physzool.68.6.30163788

Gerow, C. M., Rapin, N., Voordouw, M. J., Elliot, M., Misra, V., & Subudhi, S. (2019). Arousal from hibernation and reactivation of Eptesicus fuscus gammaherpesvirus (Ef HV) in big brown bats. Transboundary and Emerging Diseases, 66(2), 1054–1062. https://doi.org/10.1111/tbed.13102

Gilbert, R. E., Thai, K., Advani, S. L., Cummins, C. L., Kepecs, D. M., Schroer, S. A., Woo, M., & Zhang, Y. (2015). SIRT1 activation ameliorates hyperglycaemia by inducing a torpor-like state in an obese mouse model of type 2 diabetes. Diabetologia, 58(4), 819–827. https://doi.org/10.1007/s00125-014-3485-4

Girdwood, D. W. H., Tatham, M. H., & Hay, R. T. (2004). SUMO and transcriptional regulation. Seminars in Cell & Developmental Biology, 15(2), 201–210. https://doi.org/10.1016/j.semcdb.2003.12.001

Givre, L., Crola Da Silva, C., Swenson, J. E., Arnemo, J. M., Gauquelin-Koch, G., Bertile, F., Lefai, E., & Gomez, L. (2021). Cardiomyocyte Protection by Hibernating Brown Bear Serum: Toward the Identification of New Protective Molecules Against Myocardial Infarction. Frontiers in Cardiovascular Medicine, 8, 687501. https://doi.org/10.3389/fcvm.2021.687501

Grabek, K. R., Martin, S. L., & Hindle, A. G. (2015). Proteomics approaches shed new light on hibernation physiology. Journal of Comparative Physiology B, 185(6), 607–627. https://doi.org/10.1007/s00360-015-0905-9

Graham, N. A., Tahmasian, M., Kohli, B., Komisopoulou, E., Zhu, M., Vivanco, I., Teitell, M. A., Wu, H., Ribas, A., Lo, R. S., Mellinghoff, I. K., Mischel, P. S., & Graeber, T. G. (2012). Glucose deprivation activates a metabolic and signaling amplification loop leading to cell death. Molecular Systems Biology, 8(1), 589. https://doi.org/10.1038/msb.2012.20

Gröndahl, F., Sidenmark, J., & Thomsen1, A. (2009). Survey of waste water disposal practices at Antarctic research stations. Polar Research, 28(2), 298–306. https://doi.org/10.1111/j.1751-8369.2008.00056.x

Ha, M. K., Bartholomeus, E., Van Os, L., Dandelooy, J., Leysen, J., Aerts, O., Siozopoulou, V., De Smet, E., Gielen, J., Guerti, K., De Maeseneer, M., Herregods, N., Lechkar, B., Wittoek, R., Geens, E., Claes, L., Zaqout, M., Dewals, W., Lemay, A., … Ogunjimi, B. (2022). Blood transcriptomics to facilitate diagnosis and stratification in pediatric rheumatic diseases – a proof of concept study. Pediatric Rheumatology, 20(1), 91. https://doi.org/10.1186/s12969-022-00747-x

Hampton, M., Melvin, R. G., & Andrews, M. T. (2013). Transcriptomic Analysis of Brown Adipose Tissue across the Physiological Extremes of Natural Hibernation. PLoS ONE, 8(12), e85157. https://doi.org/10.1371/journal.pone.0085157

Hampton, M., Melvin, R. G., Kendall, A. H., Kirkpatrick, B. R., Peterson, N., & Andrews, M. T. (2011). Deep Sequencing the Transcriptome Reveals Seasonal Adaptive Mechanisms in a Hibernating Mammal. PLoS ONE, 6(10), e27021. https://doi.org/10.1371/journal.pone.0027021

Harlow, H. J., Lohuis, T., Beck, T. D. I., & Iaizzo, P. A. (2001). Muscle strength in overwintering bears. Nature, 409(6823), 997–997. https://doi.org/10.1038/35059165

Haugg, E., Herwig, A., & Diedrich, V. (2021). Body Temperature and Activity Adaptation of Short Photoperiod-Exposed Djungarian Hamsters (Phodopus sungorus): Timing, Traits, and Torpor. Frontiers in Physiology, 12, 626779. https://doi.org/10.3389/fphys.2021.626779

Heldmaier, G., Ortmann, S., & Elvert, R. (2004). Natural hypometabolism during hibernation and daily torpor in mammals. Respiratory Physiology & Neurobiology, 141(3), 317–329. https://doi.org/10.1016/j.resp.2004.03.014

Heldmaier, G., & Steinlechner, S. (1981). Seasonal pattern and energetics of short daily torpor in the Djungarian hamster, Phodopus sungorus. Oecologia, 48(2), 265–270. https://doi.org/10.1007/BF00347975

Hittel, D., & Storey, K. B. (2002). The translation state of differentially expressed mRNAs in the hibernating 13-lined ground squirrel (Spermophilus tridecemlineatus). Archives of Biochemistry and Biophysics, 401(2), 244–254. https://doi.org/10.1016/S0003-9861(02)00048-6

Hodgson, D. A., Doran, P. T., Roberts, D., & McMinn, A. (2004). Paleolimnological studies from the Antarctic and subantarctic islands. In J. P. Smol, R. Pienitz, & M. S. V. Douglas (Eds.), Long-term Environmental Change in Arctic and Antarctic Lakes (Vol. 8, pp. 419–474). Springer Netherlands. https://doi.org/10.1007/978-1-4020-2126-8_14

Hoffmann, K. (1973). The influence of photoperiod and melatonin on testis size, body weight, and pelage colour in the Djungarian hamster (Phodopus sungorus). Journal of Comparative Physiology, 85(3), 267–282. https://doi.org/10.1007/BF00694233

Hommes, D. W. (2003). Mitogen activated protein (MAP) kinase signal transduction pathways and novel anti-inflammatory targets. Gut, 52(1), 144–151. https://doi.org/10.1136/gut.52.1.144

Huang, W., Liao, C.-C., Han, Y., Lv, J., Lei, M., Li, Y., Lv, Q., Dong, D., Zhang, S., Pan, Y.-H., & Luo, J. (2020). Co-activation of Akt, Nrf2, and NF-κB signals under UPRER in torpid Myotis ricketti bats for survival. Communications Biology, 3(1), 658. https://doi.org/10.1038/s42003-020-01378-2

Humphries, M. M., Thomas, D. W., & Kramer, D. L. (2003). The Role of Energy Availability in Mammalian Hibernation: A Cost-Benefit Approach. Physiological and Biochemical Zoology, 76(2), 165–179. https://doi.org/10.1086/367950

Ihermann-Hella, A., Lume, M., Miinalainen, I. J., Pirttiniemi, A., Gui, Y., Peränen, J., Charron, J., Saarma, M., Costantini, F., & Kuure, S. (2014). Mitogen-Activated Protein Kinase (MAPK) Pathway Regulates Branching by Remodeling Epithelial Cell Adhesion. PLoS Genetics, 10(3), e1004193. https://doi.org/10.1371/journal.pgen.1004193

Jain, S., & Jani, A. (2020). Renal Tubular Cells from Hibernating Squirrels are Protected against Cisplatin Induced Apoptosis. International Journal of Nephrology, 2020, 1–9. https://doi.org/10.1155/2020/6313749

Jani, A., Martin, S. L., Jain, S., Keys, D., & Edelstein, C. L. (2013). Renal adaptation during hibernation. American Journal of Physiology-Renal Physiology, 305(11), F1521–F1532. https://doi.org/10.1152/ajprenal.00675.2012

Jani, A., Orlicky, D. J., Karimpour-Fard, A., Epperson, L. E., Russell, R. L., Hunter, L. E., & Martin, S. L. (2012). Kidney proteome changes provide evidence for a dynamic metabolism and regional redistribution of plasma proteins during torpor-arousal cycles of hibernation. Physiological Genomics, 44(14), 717–727. https://doi.org/10.1152/physiolgenomics.00010.2012

Jaskelioff, M., Muller, F. L., Paik, J.-H., Thomas, E., Jiang, S., Adams, A. C., Sahin, E., Kost-Alimova, M., Protopopov, A., Cadiñanos, J., Horner, J. W., Maratos-Flier, E., & DePinho, R. A. (2011). Telomerase reactivation reverses tissue degeneration in aged telomerase-deficient mice. Nature, 469(7328), 102–106. https://doi.org/10.1038/nature09603

Jiménez-Saucedo, T., Berlanga, J. J., & Rodríguez-Gabriel, M. (2021). Translational control of gene expression by eIF2 modulates proteostasis and extends lifespan. Aging, 13(8), 10989–11009. https://doi.org/10.18632/aging.203018

Khandelwal, S., Bhatia, A., & Mishra, A. (2015). Psychological health in the summer team of an Indian expedition to Antarctica. Journal of Mental Health and Human Behaviour, 20(2), 65. https://doi.org/10.4103/0971-8990.174596

Kirsch, R., Ouarour, A., & Pévet, P. (1991). Daily torpor in the Djungarian hamster (Phodopus sungorus): Photoperiodic regulation, characteristics and circadian organization. Journal of Comparative Physiology A, 168(1), 121–128. https://doi.org/10.1007/BF00217110

Kolde, R. (2019). pheatmap: Pretty Heatmaps. https://CRAN.R-project.org/package=pheatmap

Krämer, A., Green, J., Pollard, J., & Tugendreich, S. (2014). Causal analysis approaches in Ingenuity Pathway Analysis. Bioinformatics, 30(4), 523–530. https://doi.org/10.1093/bioinformatics/btt703

Kurtz, C. C., Lindell, S. L., Mangino, M. J., & Carey, H. V. (2006). Hibernation confers resistance to intestinal ischemia-reperfusion injury. American Journal of Physiology-Gastrointestinal and Liver Physiology, 291(5), G895–G901. https://doi.org/10.1152/ajpgi.00155.2006

Kurtz, C. C., Otis, J. P., Regan, M. D., & Carey, H. V. (2021). How the gut and liver hibernate. Comparative Biochemistry and Physiology Part A: Molecular & Integrative Physiology, 253, 110875. https://doi.org/10.1016/j.cbpa.2020.110875

Larkin, J. E., Yellon, S. M., & Zucker, I. (2003). Melatonin Production Accompanies Arousal from Daily Torpor in Siberian Hamsters. Physiological and Biochemical Zoology, 76(4), 577–585. https://doi.org/10.1086/375436

Lee, Y., & Hallenbeck, J. M. (2013). SUMO and ischemic tolerance. Neuromolecular Medicine, 15(4), 771–781. https://doi.org/10.1007/s12017-013-8239-9

Lee, Y., Miyake, S., Wakita, H., McMullen, D. C., Azuma, Y., Auh, S., & Hallenbeck, J. M. (2007). Protein SUMOylation is Massively Increased in Hibernation Torpor and is Critical for the Cytoprotection Provided by Ischemic Preconditioning and Hypothermia in SHSY5Y Cells. Journal of Cerebral Blood Flow & Metabolism, 27(5), 950–962. https://doi.org/10.1038/sj.jcbfm.9600395

Li, M. O., Wan, Y. Y., Sanjabi, S., Robertson, A.-K. L., & Flavell, R. A. (2006). Transforming growth factor-β regulation of immune responses. Annual Review of Immunology, 24(1), 99–146. https://doi.org/10.1146/annurev.immunol.24.021605.090737

Li, Y., Paonessa, J. D., & Zhang, Y. (2012). Mechanism of Chemical Activation of Nrf2. PLoS ONE, 7(4), e35122. https://doi.org/10.1371/journal.pone.0035122

Lin, X., Wang, Y., Jiang, Y., Xu, M., Pang, Q., Sun, J., Yu, Y., Shen, Z., Lei, R., & Xu, J. (2020). Sumoylation enhances the activity of the TGF-β/SMAD and HIF-1 signaling pathways in keloids. Life Sciences, 255, 117859. https://doi.org/10.1016/j.lfs.2020.117859

Ling, C., & Groop, L. (2009). Epigenetics: A Molecular Link Between Environmental Factors and Type 2 Diabetes. Diabetes, 58(12), 2718–2725. https://doi.org/10.2337/db09-1003

Logan, S. M., & Storey, K. B. (2017). Avoiding apoptosis during mammalian hibernation. Temperature, 4(1), 15–17. https://doi.org/10.1080/23328940.2016.1211071

Logan, S. M., & Storey, K. B. (2018). Pro-inflammatory AGE-RAGE signaling is activated during arousal from hibernation in ground squirrel adipose. PeerJ, 6, e4911. https://doi.org/10.7717/peerj.4911

López-Otín, C., Blasco, M. A., Partridge, L., Serrano, M., & Kroemer, G. (2013). The Hallmarks of Aging. Cell, 153(6), 1194–1217. https://doi.org/10.1016/j.cell.2013.05.039

Lukacs, N. W., Kunkel, S. L., Allen, R., Evanoff, H. L., Shaklee, C. L., Sherman, J. S., Burdick, M. D., & Strieter, R. M. (1995). Stimulus and cell-specific expression of C-X-C

and C-C chemokines by pulmonary stromal cell populations. American Journal of Physiology-Lung Cellular and Molecular Physiology, 268(5), L856–L861. https://doi.org/10.1152/ajplung.1995.268.5.L856

Lyman, C. P. (1982). Hibernation and Torpor in Mammals and Birds. USA: Academic Press.

Ma, Y. L., Zhu, X., Rivera, P. M., Tøien, Ø., Barnes, B. M., LaManna, J. C., Smith, M. A., & Drew, K. L. (2005). Absence of cellular stress in brain after hypoxia induced by arousal from hibernation in Arctic ground squirrels. American Journal of Physiology-Regulatory, Integrative and Comparative Physiology, 289(5), R1297–R1306. https://doi.org/10.1152/ajpregu.00260.2005

Mahlert, B., Gerritsmann, H., Stalder, G., Ruf, T., Zahariev, A., Blanc, S., & Giroud, S. (2018). Implications of being born late in the active season for growth, fattening, torpor use, winter survival and fecundity. eLife, 7, e31225. https://doi.org/10.7554/eLife.31225

Malatesta, M., Biggiogera, M., Baldelli, B., Barabino, S. M. L., Martin, T. E., & Zancanaro, C. (2008). Hibernation as a far-reaching program for the modulation of RNA transcription. Microscopy Research and Technique, 71(8), 564–572. https://doi.org/10.1002/jemt.20587

Martín, R., Berlanga, J. J., & De Haro, C. (2013). New roles of the fission yeast eIF2α kinases Hri1 and Gcn2 in response to nutritional stress. Journal of Cell Science, jcs.118067. https://doi.org/10.1242/jcs.118067

Melvin, R. G., & Andrews, M. T. (2009). Torpor induction in mammals: Recent discoveries fueling new ideas. Trends in Endocrinology & Metabolism, 20(10), 490–498. https://doi.org/10.1016/j.tem.2009.09.005

Mizushima, N., & Levine, B. (2010). Autophagy in mammalian development and differentiation. Nature Cell Biology, 12(9), 823–830. https://doi.org/10.1038/ncb0910-823

Nagafuchi, Y., Yanaoka, H., & Fujio, K. (2022). Lessons From Transcriptome Analysis of Autoimmune Diseases. Frontiers in Immunology, 13, 857269. https://doi.org/10.3389/fimmu.2022.857269

Nespolo, R. F., Mejias, C., & Bozinovic, F. (2022). Why bears hibernate? Redefining the scaling energetics of hibernation. Proceedings of the Royal Society B: Biological Sciences, 289(1973), 20220456. https://doi.org/10.1098/rspb.2022.0456

Niklas, K. J., & Kutschera, U. (2015). Kleiber's Law: How the Fire of Life ignited debate, fueled theory, and neglected plants as model organisms. Plant Signaling & Behavior, 10(7), e1036216. https://doi.org/10.1080/15592324.2015.1036216

Novoselova, E. G., Kolaeva, S. G., Makar, V. R., & Agaphonova, T. A. (2000). Production of tumor necrosis factor in cells of hibernating ground squirrels Citellus Undulatus during annual cycle. Life Sciences, 67(9), 1073–1080. https://doi.org/10.1016/S0024-3205(00)00698-6

O'Hara, B. F., Watson, F. L., Srere, H. K., Kumar, H., Wiler, S. W., Welch, S. K., Bitting, L., Heller, H. C., & Kilduff, T. S. (1999). Gene Expression in the Brain across the Hibernation Cycle. The Journal of Neuroscience, 19(10), 3781–3790. https://doi.org/10.1523/JNEUROSCI.19-10-03781.1999

Pakos-Zebrucka, K., Koryga, I., Mnich, K., Ljujic, M., Samali, A., & Gorman, A. M. (2016). The integrated stress response. EMBO Reports, 17(10), 1374–1395. https://doi.org/10.15252/embr.201642195

Palam, L. R., Baird, T. D., & Wek, R. C. (2011). Phosphorylation of eIF2 Facilitates Ribosomal Bypass of an Inhibitory Upstream ORF to Enhance CHOP Translation. Journal of Biological Chemistry, 286(13), 10939–10949. https://doi.org/10.1074/jbc.M110.216093

Palchykova, S., Deboer, T., & Tobler, I. (2003). Seasonal aspects of sleep in the Djungarian hamster. BMC Neuroscience, 4(1), 9. https://doi.org/10.1186/1471-2202-4-9

Palumbo, P. J., Wellik, D. L., Bagley, N. A., & Nelson, R. A. (1983). Insulin and Glucagon Responses in the Hibernating Black Bear. Bears: Their Biology and Management, 5, 291. https://doi.org/10.2307/3872552

Paul, S., & Lal, G. (2017). The Molecular Mechanism of Natural Killer Cells Function and Its Importance in Cancer Immunotherapy. Frontiers in Immunology, 8, 1124. https://doi.org/10.3389/fimmu.2017.01124

Puspitasari, A., Cerri, M., Takahashi, A., Yoshida, Y., Hanamura, K., & Tinganelli, W. (2021). Hibernation as a Tool for Radiation Protection in Space Exploration. Life, 11(1), 54. https://doi.org/10.3390/life11010054

Puspitasari, A., Squarcio, F., Quartieri, M., Totis, C., Hitrec, T., Takahashi, A., Yoshida, Y., Hanamura, K., Yako, T., Cerri, M., Simoniello, P., Durante, M., & Tinganelli, W. (2022). Synthetic torpor protects rats from exposure to accelerated heavy ions. Scientific Reports, 12(1), 16405. https://doi.org/10.1038/s41598-022-20382-6

Qiu, Y., Chen, Y., Zeng, T., Guo, W., Zhou, W., & Yang, X. (2016). High-mobility group box-B1 (HMGB1) mediates the hypoxia-induced mesenchymal transition of osteoblast cells via activating ERK/JNK signaling: HMGB1 mediates mesenchymal transition of osteoblasts. Cell Biology International, 40(11), 1152–1161. https://doi.org/10.1002/cbin.10616

R Core Team. (2021). R: A Language and Environment for Statistical Computing. R Foundation for Statistical Computing. https://www.R-project.org/

Rasmussen, A. T., & Rasmussen, G. B. (1917). The volume of the blood during hibernation and other periods of the year in the woodchuck (marmota monax). American Journal of Physiology-Legacy Content, 44(2), 132–148. https://doi.org/10.1152/ajplegacy.1917.44.2.132

Rouble, A. N., & Storey, K. B. (2015). Characterization of the SIRT family of NAD+-dependent protein deacetylases in the context of a mammalian model of hibernation, the thirteen-lined ground squirrel. Cryobiology, 71(2), 334–343. https://doi.org/10.1016/j.cryobiol.2015.08.009

Ruf, T., & Geiser, F. (2015). Daily torpor and hibernation in birds and mammals. Biological Reviews, 90(3), 891–926. https://doi.org/10.1111/brv.12137

Ruuskanen, S., Hsu, B.-Y., & Nord, A. (2021). Endocrinology of thermoregulation in birds in a changing climate. Molecular and Cellular Endocrinology, 519, 111088. https://doi.org/10.1016/j.mce.2020.111088

Sahdo, B., Evans, A. L., Arnemo, J. M., Fröbert, O., Särndahl, E., & Blanc, S. (2013). Body Temperature during Hibernation Is Highly Correlated with a Decrease in Circulating Innate Immune Cells in the Brown Bear (Ursus arctos): A Common Feature among Hibernators? International Journal of Medical Sciences, 10(5), 508–514. https://doi.org/10.7150/ijms.4476

Sajeev, T. K., Joshi, G., Arya, P., Mahajan, V., Chaturvedi, A., & Mishra, R. K. (2021). SUMO and SUMOylation Pathway at the Forefront of Host Immune Response. Frontiers in Cell and Developmental Biology, 9, 681057. https://doi.org/10.3389/fcell.2021.681057

Sanchez, M., Lin, Y., Yang, C.-C., McQuary, P., Rosa Campos, A., Aza Blanc, P., & Wolf, D. A. (2019). Cross Talk between eIF2α and eEF2 Phosphorylation Pathways Optimizes Translational Arrest in Response to Oxidative Stress. iScience, 20, 466–480. https://doi.org/10.1016/j.isci.2019.09.031

Sandal, G. M., Van deVijver, F. J. R., & Smith, N. (2018). Psychological Hibernation in Antarctica. Frontiers in Psychology, 9, 2235. https://doi.org/10.3389/fpsyg.2018.02235

Sauer, H., Wartenberg, M., & Hescheler, J. (2001). Reactive Oxygen Species as Intracellular Messengers During Cell Growth and Differentiation. Cellular Physiology and Biochemistry, 11(4), 173–186. https://doi.org/10.1159/000047804

Scherbarth, F., Diedrich, V., Dumbell, R. A., Schmid, H. A., Steinlechner, S., & Barrett, P. (2015). Somatostatin receptor activation is involved in the control of daily torpor in a seasonal mammal. American Journal of Physiology-Regulatory, Integrative and Comparative Physiology, 309(6), R668–R674. https://doi.org/10.1152/ajpregu.00191.2015

Scherbarth, F., & Steinlechner, S. (2010). Endocrine mechanisms of seasonal adaptation in small mammals: From early results to present understanding. Journal of Comparative Physiology B, 180(7), 935–952. https://doi.org/10.1007/s00360-010-0498-2

Schieber, M., & Chandel, N. S. (2014). ROS Function in Redox Signaling and Oxidative Stress. Current Biology, 24(10), R453–R462. https://doi.org/10.1016/j.cub.2014.03.034

Scholander, P. F., Hammel, H. T., Andersen, K. L., & L⊘yning, Y. (1958). Metabolic Acclimation to Cold in Man. Journal of Applied Physiology, 12(1), 1–8. https://doi.org/10.1152/jappl.1958.12.1.1

Schwartz, C., Hampton, M., & Andrews, M. T. (2013). Seasonal and Regional Differences in Gene Expression in the Brain of a Hibernating Mammal. PLoS ONE, 8(3), e58427. https://doi.org/10.1371/journal.pone.0058427

Shanker, S., Paulson, A., Edenberg, H. J., Peak, A., Perera, A., Alekseyev, Y. O., Beckloff, N., Bivens, N. J., Donnelly, R., Gillaspy, A. F., Grove, D., Gu, W., Jafari, N., Kerley-Hamilton, J. S., Lyons, R. H., Tepper, C., & Nicolet, C. M. (2015). Evaluation of Commercially Available RNA Amplification Kits for RNA Sequencing Using Very Low Input Amounts of Total RNA. Journal of Biomolecular Techniques : JBT, 26(1), 4–18. https://doi.org/10.7171/jbt.15-2601-001

Sharma, S., & Kavuru, M. (2010). Sleep and Metabolism: An Overview. International Journal of Endocrinology, 2010, 1–12. https://doi.org/10.1155/2010/270832

Shimozuru, M., Iibuchi, R., Yoshimoto, T., Nagashima, A., Tanaka, J., & Tsubota, T. (2013). Pregnancy during hibernation in Japanese black bears: Effects on body temperature and blood biochemical profiles. Journal of Mammalogy, 94(3), 618–627. https://doi.org/10.1644/12-MAMM-A-246.1

Singer, D. (2004). Metabolic adaptation to hypoxia: Cost and benefit of being small. Respiratory Physiology & Neurobiology, 141(3), 215–228. https://doi.org/10.1016/j.resp.2004.02.009

Singer, D. (2006). Human Hibernation for Space Flight: Utopistic Vision or Realistic Possibility? Journal of the British Interplanetary Society, 59, 139–143.

Singer, D., & Mühlfeld, C. (2007). Perinatal adaptation in mammals: The impact of metabolic rate. Comparative Biochemistry and Physiology Part A: Molecular & Integrative Physiology, 148(4), 780–784. https://doi.org/10.1016/j.cbpa.2007.05.004

Solari, S., & Baker, R. J. (2007). Mammal species of the world: A taxonomic and geographic reference. Journal of Mammalogy, 88(3), 824–830. https://doi.org/10.1644/06-MAMM-R-422.1

Squidonius. (2008). Qiagen Mini Spin Column.svg [Digital]. https://commons.wikimedia.org/wiki/File:Qiagen_Mini_Spin_Column.svg

Staples, J. F. (2014). Metabolic suppression in mammalian hibernation: The role of mitochondria. Journal of Experimental Biology, 217(12), 2032–2036. https://doi.org/10.1242/jeb.092973

Stawski, C., & Geiser, F. (2010). Fat and fed: Frequent use of summer torpor in a subtropical bat. Naturwissenschaften, 97(1), 29–35. https://doi.org/10.1007/s00114-009-0606-x

Steinlechner, S. (1998). Djungarian hamster and/or Siberian hamster: Who is who? Eur Pin Soc News, 38, 6.

Steinlechner, S., & Heldmaier, G. (1982). Role of photoperiod and melatonin in seasonal acclimatization of the djungarian hamster,Phodopus sungorus. International Journal of Biometeorology, 26(4), 329–337. https://doi.org/10.1007/BF02219503

Stenvinkel, P., Fröbert, O., Anderstam, B., Palm, F., Eriksson, M., Bragfors-Helin, A.-C., Qureshi, A. R., Larsson, T., Friebe, A., Zedrosser, A., Josefsson, J., Svensson, M., Sahdo, B., Bankir, L., & Johnson, R. J. (2013). Metabolic Changes in Summer Active and Anuric Hibernating Free-Ranging Brown Bears (Ursus arctos). PLoS ONE, 8(9), e72934. https://doi.org/10.1371/journal.pone.0072934

Stevens, E. D., Kanwisher, J. W., & FG, C. cross. (2000). Muscle temperature in free-swimming giant Atlantic bluefin tuna (Thunnus thynnus L.). Journal of Thermal Biology, 25(6), 419–423. https://doi.org/10.1016/s0306-4565(00)00004-8

Storey, K. B. (2010). Out Cold: Biochemical Regulation of Mammalian Hibernation – A Mini-Review. Gerontology, 56(2), 220–230. https://doi.org/10.1159/000228829

Storey, K. B., Heldmaier, G., & Rider, M. H. (2010). Mammalian Hibernation: Physiology, Cell Signaling, and Gene Controls on Metabolic Rate Depression. In E. Lubzens, J. Cerda, & M. Clark (Eds.), Dormancy and Resistance in Harsh Environments (Vol. 21, pp. 227–252). Springer Berlin Heidelberg. https://doi.org/10.1007/978-3-642-12422-8_13

Strewe, C., Thieme, D., Dangoisse, C., Fiedel, B., van den Berg, F., Bauer, H., Salam, A. P., Gössmann-Lang, P., Campolongo, P., Moser, D., Quintens, R., Moreels, M., Baatout, S., Kohlberg, E., Schelling, G., Choukèr, A., & Feuerecker, M. (2018). Modulations of Neuroendocrine Stress Responses During Confinement in Antarctica and the Role of Hypobaric Hypoxia. Frontiers in Physiology, 9, 1647. https://doi.org/10.3389/fphys.2018.01647

Tessier, S. N., Breedon, S. A., & Storey, K. B. (2021). Modulating Nrf2 transcription factor activity: Revealing the regulatory mechanisms of antioxidant defenses during hibernation in 13-lined ground squirrels. Cell Biochemistry and Function, cbf.3627. https://doi.org/10.1002/cbf.3627

Tessier, S. N., Katzenback, B. A., Pifferi, F., Perret, M., & Storey, K. B. (2015). Cytokine and Antioxidant Regulation in the Intestine of the Gray Mouse Lemur (Microcebus murinus) During Torpor. Genomics, Proteomics & Bioinformatics, 13(2), 127–135. https://doi.org/10.1016/j.gpb.2015.03.005

Tessier, S. N., & Storey, K. B. (2014). To be or not to be: The regulation of mRNA fate as a survival strategy during mammalian hibernation. Cell Stress and Chaperones, 19(6), 763–776. https://doi.org/10.1007/s12192-014-0512-9

Thomas, M. C., & Chiang, C.-M. (2006). The General Transcription Machinery and General Cofactors. Critical Reviews in Biochemistry and Molecular Biology, 41(3), 105–178. https://doi.org/10.1080/10409230600648736

Turbill, C., Smith, S., Deimel, C., & Ruf, T. (2012). Daily torpor is associated with telomere length change over winter in Djungarian hamsters. Biology Letters, 8(2), 304–307. https://doi.org/10.1098/rsbl.2011.0758

van Breukelen, F., & Martin, S. L. (2001). Translational initiation is uncoupled from elongation at 18°C during mammalian hibernation. American Journal of Physiology-Regulatory, Integrative and Comparative Physiology, 281(5), R1374–R1379. https://doi.org/10.1152/ajpregu.2001.281.5.R1374

van Breukelen, F., & Martin, S. L. (2002). Invited Review: Molecular adaptations in mammalian hibernators: unique adaptations or generalized responses? Journal of Applied Physiology, 92(6), 2640–2647. https://doi.org/10.1152/japplphysiol.01007.2001

van Breukelen, F., Sonenberg, N., & Martin, S. L. (2004). Seasonal and state-dependent changes of eIF4E and 4E-BP1 during mammalian hibernation: Implications for the control of translation during torpor. American Journal of Physiology-Regulatory, Integrative and Comparative Physiology, 287(2), R349–R353. https://doi.org/10.1152/ajpregu.00728.2003

Vitt, L. J., & Caldwell, J. P. (2009). Chapter 7—Thermoregulation, Performance, and Energetics. In L. J. Vitt & J. P. Caldwell (Eds.), Herpetology (Third Edition) (pp. 191–213). Academic Press. https://doi.org/10.1016/B978-0-12-374346-6.00007-9

Wang, Z., Gerstein, M., & Snyder, M. (2009). RNA-Seq: A revolutionary tool for transcriptomics. Nature Reviews Genetics, 10(1), 57–63. https://doi.org/10.1038/nrg2484

Wei, Y., Zhang, J., Xu, S., Peng, X., Yan, X., Li, X., Wang, H., Chang, H., & Gao, Y. (2018). Controllable oxidative stress and tissue specificity in major tissues during the torpor–arousal cycle in hibernating Daurian ground squirrels. Open Biology, 8(10), 180068. https://doi.org/10.1098/rsob.180068

Wei, Y., Zhang, J., Yan, X., Peng, X., Xu, S., Chang, H., Wang, H., & Gao, Y. (2019). Remarkable Protective Effects of Nrf2-Mediated Antioxidant Enzymes and Tissue Specificity in Different Skeletal Muscles of Daurian Ground Squirrels Over the Torpor-Arousal Cycle. Frontiers in Physiology, 10, 1449. https://doi.org/10.3389/fphys.2019.01449

Wiersma, M., Beuren, T. M. A., de Vrij, E. L., Reitsema, V. A., Bruintjes, J. J., Bouma, H. R., Brundel, B. J. J. M., & Henning, R. H. (2018). Torpor-arousal cycles in Syrian hamster heart are associated with transient activation of the protein quality control system. Comparative Biochemistry and Physiology Part B: Biochemistry and Molecular Biology, 223, 23–28. https://doi.org/10.1016/j.cbpb.2018.06.001

Wu, C.-W., & Storey, K. B. (2012). Pattern of cellular quiescence over the hibernation cycle in liver of thirteen-lined ground squirrels. Cell Cycle, 11(9), 1714–1726. https://doi.org/10.4161/cc.19799

Wu, C.-W., & Storey, K. B. (2016). Life in the cold: Links between mammalian hibernation and longevity. Biomolecular Concepts, 7(1), 41–52. https://doi.org/10.1515/bmc-2015-0032

Wu, C.-W., & Storey, K. B. (2018). Regulation of Smad mediated microRNA transcriptional response in ground squirrels during hibernation. Molecular and Cellular Biochemistry, 439(1–2), 151–161. https://doi.org/10.1007/s11010-017-3144-4

Xia, X. (1995). Body temperature, rate of biosynthesis, and evolution of genome size. Molecular Biology and Evolution, 12(5), 834–842. https://doi.org/10.1093/oxfordjournals.molbev.a040260

Xie, L.-H., Gwathmey, J. K., & Zhao, Z. (2021). Cardiac adaptation and cardioprotection against arrhythmias and ischemia-reperfusion injury in mammalian hibernators. Pflügers Archiv - European Journal of Physiology, 473(3), 407–416. https://doi.org/10.1007/s00424-020-02511-0

Yan, J., Barnes, B. M., Kohl, F., & Marr, T. G. (2008). Modulation of gene expression in hibernating arctic ground squirrels. Physiological Genomics, 32(2), 170–181. https://doi.org/10.1152/physiolgenomics.00075.2007

Zhang, J., Tessier, S. N., Biggar, K. K., Wu, C.-W., Pifferi, F., Perret, M., & Storey, K. B. (2015). Regulation of Torpor in the Gray Mouse Lemur: Transcriptional and Translational Controls and Role of AMPK Signaling. Genomics, Proteomics & Bioinformatics, 13(2), 103–110. https://doi.org/10.1016/j.gpb.2015.03.003

Zhao, Z., Miki, T., Van Oort-Jansen, A., Matsumoto, T., Loose, D. S., & Lee, C. C. (2011). Hepatic gene expression profiling of 5′-AMP-induced hypometabolism in mice. Physiological Genomics, 43(7), 325–345. https://doi.org/10.1152/physiolgenomics.00174.2010

Zhou, S., Tang, X., & Chen, H.-Z. (2018). Sirtuins and Insulin Resistance. Frontiers in Endocrinology, 9, 748. https://doi.org/10.3389/fendo.2018.00748

9 Acknowledgements

The last four years have brought me into contact with many people whom I would like to thank.

First of all, I would like to thank Prof Dr Alexander Choukér, who allowed me to work in the field of torpor research and supported my thesis. From the very beginning his ideas and motivation were absolutely unprecedented and made the teamwork very pleasing. Also, I would like to thank my supervisor Dr Dominique Moser, who, with her determination, impulse and patience, pushed me every step of the way even when there seemed to be no solution regarding *P. sungorus* the reference genome. Many thanks to both of you for showing me a path full of suggestions, fruitful discussions, dedication and for the time you took to make me a better researcher during the development of my project. To the whole working group, thank you for every moment, for being available and supportive. Further I would like to thank my dear colleague Marion Hörl, for the fun lunchtimes even during the pandemic and Florian Brandes, working with IPA would have been exhausting without his music.

I would also like to express my gratitude to Prof Dr Annika Herwig and Dr Victoria Diedrich from the University of Ulm, Prof Dr Dominique Singer and Dr Melanie Heidkamp from the University of Hamburg for the study material and impulse to go on, and for their guidance during this academic stage.

Of course, a special thanks goes to Prof Dr Jürgen Bereiter Hahn, for his constructive feedback and critical spirit that gave me advice and support to move forward. Without him this project would not have been possible. Furthermore, I would also like to thank the Uniscientia foundation.

My thanks also goes to Prof Dr Gustav Schelling for his understanding and organization regarding the use of the IPA software. Special thanks also to Dr Yiming Chen and Dr Jean Noel Billaud for their support with bioinformatics and IPA software handling respectively.

I would like to thank the LMU, my alma mater, the institution where I was able to do my thesis and the evaluation committee, my other fellow graduate students in the seminars.

And finally, I would like to thank my masters of life, my whole family, for their unconditional support, for the conversations at any time of the day, for the trips, for always being there.

10 Appendix

10.1 Publications

- Cuyutupa, V. R., Moser, D., Diedrich, V., Cheng, Y., Billaud, J. N., Haugg, E., Singer, D., Bereiter-Hahn, J., Herwig, A., & Choukér, A. (2023). Blood transcriptomics mirror regulatory mechanisms during hibernation-a comparative analysis of the Djungarian hamster with other mammalian species. *Pflugers Archiv: European journal of physiology*, *475*(10), 1149–1160. https://doi.org/10.1007/s00424-023-02842-8

10.2 Conference Presentation

- 16th International Hibernation Symposium: “Whole blood transcriptome analysis at different phases of daily torpor in Djungarian hamsters”
- ESA Topical Team Meeting Hibernation: “Learning from blood in torpor: comparative transcriptomics of *P. sungorus* with other mammals”

10.3 Supplementary Data

Table 7. Fold Change of genes for the respective *zeitgeber* time point (ZT). At the entry of torpor (ZT1), at torpor nadir (ZT4), during arousal (ZT7) and after torpor (ZT16).

Gene name	ZT 1	ZT 4	ZT 7	ZT 16
AARS1	-1.14	-1.20	-1.89	-1.25
AARS2	-1.19	1.52	1.17	NA
ABCA1	1.16	1.38	2.10	NA
ABL1	1.31	1.45	1.19	NA
ACADL	-1.58	-1.12	-1.65	-1.15
ACLY	1.07	-1.36	-1.37	1.12
ACSS2	-1.60	-1.12	-1.59	NA
ACTN1	1.08	1.43	-1.34	-1.09
ACVR2A	1.39	-1.07	1.70	NA
AKT1	1.30	1.56	1.39	NA
AKT3	1.05	-1.65	-1.11	NA
ANAPC10	1.30	-2.47	-1.21	NA
ANAPC11	-1.16	NA	-6.04	NA
ANAPC13	1.22	1.02	1.67	NA
ANAPC2	1.14	1.32	1.42	NA
ANAPC7	-1.16	-1.47	-1.30	NA
APP	1.07	1.44	-1.68	-1.45
ARG2	-1.64	1.05	-1.99	NA
ARHGAP4	1.23	1.67	1.42	NA
ARHGAP6	1.02	1.53	-1.25	NA
ASXL1	1.08	1.70	1.92	-1.00
ATF5	-1.50	1.80	1.34	NA
ATG101	1.12	1.66	1.42	NA
ATG12	-1.19	17.98	3.04	1.07
ATG13	1.12	1.26	1.62	NA
ATG14	-1.11	1.36	1.46	NA
ATG16L1	1.04	1.29	1.85	NA
ATG2A	1.08	1.53	1.50	NA
ATG2B	1.13	1.56	1.68	NA
ATG3	1.19	2.12	2.26	NA
ATG4A	1.29	1.31	1.11	NA
ATG9A	-1.05	1.28	1.12	NA
ATG9B	-2.11	-1.77	-2.31	NA
ATP5F1C	1.06	1.05	1.31	1.15
BCL2L1	-1.09	-1.49	-1.76	-1.20
BCL2L11	1.40	1.75	1.71	NA
BHLHE40	1.49	2.01	3.38	NA
BMAL1	1.02	-1.04	1.39	NA
BTK	-1.04	-1.47	-1.15	1.04
C1QB	-1.36	1.10	2.39	NA
C1QC	-1.10	1.15	1.80	NA
CACNA1A	1.85	2.99	-1.43	-1.51
CACNA1E	-2.33	3.22	1.80	NA
CACNB4	-1.93	1.19	-1.00	NA
CACNG5	1.30	1.54	3.75	NA
CALM1	1.11	2.08	1.99	NA
CAMK1	1.09	1.05	-1.65	NA
CAMK1D	1.65	1.98	-1.21	NA
CAPN1	-1.15	-1.38	-1.75	-1.55
CAPN2	1.28	1.28	-1.20	-1.03

Gene name	ZT 1	ZT 4	ZT 7	ZT 16
MAP3K8	1.12	1.04	1.39	NA
MAP4K1	-1.32	1.12	-1.18	1.88
MAPK13	1.07	1.53	2.75	NA
MAPK15	-14.22	-2.41	NA	NA
MAPK3	1.05	1.02	1.13	-1.35
MAPK6	1.15	1.78	1.93	NA
MAPK9	-1.02	1.16	1.55	NA
MARS2	-1.10	-1.97	-2.30	NA
MAVS	-1.04	-2.04	-2.08	NA
MDM2	-1.07	1.28	1.80	-1.04
MLYCD	1.09	1.77	1.63	NA
MMP11	1.10	1.39	2.17	NA
MMP2	1.32	-2.03	-2.17	NA
MMP8	3.61	24.91	5.38	NA
MMP9	1.53	1.73	2.79	NA
MYL6	-1.16	1.13	-1.60	-1.39
NARS2	1.30	-1.02	1.82	NA
NCF1	-1.02	-1.34	-1.51	-1.13
NCF4	1.07	-1.04	1.73	1.06
NCR1	1.62	-1.77	-2.00	NA
NDUFA13	1.41	2.49	2.29	NA
NDUFA4	1.00	1.04	-1.50	NA
NDUFA8	-1.28	-1.11	-1.66	NA
NDUFB1	1.27	2.09	2.93	NA
NDUFB11	1.20	2.49	3.91	NA
NDUFB4	1.15	1.27	1.52	NA
NDUFB5	-1.13	-1.78	-1.62	NA
NDUFB9	-1.05	1.19	1.45	NA
NDUFS1	1.19	1.13	1.56	NA
NDUFS5	1.13	-1.15	-1.58	NA
NDUFV3	1.04	-1.14	-1.54	NA
NF1	1.35	1.07	1.52	NA
NFATC3	-1.06	-1.32	1.17	-1.01
NFKB1	1.20	-1.19	-1.47	1.01
NFKBIA	1.00	1.42	1.73	1.01
NOD2	1.01	-1.63	-1.32	NA
PAG1	1.10	1.15	1.43	-1.08
PAK1	-1.07	-1.15	-1.73	NA
PAK3	-1.30	1.56	3.02	NA
PAM16	-1.12	-1.64	-1.51	NA
PARS2	-1.71	-1.19	-1.89	-1.17
PAX5	-1.01	1.41	1.50	1.18
PCK1	-1.84	-1.08	-2.08	NA
PCK2	-1.50	-1.33	-1.95	NA
PCNA	-1.05	-1.73	-1.37	NA
PDHA1	-4.35	8.16	NA	NA
PDHB	-1.02	1.19	1.47	NA
PECAM1	1.19	1.19	-1.26	-1.33
PIK3C2A	1.10	1.48	1.48	NA
PIK3CB	1.11	-1.02	1.54	NA

CASP1	1.17	1.30	1.46	NA	PIK3CD	1.14	1.28	1.33	1.16
CAT	-1.47	-1.21	-1.66	-1.45	PIK3CG	1.08	-1.27	-1.00	-1.38
CBX4	1.01	1.72	1.49	NA	PIK3R4	1.09	-1.73	-1.30	NA
CBX7	1.10	1.59	1.23	NA	PIK3R5	-1.11	-1.26	-1.32	-1.09
CBX8	-1.56	-1.20	-1.56	NA	PIK3R6	-1.14	-1.20	-1.54	NA
CCL4	-1.06	-4.17	-2.54	NA	PLA2G10	1.24	2.52	-1.72	NA
CCL5	1.29	-2.00	1.03	-1.09	PLA2G2D	-1.20	-1.93	1.31	NA
CCND2	-1.22	-1.54	-1.51	NA	PLA2G6	1.06	-1.43	-1.52	NA
CCND3	1.05	-1.45	-1.53	NA	PLCB2	-1.14	-1.16	-1.51	1.23
CCR5	1.09	-2.07	-2.95	NA	PLCB4	-1.25	1.18	-1.54	NA
CCR7	-1.04	-2.00	-2.03	1.08	PML	-1.04	-1.37	-1.48	1.02
CD28	1.21	1.35	1.41	-1.01	POLR1A	-1.14	1.00	-1.59	NA
CD48	1.20	1.01	-1.53	-1.14	POLR1B	1.16	-1.54	-1.21	NA
CD69	1.02	-1.55	-1.05	NA	POLR2B	1.05	-1.71	-1.57	NA
CD83	-1.35	-1.45	-1.10	NA	POLR2E	-1.48	-1.56	-1.81	-1.08
CDC25B	-1.27	-1.47	-1.71	1.01	POLR3D	-1.28	-2.12	-1.71	NA
CDC26	-1.04	-1.42	-1.38	NA	PPIF	1.05	-1.01	-1.47	NA
CDC27	1.50	1.43	2.50	NA	PPP1CB	-1.11	1.00	1.05	-2.00
CDK11A	-1.05	1.13	2.31	NA	PPP1R10	1.04	-1.83	-2.94	NA
CDK2	1.01	1.76	1.65	NA	PPP1R14A	-1.13	1.59	-2.53	NA
CDK4	-1.05	-1.26	-1.51	NA	PPP2CA	-1.00	-1.34	-1.09	1.05
CDKN2B	1.12	1.83	-1.79	NA	PPP2CB	-1.03	1.01	1.50	NA
CEBPB	-1.23	1.14	-1.02	-1.73	PPP2R5B	1.02	-1.35	-1.68	NA
CGAS	-1.15	-1.58	-1.24	NA	PPP2R5C	1.11	1.31	1.68	1.03
CLCF1	1.13	1.21	1.37	-1.08	PPP2R5E	-1.04	-1.06	1.37	NA
CLOCK	-1.02	1.25	1.66	NA	PPP3CB	1.08	1.23	1.68	1.08
CNTF	1.01	1.23	1.68	NA	PPP3R1	1.02	-1.41	1.08	NA
COL11A2	-1.20	1.71	-1.50	1.09	PRF1	1.21	-2.07	-1.44	-1.02
CPS1	-1.75	-1.08	-1.80	-1.13	PRKAA2	1.26	1.58	1.66	NA
CREB3L4	-1.72	-2.77	-2.06	NA	PRKACA	1.34	-1.59	-1.81	NA
CREBBP	1.16	1.30	1.40	-1.05	PRKAR2B	1.29	1.22	-1.46	-1.06
CSF2RB	1.04	-1.36	-1.63	NA	PRKCD	1.04	1.31	1.40	NA
CTBP2	-1.01	-1.76	-1.31	NA	PRKCZ	-1.13	1.33	-1.88	NA
CTNNB1	-1.09	-1.32	-1.23	-1.01	PTPA	1.27	1.89	1.74	NA
CTTN	1.63	2.00	-1.94	NA	PTPN6	1.14	1.34	1.35	1.00
CXCR4	-1.16	-1.83	1.54	-1.49	PVR	1.10	1.78	4.04	NA
CYBB	1.22	1.15	1.63	-1.13	PXN	1.10	1.33	1.19	-1.03
DAPP1	-1.00	1.20	1.51	NA	RAF1	1.08	1.17	1.32	-1.25
DARS1	-1.04	-1.38	-1.36	-1.21	RALA	-1.17	-1.41	-1.58	NA
DAXX	-1.07	-1.32	-1.53	NA	RALB	1.12	-1.46	-1.64	NA
DHCR24	1.19	-1.80	-1.03	NA	RAP1B	1.08	1.23	1.39	-1.05
DLD	-1.54	-1.09	-1.80	-1.13	RAPGEF1	1.07	1.16	1.31	-1.09
DMTF1	1.04	1.39	1.44	NA	RAPGEF3	-16.20	NA	NA	NA
DOT1L	-1.03	-1.38	-1.43	NA	RASSF5	1.14	1.04	1.31	-1.06
DR1	1.20	4.75	3.81	NA	RCC1	1.31	-1.08	-1.88	NA
DUSP1	1.42	-1.37	2.11	NA	RCOR1	-1.06	-1.02	1.42	NA
E2F1	-1.47	-1.20	-1.70	NA	RDX	1.02	-1.44	1.04	NA
E2F2	1.14	1.23	-1.21	-1.42	REL	1.01	1.26	3.02	NA
E2F3	-1.28	-1.45	-2.48	NA	RELB	-1.03	1.44	1.27	NA
E2F5	1.08	-1.84	-1.68	NA	RFC1	-1.15	-1.61	-1.26	NA
E2F8	-1.81	6.86	NA	NA	RHOB	-1.05	-1.49	-1.10	NA
EBF1	1.04	1.48	1.63	NA	RHOD	-25.97	-1.50	-3.35	NA
EIF2A	-1.09	-1.35	-1.19	-1.05	RHOQ	-1.74	-1.46	1.16	NA
EIF2AK3	1.18	1.00	1.43	NA	RNF4	1.10	1.20	1.46	1.03
EIF2B3	1.39	1.14	-2.07	NA	RPA1	1.02	-1.19	-1.30	NA
EIF2B5	1.02	1.33	1.32	NA	RPL7L1	1.15	1.53	1.81	1.12
EIF2S3	-1.13	-1.29	-1.11	-1.12	RPS6KA5	-1.56	1.06	-1.62	-1.08

EIF3D	-1.04	-1.25	-1.41	1.05	RRAS	-1.12	-1.03	-2.21	NA
EIF4E	-1.13	-1.03	1.38	NA	RRAS2	-1.13	-1.53	-1.16	NA
EIF4EBP1	-1.01	-1.66	-2.74	NA	RRP9	-1.15	1.64	1.20	NA
EIF4G3	1.16	1.34	1.18	-1.03	RUNX3	1.14	1.08	1.35	1.11
ELF1	1.08	1.24	1.35	-1.16	SAA1	1.21	5.54	5.58	NA
ELF2	1.05	1.24	1.42	NA	SAE1	-1.11	-1.26	-1.88	NA
ELK3	1.15	-1.21	-1.40	-1.08	SARS2	-1.51	-1.14	-2.53	NA
ERCC2	1.03	1.24	-1.44	1.08	SCNN1A	1.43	-1.15	-10.13	NA
ESRRA	-1.15	1.51	1.72	NA	SDHB	-1.03	1.18	1.33	NA
EZH2	1.11	1.57	1.81	NA	SENP2	1.10	1.39	1.47	NA
FARSB	-1.22	-1.84	-1.89	NA	SENP7	-1.11	-1.41	-2.36	NA
FCER1G	1.17	1.56	2.44	NA	SF3A1	1.15	1.12	1.42	-1.08
FCGR2B	-1.16	-1.42	-1.57	1.03	SHC1	-1.21	-1.34	-1.35	-1.04
FER	-1.68	1.08	-1.32	NA	SIPA1	-1.05	-1.08	-1.30	1.18
FOS	-1.03	-3.62	1.60	NA	SIRT3	-1.41	4.78	5.10	NA
FOXO3	-1.18	-1.40	-1.06	-1.38	SIRT6	1.18	1.11	-2.12	NA
FOXO4	1.05	-1.08	-1.70	-1.64	SKI	1.35	1.98	1.40	NA
FYN	1.05	1.34	1.21	1.06	SLC2A1	1.30	1.05	1.40	NA
FZR1	-1.50	-1.34	-2.23	-1.65	SMAD1	1.10	1.15	1.65	NA
GAB1	-1.21	-1.63	-1.59	NA	SMAD4	1.15	1.37	1.72	-1.13
GABARAP	-1.15	-1.17	-1.70	-1.20	SMAD5	-1.01	-1.01	1.41	NA
GABPB2	1.37	1.80	1.33	NA	SMARCA5	-1.02	-1.28	1.14	1.02
GADD45A	1.28	-1.65	-1.75	-1.12	SMURF1	-1.04	1.29	1.52	NA
GADD45G	1.67	1.84	3.25	NA	SNCA	-1.25	-1.16	-1.15	-1.57
GLS	1.04	1.12	1.61	-1.00	SOD3	1.59	1.69	-1.66	-1.33
GLUD2	-1.12	3.64	NA	NA	SOS1	1.20	1.14	1.49	NA
GOT2	1.09	-1.05	-1.46	NA	SOS2	1.25	1.20	1.62	NA
GTF2A1	-1.39	-1.47	-1.20	NA	SP3	1.11	1.05	1.34	-1.08
GTF2E1	-1.16	-2.59	-1.51	NA	SUMO3	-1.08	1.08	3.45	NA
GTF2E2	-1.07	-1.41	-1.11	NA	SUV39H1	1.03	1.46	1.46	NA
GTF2H1	-1.58	1.09	1.54	NA	SYNJ1	1.22	1.47	1.66	-1.02
GTF2H4	1.13	-1.23	-1.80	NA	TAB1	-1.10	1.16	-1.59	NA
GTF2H5	NA	1.12	1.55	NA	TAF1	1.01	-1.11	-1.62	1.17
H1-0	-1.16	1.83	NA	NA	TAF12	-1.03	-1.54	-2.21	NA
H1-10	-1.30	2.64	1.37	NA	TAF13	-1.33	-1.84	-1.13	NA
H1-3	-1.30	1.55	-1.00	1.09	TAF15	-1.01	1.33	1.05	1.06
H3-3A	-1.03	1.11	1.10	-1.73	TAF5L	-1.21	1.19	1.79	NA
HARS1	-1.30	-1.49	-1.70	NA	TAF7	-1.00	-1.69	1.07	NA
HBP1	1.08	1.24	1.50	1.03	TARS1	-1.02	-1.43	-1.31	NA
HDAC1	-1.07	-1.36	-1.15	1.21	TARS3	-1.76	-1.16	-1.89	-1.12
HDAC2	-1.05	-1.54	-1.52	NA	TBK1	1.23	-1.41	-1.10	NA
HSPA1A	-1.32	1.31	-1.98	NA	TDG	1.04	1.25	1.56	NA
HSPA4	-1.01	-1.38	-1.34	-1.07	TEC	1.29	-1.45	-1.21	NA
HSPA8	-1.13	-1.56	-1.68	-1.13	TGIF1	-1.10	-1.68	-1.45	NA
IARS2	-1.55	-1.18	-1.77	-1.11	TIMM17B	-1.09	1.01	-1.96	NA
ICAM3	-1.33	11.10	9.32	NA	TIMM22	-1.00	-1.75	-1.70	NA
IFNB1	1.10	-3.21	-1.78	NA	TIMM23B	1.07	1.02	2.58	NA
IGHD	NA	-2.00	-3.46	NA	TIMM44	-1.40	-1.26	-1.36	NA
IGHG2	1.10	2.02	1.62	NA	TIMM8A	1.19	-1.66	1.50	NA
IKBKB	-1.02	1.53	1.59	NA	TIMP3	1.50	-1.41	-1.63	NA
IL2RG	1.07	-1.26	-1.46	1.08	TLN1	1.22	1.35	-1.14	-1.18
IL3RA	-1.07	1.27	-1.42	NA	TLR2	-1.22	-2.69	-2.77	NA
IL6	-1.25	-3.03	-1.09	NA	TLR3	-1.27	-2.46	-1.75	NA
INPP5B	-1.07	-1.13	-1.57	NA	TLR4	2.28	-2.32	1.02	NA
INPPL1	1.15	1.22	1.42	NA	TLR6	1.37	-2.79	-2.91	NA
IRF3	-1.05	-1.24	-2.10	1.28	TLR7	1.19	-1.47	-1.72	NA
ITGA1	-1.22	3.35	3.26	NA	TLR8	-1.03	-2.94	-4.49	NA

ITGA2B	-1.05	1.87	-1.52	-1.46	TMEM173	-1.14	-1.34	-1.49	1.01
ITGA3	1.42	-1.82	-4.69	NA	TNFSF10	-1.18	-1.77	1.26	NA
ITGA4	-1.32	1.26	1.16	-1.25	TNFSF11	1.02	-2.42	-8.82	NA
ITGA7	1.21	1.20	-6.28	NA	TNFSF14	1.16	-1.79	-1.25	NA
ITGB1	1.17	1.21	-1.12	-1.34	TNFSF8	1.07	-1.32	-1.94	NA
ITGB3	1.20	1.35	-1.70	-1.24	TNFSF9	1.89	1.26	3.30	NA
ITGB5	1.22	-21.17	NA	NA	TOMM20	-1.08	1.13	1.47	1.03
ITGB7	2.33	1.00	-1.43	1.05	TOMM34	1.04	1.39	1.26	1.08
ITK	-1.04	-1.35	-1.60	-1.07	TOMM7	1.23	-1.13	-1.47	NA
ITPR3	-1.05	1.40	1.16	1.07	TP53BP1	-1.17	-1.22	-1.95	NA
JAK3	1.04	1.39	1.15	1.21	TRAF6	1.12	1.74	1.98	NA
KARS1	-1.09	NA	NA	NA	TREM2	1.01	1.33	-1.48	-1.58
KAT2A	1.02	-1.53	-1.34	NA	TUBA3C	1.11	5.24	-1.15	NA
KDM1A	-1.01	1.68	1.60	NA	TUBA8	1.49	1.09	-1.63	NA
KIR3DL3	1.33	-2.77	-3.83	NA	TYK2	1.13	1.37	1.38	1.07
KLRD1	1.26	-2.50	-2.89	NA	UBE2I	1.09	1.23	1.58	1.11
KRAS	1.57	3.41	3.86	NA	UCP2	-1.20	-1.26	-2.29	-1.79
LAMTOR3	1.02	1.06	1.37	NA	UQCRC2	-1.33	-1.15	1.28	-1.22
LARS1	1.10	-1.40	-1.99	NA	UQCRFS1	-1.33	-1.02	1.19	NA
LAT	-1.18	1.20	-1.37	1.06	VARS2	-1.07	1.49	-1.12	NA
LDHB	-1.28	-2.79	-3.05	NA	VCL	1.48	1.68	-1.14	1.04
LTA	1.08	1.73	1.62	NA	VDAC2	1.05	1.22	1.55	1.04
MALT1	1.00	1.24	1.58	1.09	VDAC3	-1.05	-1.03	-1.60	-1.13
MAP1LC3B2	1.52	3.71	1.90	NA	VHL	1.05	1.27	1.63	NA
MAP2K1	-1.06	-1.50	-1.25	-1.07	WARS2	-1.77	-1.23	-1.67	NA
MAP2K3	1.07	1.05	-1.49	-1.15	WIPF1	1.02	1.26	-1.27	-1.33
MAP3K10	1.06	-1.04	-2.09	NA	XRCC5	-1.06	1.47	1.30	NA
MAP3K11	1.18	1.14	1.68	NA	YPEL3	1.29	1.78	1.32	NA
MAP3K13	-1.42	-1.72	-2.41	NA	ZBTB14	-1.13	1.30	-1.27	NA
MAP3K2	-1.07	1.51	2.44	NA	ZEB1	-1.05	-1.44	1.16	NA
MAP3K7	1.01	1.30	1.85	NA	ZFP36L1	1.09	1.30	1.51	1.14